International Parallel Test on the Measurement of G_{max} Using Bender Elements Organized by TC-29

Japanese Domestic Committee for TC-29

S. Yamashita	*Kitami Institute of Technology*
T. Fujiwara	*Geo-Research Institute*
T. Kawaguchi	*Hakodate National College of Technology*
T. Mikami	*OYO Corporation*
Y. Nakata	*Yamaguchi University*
S. Shibuya	*Kobe University*

1. ABSTRACT

Technical committee, TC29 (Stress-strain and Strength Testing of Geomaterials) of International Society of Soil Mechanics and Geotechnical Engineering (ISSMGE), has started international parallel test on the measurement of G_{max} using bender elements (BE) as one of its main activities in the year 2003. The purpose was to evaluate the consistency of the BE test results obtained by using the exactly similar test material and test method besides identifying the various existing hardware and software being used in this test. It was decided that the domestic TC29 group of Japanese Geotechnical Society (TC29-JGS) leads this group.

By 2005, reports of the test result were obtained from 23 institutions from 11 countries. This report has been prepared by TC29-JGS taking a leading role from the beginning. Standard test method is proposed here in order to obtain the more accurate data from the bender element test by examining various test methods adopted at different institutions worldwide and the effect of different factors on test results.

2. INTRODUCTION

Parameters (shear modulus, G_{max} and damping, h) required for the dynamic response of geomaterials due to dynamic loads, such as traffic loads, earthquakes and machine vibrations, are being evaluated by using laboratory tests at small strain level and from in-situ seismic tests. It is now commonly known that stress-strain behavior of a geomaterials is non-linear and G value decreases but damping ratio increases with the increase in strain level. In order to evaluate this non-linearity, stress-strain responses at very small strains due to monotonic or cyclic loadings are evaluated by using triaxial or torsional shear testing machines, commonly known as static loading methods. On the other hand, applying wave motions in the test specimens and observing their behavior at resonance including free oscillation time, such as resonant column apparatus, are other kinds of evaluation methods, called as vibration test methods. Besides them, some methods, such as ultrasonic pulse test, the bender element test etc., which calculate deformation constants based on the wave velocity, are called as pulse transmission techniques.

Among these testing methods described in previous paragraphs, the test procedures for the first two methods are well written and are being used worldwide though still short of being universal. The need was felt for examining the effects of sampling and preparation methods, effects due to the change in experimental method and application of test result into practice, which are said to affect largely on the test results. In addition, sharing the information internationally and preparing international guideline was also felt necessary. TC29 was formed under such background in 1994 with Prof. F. Tatsuoka as its Chairperson. The aim of this group was: 1) to share information about laboratory tests internationally, 2) suggest the working guideline for laboratory tests, and 3) perform case studies to apply the result obtained from laboratory tests. On completing the first two periods (1994-2000) under the leadership of Prof. F.Tatsuoka, the third period (2001-2005) was led by Prof. R. Jardine from Imperial College. The same group is continuing at present for the fourth working period (2005-2009) of TC29.

In the last 10 years, TC29 is active with the aim of improving laboratory shear testing apparatus and test methods, generalization of the mechanical properties of different types of geomaterials and their engineering applications. In doing that, four international conferences, IS-Hokkaido (1994), Geotechnique

Symposium (1997), IS-Torino (1999) and IS-Lyon (2003), have been sponsored by now along with the publication of proceedings and a summary book (Tatsuoka et al., 2001).

One of the prime missions of TC29 is to optimize and internationalize the laboratory test apparatus and test methods being used in characterizing deformation behavior of geomaterials. TC29 has already conducted two international parallel tests in the past by using the same soil and the same test method (Toki et al. 1995, Yamashita et al. 2001).

The BE test is becoming quite popular in the last ten years due to its simplicity, low cost and being non-destructional type. The test is not only limited to the leading countries for laboratory tests, such as United Kingdom, United States, Italy, Japan, Australia, Norway, and Sweden, but has extended globally via foreign graduates from these countries. However, the process of defining the travel distance of shear wave, time of travel, the input wave type, input frequency, the hardware and software for removing the noise and so many other factors differ in each laboratory. Most of the times, these factors are decided on personal judgments rather than guided by procedures. To take up this issue seriously, TC29 has started international parallel test on bender element (BE) in 2003 as one of its main activities.

Under the aforementioned background, the purpose of international parallel test on the bender element was: 1) to grasp the present condition of hardware/software being utilized in the bender element test, 2) to strictly evaluate the consistency of test results from this test by using the same material and test procedures, and 3) to produce the original concept and international test guideline for measuring shear modulus, G_{max} of different geomaterials. Having abundant backup data and track record, it was decided that domestic TC29 committee of Japan, TC29-JGS takes the leading role for its execution.

3. INTERNATIONAL PARALLEL TEST

3.1 Test Specification

Test specifications (see Appendix-1) were published on September 2003 at the 3rd Symposium on the Deformation Behavior of Geomaterials (IS-Lyon03), which was held in Lyon, France. Regarding the test material, Toyoura sand was purchased at once by TC29-JGS and distributed to the participating institutions as 5 kg packs (more if desired by laboratories) including a nozzle for sample preparation. Here, the reasons of selecting the Toyoura sand as test material and air-pluviation method as the test method were: i) the past parallel tests using laboratory test equipment were conducted with this material (Tatsuoka et al 1986, Toki et al 1986, Miura et al 1994), ii) the same sand was used for the parallel tests performed to evaluate the deformation behavior (Toki et al 1995), and iii) the previous international simultaneous test by TC-29 (Yamashita et al 2001) also used the same test material. In addition, the large chunk of accumulated test data on Toyoura sand in Japan as well as in many other countries worldwide ascertained ample opportunities to compare the results with past records.

The reason of selecting air pluviation technique for sample preparation was also due to the past record of being used in international parallel tests. In principle, JGS 0520-2000 and JGS 0542-2000 were followed for specimen preparation as well as for testing. Furthermore, because there were queries from the participated institutions about the drop height during specimen preparation, Appendix-3 that showed the relationship between specimen densities against the drop height was attached for reference.

It was decided to test the specimen at relative density of 80% & 50%. However, in order to obtain a relative density, it was necessary to calculate the maximum and minimum density ($\rho_{d,max}$ and $\rho_{d,min}$) and the results could differ among participated institutions. To overcome this difficulty, members of TC29-JGS had performed the tests beforehand to evaluate $\rho_{d\,max}$ and $\rho_{d\,min}$ and the average value of required dry density was supplied to the institutions. Table 3.1 shows the participated institutions and obtained results. Figure 3.1 provides the gradation of sand used for testing.

Table 3.1 Physical properties of Toyoura sand

Lab. No.	ρ_s (g/cm^3)	$\rho_{d\,max}$ (g/cm^3)	$\rho_{d\,min}$ (g/cm^3)	e_{max}	e_{min}
1	2.636	1.619	1.337	0.972	0.628
2	2.636	1.622	1.341	0.966	0.625
3	2.633	1.614	1.338	0.968	0.631
Ave	2.635	1.618	1.339	0.968	0.628

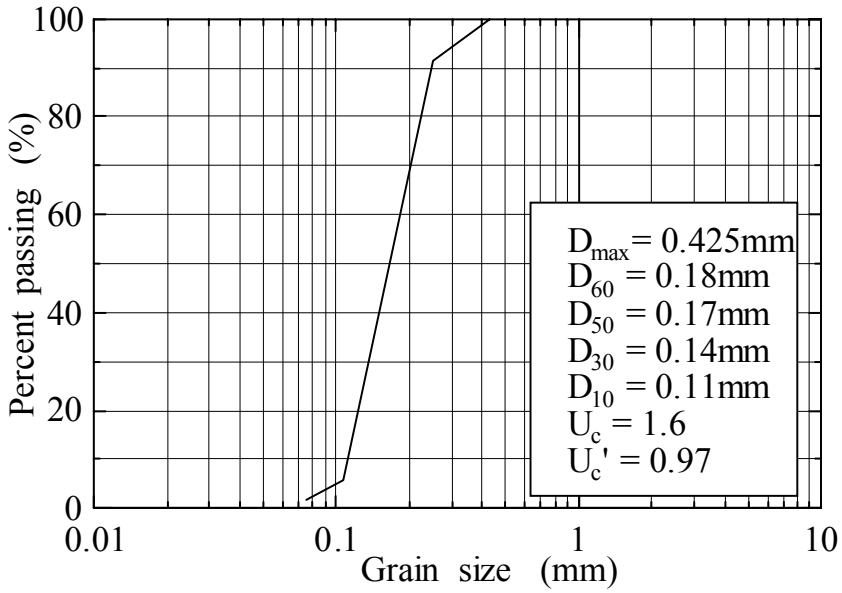

Fig. 3.1 Grain size of Toyoura sand

3.2 Participated Laboratories

Application for participation in the international parallel test was started in September, 2003 at the 3rd international conference on deformation behavior of geomaterials held in Lyon, France. This was followed by uploading the information for test specification and details in the TC29 homepage. There was an overwhelming response, altogether 30 institutions from 13 different countries applied for participation before the year end.

The international parallel test was formally started by dispatching Toyoura sand and the nozzle for test to the participated institutions before March, 2004. In the beginning, the deadline for submitting the report was fixed as June, 2004. However, the deadline was extended to December, 2004 due to the fact that dispatching of the sample was late besides other reasons. Finally, report of the test result was prepared on September, 2005 based upon the submissions from 23 institutions worldwide. While Table 3.2 shows the list of the participated institutions, Figure 3.2 shows their distribution worldwide. The participated institutions were total of 15 from Asia (Japan-11, China-1 & Korea-1), 9 from Europe (France-2, Italy-2, Finland-1, Holland-1, Portugal-1, Rumania-1 & England-1) and one from North America (Canada-1). By comparing the participated international institutions in the previous parallel test organized by TC29, which was just 19 institutions from 6 countries (Japan-11, Greece-1, Italy-4, Korea-1, Portugal-1 & Spain-1) as shown in Figure 3.3, it is quite understandable that bender element test is spreading worldwide and being quite popular.

Table 3.2 Participated laboratories

No.	Names	Affiliation	Country
1	Dr. D. Wijewickreme	University of British Columbia	Canada
2	Dr. Y.-g. Zhou	Zhejiang University	China
3	Dr. T. Länsivaara	Tampere University of Technology	Finland
4	Dr. C. Dano	Research Institute in Civil and Mechanical Engineering	France
5	Dr. H. Geoffroy & Dr. A. Ezaoui	ENTPE	France
6	Prof. D.C.F. Lo Presti & Dr. D. Androne	Politecnico di Torino	Italy
7	Dr. R. Castellanza & Dr. C. Zambelli	Politecnico di Milano	Italy
8	Mr. N. Takehara	Tokyo Soil Research Co., Ltd.	Japan
9	Prof. J. Kuwano & Dr. Tay	Tokyo Institute of Technology	Japan
10	Dr. T. Ogino	Akita University	Japan
11	Dr. Y. Nakata	Yamaguchi University	Japan
12	Mr. T. Fujiwara	Geo-Resurch Institute	Japan
13	Mr. K. Nishida	Hokkaido University	Japan
14	Mr. M.K. Mostafa	Osaka City University	Japan
15	Prof. J. Koseki	Institute of Industrial Science, University of Tokyo	Japan
16	Dr. T. Kawaguchi	Hakodate National College of Technology	Japan
17	Dr. S. Yamashita	Kitami Institute of Technology	Japan
18	Dr. Y. Mohri & Dr. T. Lohani	National Research Institute of Agricultural Engineering	Japan
19	Prof. D.-S. Kim	Korea Advanced Institure of Science and Technology	Korea
20	Dr. E. d. Haan	GeoDelft	Netherlands
21	Dr. C. Ferreira	Universidade do Porto	Portugal
22	Dr. A. Cristian	National Center for Seismic Risk Reduction	Romania
23	Dr. A. Takahashi	Imperial College London	UK

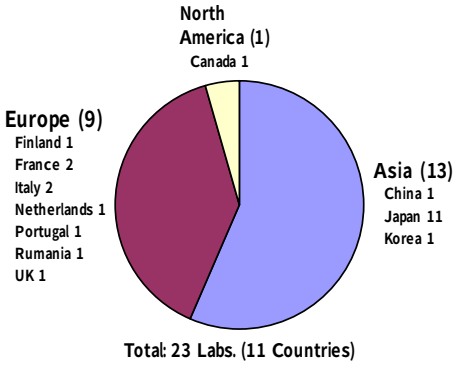

Fig. 3.2 Regions and countries

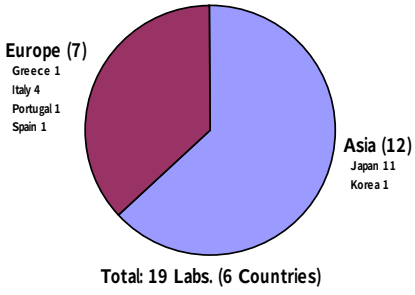

Fig. 3.3 Regions and countries (last RR-test)

3.3 Test Apparatus and Test Conditions

Table 3.3 enlists the details on test apparatus, specimen size and number of tests at different participated laboratories. It is to be noted here that Laboratory No. in this table does not match with Table 3.2. Figures 3.4 to 3.7 give us a look on the test distributions based on the apparatus type, specimen diameter, ratio of height (H) to diameter (D) and number of different test types.

The number of different type of test equipments, triaxial testing device (TX) -17, consolidation (OM) and direct shear test equipment (DS) that use stiff metal container -5, resonant column apparatus (RC) -2 (including one torsional shearing (TS) apparatus), shows that triaxial device was primarily used. Regarding the specimen size in triaxial test, diameters of 50 mm and 70 mm totaled almost 80%. There were two cases where diameter above 100 mm was used. When examined for the ratio, H/D, it was above 1.0 and equaled 2.0 in triaxial and resonant column method tests. In contrast, H/D was relatively small in consolidation and direct shear test equipments, where the specimens were put inside stiff metal containers.

On categorizing according to saturation condition, there were total of 60 tests on dry specimen and 45 with saturated specimen, thus making 105 in total. The relatively large number of tests on dry specimen could be due to simple test condition without necessitating saturation. However, there is another difficulty in accurate specimen volume change measurement when tested dry because it either needs double cell type arrangement or needs lateral strain measurements. In the tests performed, it was mostly found that volume change of dry specimen was simply taken as three times that the axial strain. The tests on dry specimens may also cause the difficulty in identifying the shear wave arrival time due to a near-field-effect that goes up when the distance between the bender pairs decreases. It is reported that near-field-effect are mainly influenced by P wave signals that reach the receiving end before true shear wave signal. As the difference in propagation velocity of the P wave and S wave is smaller in dry specimen than saturated specimen, there is high possibility that near-field-effect is higher in dry specimens.

Regarding the stress condition at consolidation, isotropic stress state was followed in 55 test cases, which is more than half of the total. Tests under K_0 conditions were performed in consolidation or direct shear apparatus using stiff container. There was one case that used triaxial apparatus (No.5) but K_0 condition was not obtained by controlling the lateral stress so that no lateral strain was developed. In this test, a hard cylindrical Perspex glass was used to restrain the side displacement, which was principally similar to oedometer or direct shear devices, and was put in OM category.

Table 3.3 Test apparatus and test conditions

Lab. No.	Apparatus	Specimen size			Dry						Saturated					
		D	H	H/D	Dr=50%			Dr=80%			Dr=50%			Dr=80%		
		mm	mm		K=1	K=0.5	K_0	K=1	K=0.5	K_0	K=1	K=0.5	K_0	K=1	K=0.5	K_0
1	TX	100	200	2.00	2			2								
2	TX	50	100	2.00							1	1		1	1	
3	TX	38	80	2.11	1	1		2	2						1	
4	OM	75	40	0.53			1			1			1			1
5	OM(TX)	50	50	1.0			1			1						
			90	1.8			1			2						
6	TX	66	70	1.06	1											
7	TX	75	150	2.00							1	1			1	
8	TX	76	150	1.97	2			1								
9	RC/TS	50	100	2.00	1			1			1			1		
10	DS	75	100	1.33			1			1						
11	TX	50	100	2.00							1	1		1	1	
12	RC	50	110	2.20	1	1		1	1		2	1		1	1	
13	TX	70	140	2.00	1	1		1	1							
14	TX	50	100	2.00							1					
15	OM	62	55	0.89									1			1
	TX	39	85	2.18							1	1		1	1	
16	TX	50	100	2.00	1	1		1	1		1	1		1	1	
17	DS	48	60	1.25			5			5						
18	TX	70	140	2.00				3								
19	TX	50	100	2.00							1					
20	TX	50	100	2.00	1			1	1							
21	TX	53	115	2.17	2	1		1	1		1	1		1	1	
22	TX	70	70	1.00							1			1		
			100	1.40							1			1		
			150	2.14							1			1		
23	TX	200	390	1.95	1			1			1			1		
Total					14	5	9	15	7	10	15	7	2	11	8	2
					60						45					
					105											

* Lab. No. does not coincide with Table 3.2.

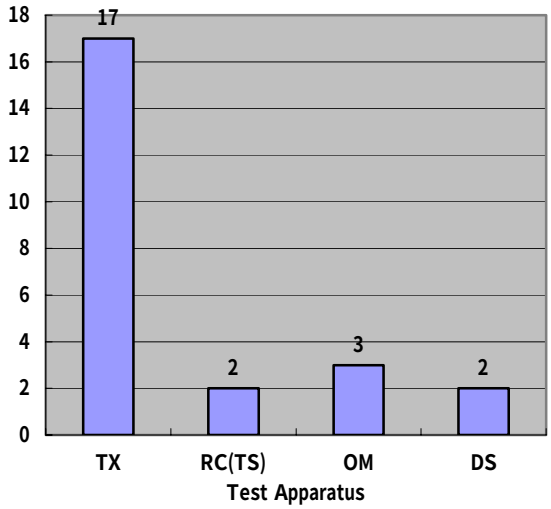

Fig. 3.4 Test apparatus

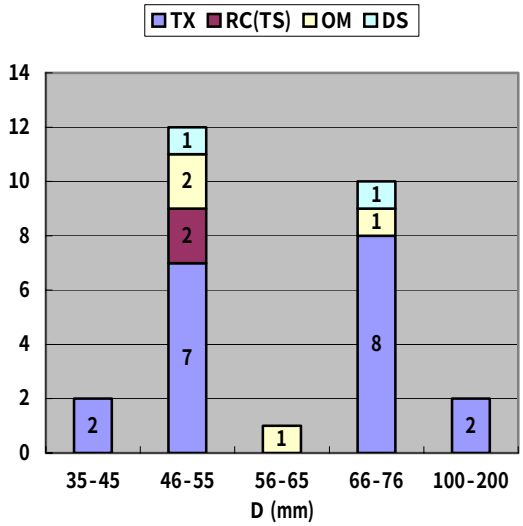

Fig. 3.5 Specimen diameter

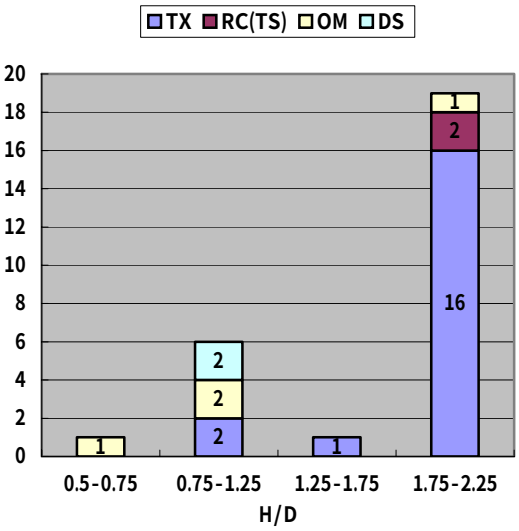

Fig. 3.6 Ratio of H to D

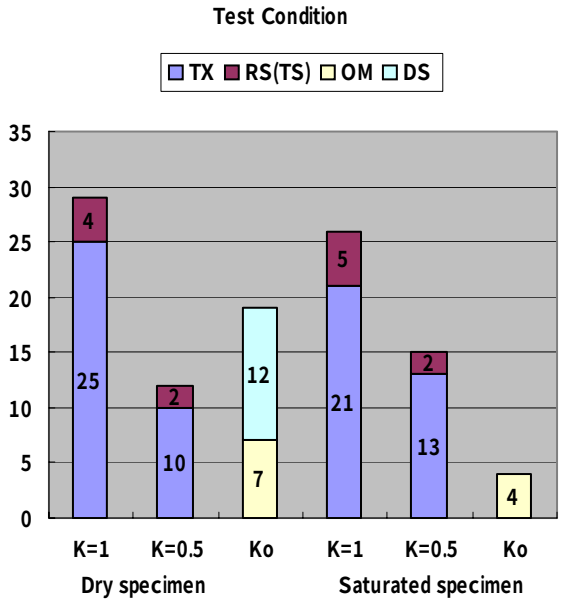

Fig. 3.7 Number of tested samples

3.4 Specifications of Bender Elements

Table 3.4 plots the specifications of bender elements (BE) that were used in the tests. The dimensions and signs are as shown in the Figure 3.8. In the table, some of the columns include two rows of information for BE dimensions, the top of which indicates the property of transmitter bender and the bottom one, the receiver bender.

Information on the thickness of epoxy coating, t_c and the total thickness, t are inscribed wherever available. Where there are no reports or unclear, columns are left blank.

Figure 3.9 shows a typical example of BE set up. Here, BE is a bimorph electric actuator that polarize in the direction of thickness. Two ceramic elements are bonded together with a flexible shim of metal such as nickel acting as an electrode. In general, the material of the piezo-electric device was Lead Zirconium Titanate (Pb (Ti.Zr) O_3), called PZT. When electric voltage is applied on a bimorph piezo-electric element, one of the layer shrinks and the other extends due to piezoelectric effect, ultimately producing a bend in a whole element. On the other hand, when deformation is applied, the piezoelectric transducer generates a voltage. By using this property of BE, either of the elements installed in a cap or pedestal are applied with electric voltage to generate shear waves and the element at the other end receives the signal enabling the measurement of shear wave velocity in the soil element.

In all the tests performed here, BE transducers were entirely made of PZT wherever the reporting was done. On observing the size, the length, L_t of 12-20 mm, the width, W of 10-12 mm and the thickness, t of 0.5-1.0 mm was used. Thickness of waterproofing insulation, such as epoxy coating, t_c seemed to be 0.5 mm in general.

There are two different ways of electric wirings to activate such piezo-electric devices to transmit or receive a shear wave, namely parallel type and series type. In a parallel type connection, polarization direction in both layers of a bimorph specimen becomes identical whereas, in a series type, polarization direction is opposite. The result is such that parallel type vibrates larger than the series type vis-a-vis the same applied voltage and is used for transmission. On the other hand, the generated voltage becomes larger in a series type connection than the parallel type vis-a-vis the same vibration, and is used at receiving end.

As shown in Figure 3.10, institutions using parallel type benders (P) at transmitting end and series type benders (S) at the receiving end were the most. By using series type connection in parallel benders and parallel type connection in series benders, all the bender body can be compressed or extended together, thus enabling it to measure P wave velocity (Lings & Greening, 2001). As discussed later in Section 4.6, P wave velocity was measured by one of the institutions by using this principle.

In order to pass a shear wave into the specimen through BE and receive it from other end, it is necessary that BE penetrate into the specimen from either ends. There is no clear conclusion about the ideal penetration length. When the penetration is too long, it can disturb the specimen excessively. On the other hand, when it is too short, strength of shear wave may be too weak either in transmission or at reception. In addition, it is possible that near-field-effect is also affected by such changes in penetration length.

Figure 3.11 shows the average penetration length, L_c of benders into the specimen that was used by the participated laboratories (mean penetration length at specimen top and bottom). The length differs largely from institutions to institutions ranging from 1.2 to 14 mm, with the average of 6.0 mm. On excluding the relatively large penetration from Laboratory No.17, the mean value of penetration comes out to be 4.7 mm.

Figure 3.12 shows the variation of $2L_c/H$, depicting the proportion of penetration as compared to the specimen height, H. For the tests conducted, the range varied from 1.6 to 58% with a mean value of 17.5%. The mean value of penetration ratio in triaxial test apparatus and resonance method test comes out to be 8.6%. It became larger and reached 36% in a consolidation and shear test equipments whose specimen height is relatively low.

Table 3.4 Size and mounting of BE

Lab. No.	Apparatus	Dimension of BE					Material	Electrical connections		Lc. ave. mm	H mm	2Lc/H %
		Lt mm	W mm	t mm	Lc mm	tc mm		Transmitter	Receiver			
1	TX		10	1	2.5					2.5	200	2.5
2	TX		12	1.5	4.5					4.5	100	9
3	TX	13	12.5 12.6	1.6 1.8	3.2 3.6		PZT			3.4	80	8.5
4	OM	20	10	0.5	3		PZT			3	40	15
5	OM(TX)		12.5	0.51	10			Parallel	Series	10	50 90	40 22.2
6	TX	-	10	0.5	5	0.5	PZT	Parallel	Series	5	70	14.3
7	TX	13	10	0.5	7			Parallel	Series	7	150	9.3
8	TX		11	1.2	1.2					1.2	150	1.6
9	RC/TS	12.7	8	0.6	3.705	0.25	PZT	Series	Series	3.705	100	7.4
10	DS	13	10	0.5	7.27 6.98		PZT	Series	Series	7.125	70	20.4
11	TX		12	1.2 1.4	4.1 4.4					4.25	100	8.5
12	RC	12.7	10	0.5	4.9 3.3			Parallel	Series	4.1	110	7.5
13	TX	20	10	0.5	2		PZT			2	140	2.9
14	TX	12.7	10	0.5	4.575	0.25				4.575	100	9.2
15	OM TX	31.8	12.7	0.38	4	0.7	PZT	Parallel	Parallel	4	55 85	14.5 9.4
16	TX	20	5	1	8.8 9.4	0.25	PZT	Parallel	Parallel	9.1	100	18.2
17	DS	15	10	0.5 2	10.23 12.63	0.5	PZT	Parallel	Series	11.43	48	47.6
		15	10	0.5 2	10.23 17.62	0.5	PZT	Parallel	Series	13.925	48	58
		15	10	0.5 0.5	10.23 12.75	0.5	PZT	Parallel	Series	11.49	48	47.9
		15	10	0.5 0.5	10.23 17.15	0.5	PZT	Parallel	Series	13.69	48	57
		15	10	0.5 0.5	10.23 8.45	0.5	PZT	Parallel	Series	9.34	48	38.9
18	TX	20	10	3	2					2	140	2.9
19	TX	12.7	1.65	0.6	1.95					1.95	100	3.9
20	TX	20	10	0.65	3		PZT	Parallel	Parallel	3	100	6
21	TX	12 13	10	0.5	10.5 10.48	0.5	PZT	Parallel	Series	10.49	115	17.9
22	TX	20	10	0.5	5.95 6.30	0.5	PZT	Series	Series	6.125	70 100 150	17.5 12.3 8.2
23	TX	12	10	0.5	7.0 5.0	0.5	PZT	Parallel	Series	6	390	3.1

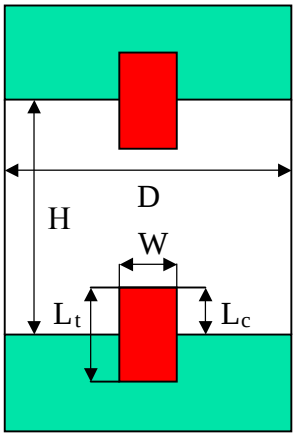

Fig. 3.8 Dimensions of BE

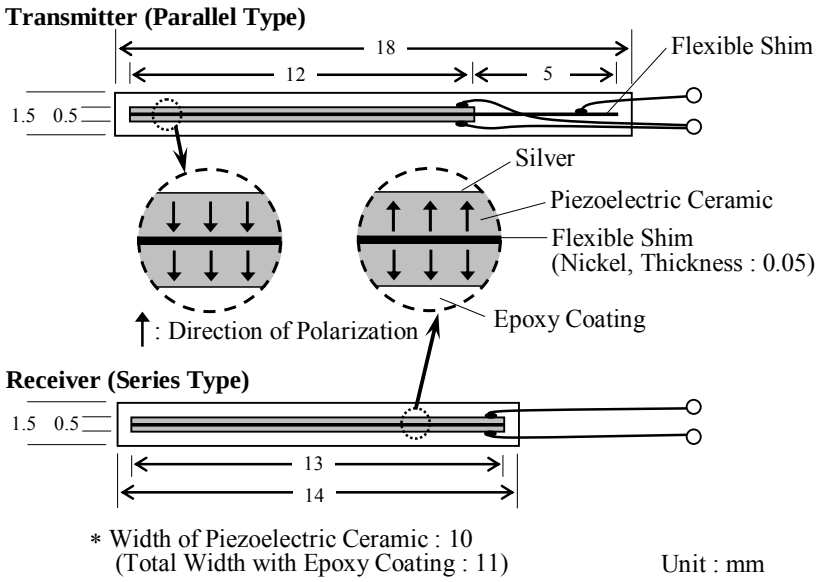

Fig. 3.9 An example of BE

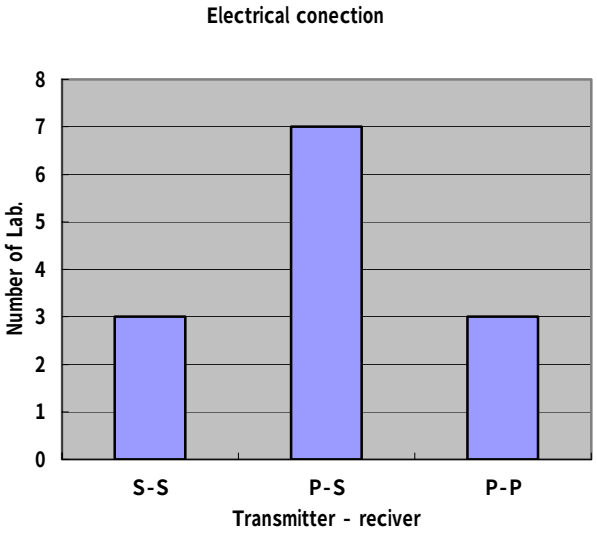

Fig. 3.10 Electrical connection of BE

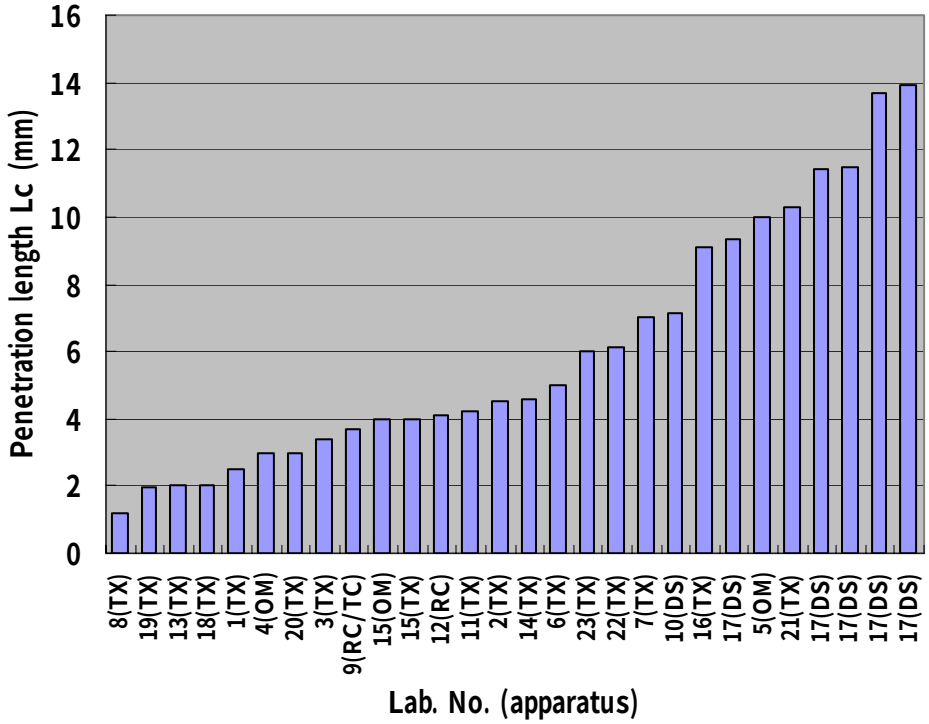

Fig. 3.11 Penetration length of BE

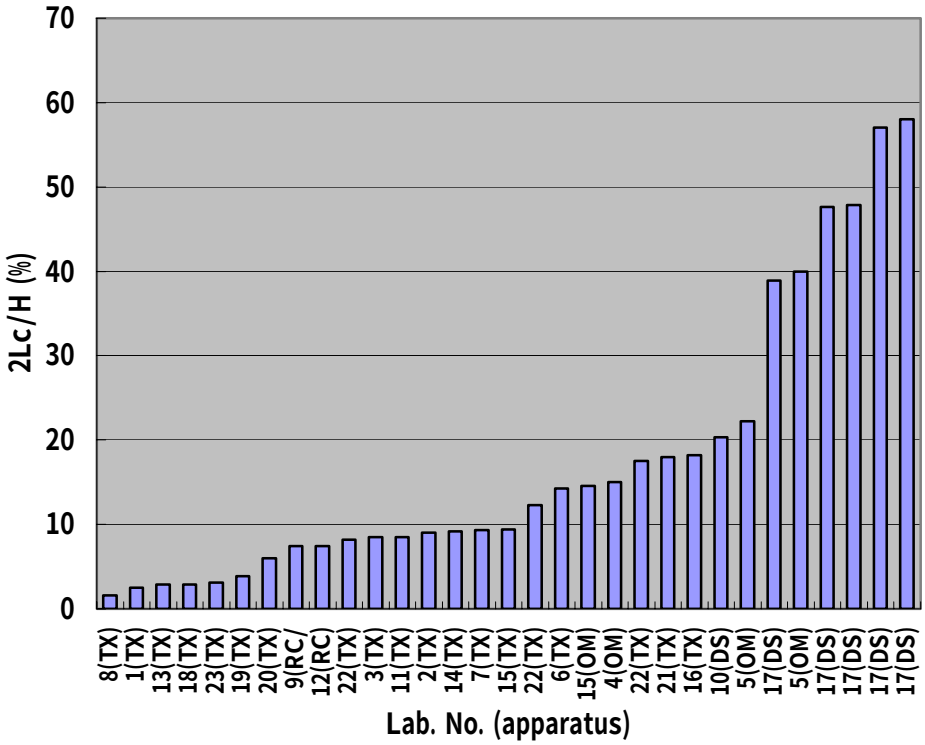

Fig. 3.12 2Lc/H

3.5 Identification of Travel Time

Table 3.5 shows the type of input wave and identification method of shear wave arrival time used by different institutions. In the test, shear wave velocity (V_S) is calculated from the simple measurement of propagation distance (Δs) and propagation time (Δt). It is thus a very simple test.

Regarding the propagation distance, except two institutions, which designated a distance between the central part of benders and the whole specimen height of sample as Δs, all other 21 institutions considered the tip-to-tip distance between bender pairs as Δs. Thus it is taken that there is consensus on the definition of Δs as the tip-to-tip distance between bender pairs. On the one hand, there was no such international consensus for the identification of arrival time of received wave. It differed at different tested institutions and is the main issue of discussion in BE test.

Currently, there are three different approaches in identifying the arrival time. The first one is by actually observing the transmission and received wave signal and finding their difference as a propagation time in the soil specimen. As this method uses a time base axis in order to identify the propagation time, this is often called as time domain technique (T.D.). With this method, when the distance between the bender pairs is short, received waves are often affected by near-field-effect disturbances that are believed to be the influence of P wave signals that reach before the actual shear waves. In addition, additional effects by other electric noises and reflections etc, often makes the reading of arrival time quite difficult. To separate the near-field-effect and noises, signal arrival is often observed by passing waves of different frequencies. In addition, measuring the time difference between the first peak of the transmission wave and the corresponding peak of received wave is yet another technique.

The second method is to calculate the cross-correlation (C.C.) between transmitted and received wave. This is based with the presumption that the transmitted shear wave retains its wave shape, i.e., frequency even when it is passed into the soil. In this method, C.C. of transmitted and the received wave is first evaluated and the position at the maximum amplitude is taken as propagation time. However, there are times when frequencies of transmitted and received waves do not agree and second peak or later at the received wave, rather than the first one, becomes larger in amplitude. In such condition, there needs an experienced person with a proper knowledge to interpret the correlated result and is a problematic aspect of this testing technique. Furthermore, as this method calculates arrival time using the time base axis, it is often said to be identical to T.D. The third method calculates the cross spectrum of the transmitting and receiving waves producing the relations of amplitude and phase angle with frequency axis. The arrival time is then calculated from the inclination of phase spectrum. As it uses the frequency characteristics of input and output waves, it is often called as frequency domain technique (F.D.).

At the early days when BE was used, shear wave velocity was calculated based on the travel time of a square wave signal and considering the time to the first peak of the received wave as a propagation time (e.g. Dyvik & Madshus 1985). But, considering the fact that a square wave is simply a summation of number of sine waves of various frequencies, it was considered to use sine wave input that has single frequency. Because of the difficulty in identifying arrival time due to the influence of aforementioned near-field-effect, C.C. method was proposed as a better alternative by some researchers (e.g. Viggiani & Atkinson 1995). Identification of signal arrivals with frequency domains is discussed in Greening & Nash (2004).

Figure 3.13 shows the identification method used in defining propagation time for this study. There are laboratories which used multiple methods but T.D. technique was most commonly used. Regarding the input wave shape in T.D. method, 10 laboratories used only the sine wave, 3 laboratories used only the rectangular wave and 5 laboratories used both types. Thus 15 out of 18 laboratories were using sine wave input for their study.

For C.C. method, using sine wave input is general because of the need to calculate cross-correlation function of the transmitted and the received wave. One of the laboratories used continuous sine wave signal modified with PRBS (Pseudo Random Binary Sequence). In case of F.D. method, in order to obtain the frequency characteristic of the transmitted and received wave, either the sweep or the continuous signal of sine wave was applied. Besides, there were two institutes which did not report identification method.

Regarding the voltage for the input signal, the institutes which used ±10V were the most. A few of the laboratories used voltage amplifier to magnify the input voltage and it was as high as ±50V at the maximum. Relating the frequency for the test cases using sinusoidal input wave and considering T.D. method, 5 institutes used single frequency input wave under the same consolidation conditions but 9 others varied the input frequency.

Figure 3.14 shows the identification method of propagation time being followed by the laboratories following T.D. method of defining arrival time. The time difference between the starting point of the transmitted wave and the corresponding point in received wave (start-to-start: S-S) has been considered as the propagation time by 13 institutes whereas, time difference between the peak point of the transmission wave and the corresponding peak in received wave (peak-to-peak: P-P) is considered by two institutes. Besides, there were records by three other institutes which observed the definition of arrival time by considering different points in the received wave.

It is to be noted that accurate arrival point is not understood correctly from the received wave if the sampling interval is too large. Table 3.4 shows the sampling interval of the wave data reported by different institutes. For example, in case of dry sand having propagation velocity, V_S of 250 m/sec (80% relative density, i.e., ρ_d=1.553 g/cm^3 & G_{max} =97 MPa) and propagation distance, ΔS of 100 mm, propagation time (Δt)=0.1/250 sec = 400 μs. To read the arrival time in the order of 1% accuracy, the sampling interval should be at least 4 μs. When the frequency of received portion of wave becomes as high as 10 kHz, as an example, reading 100 points per wave needs the accuracy of 1 μs. Although actual sampling interval also depends upon the travel distance of shear wave signal, it is expected that interval lies within a single digit. Among the intervals shown in Table 3.4, there are cases which used 10 sec or more time interval. There is a need for the participated laboratories to increase the sampling speed, in order to increase the precision in identifying the true received signal.

In this way, although various methods were adopted for the identification of propagation time by different institutes, time difference between the start of transmitted and received wave (start-to-start, S-S) was mostly used by using single cycle of sinusoidal wave and considering the influence of near-field-effect by passing waves of different frequencies.

Table 3.5 Input wave and identification method of travel time

Lab. No.	Apparatus	Wave shape	Input V ±V	Frequency kHz	Identification of Travel Time			Δs	Data time Inter. μs
					Time domain	Cross-correlation	Frequency domain		
1	TX	sin pulse	5	5-10	start-to-start			tip-to-tip	10
		rect. pulse	5	5-10					
2	TX	rect. pulse	15-25	5(10)	start-to-start			mid.-to-mid.	0.1-0.5
3	TX	sin pulse	10	4-10		○	unit-inpuls response frequency response	tip-to-tip	-
4	OM	sin pulse	10	15 (20,30)	peak-to-peak			tip-to-tip	1-10
5	OM(TX)	sin pulse	10	15	plural points with S-S	○		tip-to-tip	10
		sin sweep	10	1.5-20			ABETS		
6	TX	rect. pulse	10	-	start-to-start			tip-to-tip	12
7	TX	sin pulse	20	4	start-to-start			tip-to-tip	2
8	TX	sin pulse	5	10		○		tip-to-tip	10
9	RC/TS	sin pulse	10	11-15	start-to-start			tip-to-tip	0.5
		rect. pulse	10	0.6-15					
10	DS	rect. pulse	10	0.027	peak-to-peak			tip-to-tip	0.25
11	TX	sin pulse	10-30	5-15	start-to-start	○		tip-to-tip	2
12	RC	sin pulse	10	15	?			tip-to-tip	-
13	TX	sin pulse	10	10-20	start-to-start			tip-to-tip	2
14	TX	sin pulse	10	15	?			base-to-base	-
15	OM	sin pulse	10	55(60)	start-to-start			tip-to-tip	0.04
	TX	sin pulse	10	10(-20)					0.1-0.2
16	TX	sin pulse	10	1.5(-10)	start-to-start			tip-to-tip	1-5
17	DS	sin pulse rect. pulse	10	0.1-10	plural points with S-S			tip-to-tip	2.5
18	TX	sin pulse	10	2-8	start-to-start			tip-to-tip	0.4-12
		sin cont.	10	5-27			π-point (Lissajous)		
		sin sweep	10	5-19			ABETS		
19	TX	sin pulse	-	-	start-to-start			tip-to-tip	0.4
20	TX	sin pulse	10	2.7-33	plural points with S-S			tip-to-tip	1
		rect. pulse	10	0.005					
21	TX	sin pulse	20	5-20	start-to-start			tip-to-tip	0.1
		rect. pulse	20	0.1					
22	TX	sin pulse	10-50	5-20	start-to-start			tip-to-tip	0.5-1
23	TX	PRBS	25	4		○		tip-to-tip	15

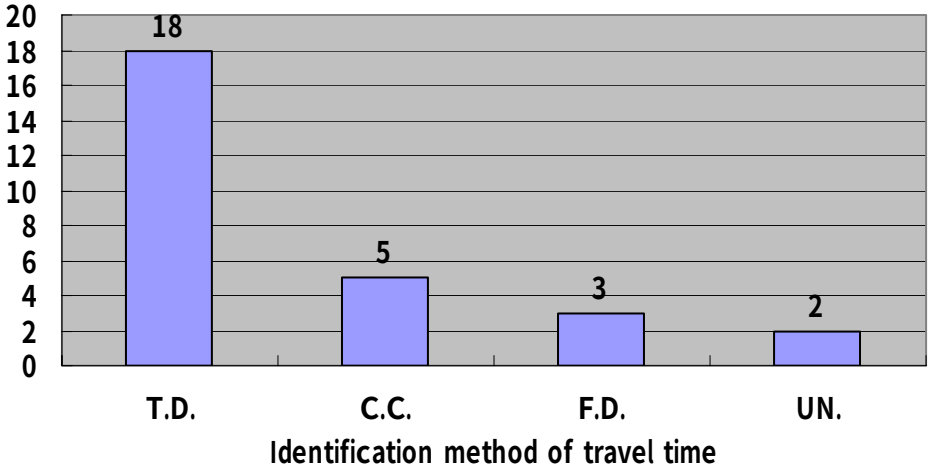

Fig. 3.13 Identification of travel time

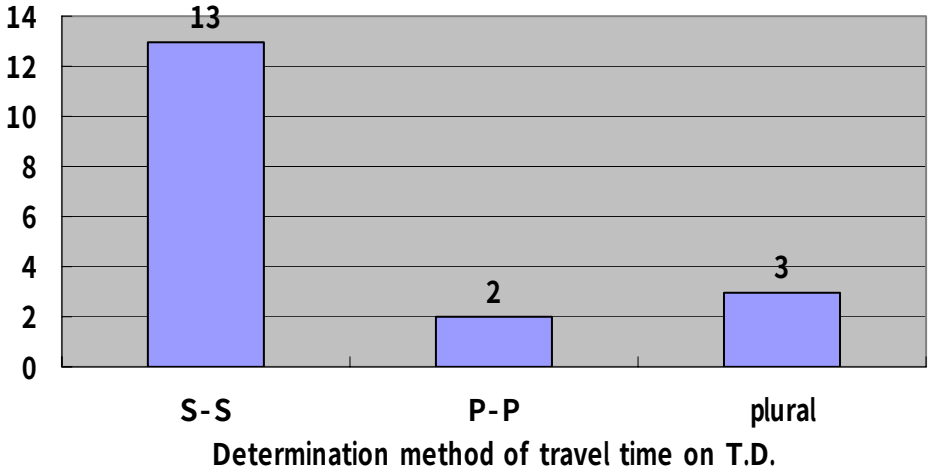

Fig. 3.14 Identification of travel time (time domain)

4. TEST RESULTS

4.1 Relations between G_{max} and e

Figures 4.1 to 4.3 show the relation between shear modulus, G_{max} and void ratio, e for isotropically consolidated specimens ($K=\sigma_h'/\sigma_v'=1.0$), anisotropically consolidated specimen with K=0.5 and K_0 consolidated specimen at the vertical stress, σ_v' of 50, 100, 200 and 400 kPa. In the figures, results of saturated specimens as well as dry specimens are shown collectively. A solid line in each plot shows the relation between G_{max} and e at the shearing strain of 10^{-6} and at different confinements (Iwasaki & Tatsuoka, 1977). The relation was obtained from the test performed in a resonant column apparatus by using a clean sand of very small U_C, similar to the Toyoura sand.

The result (Fig. 4.1) for the specimen at isotropic consolidation (IC) shows that an increase in isotropic stress narrows down the amount of scatter in the data. Furthermore, the scatter in test data is large for dry specimens than the saturated ones. Figure 4.2, showing the plot for anisotropically consolidated specimen, also shows the very similar trend of the decrease in scatter at higher stress and when saturated as discussed above for an isotropic case. On the other hand, Figure 4.3 that plots the results for K_0-consolidated specimens shows a very large variation in the value of G_{max} for dry specimens.

Figures 4.4 and 4.5 are prepared for the G_{max} vs. e relation by considering the consolidation condition (K values) for saturated and dry specimens respectively. Figure 4.4 shows that the results from saturated samples have comparatively smaller scatter and their scatter magnitude is indifferent to the K-value. The data scatter becomes relatively large when the results of the dry specimen are plotted (Fig. 4.5).

The above discussion, based on the plots of entire data, shows that data scatter varies depending upon the test condition, especially, when the specimen is dry and for K_0-consolidated specimens that are performed in a stiff metal containers and comparatively smaller travel length. The following could be some of the several reasons for these variations:

As explained in Section 3.5, the arrival time identification method differed at each of the laboratories who performed the tests. For example, in a T.D. method that measures the arrival position of the shear wave from the received signal, various groups assumed different points in the received wave as the true arrival position and calculated the G_{max} values accordingly. In this way, calculated G_{max} value was different even for the identical specimens and prepared in the same laboratory. In addition, one can expect very large effect of time definition in the result of G_{max} value when the travel path through the soil specimen is smaller, such as for K_0 consolidation tests and direct shear apparatus. Furthermore, even when the start-to-start definition has been considered as the arrival time, the exact location considered for the wave arrival in a received wave differed among the testing group. When asked with an example of received wave, such as in Figure 4.6, the reading point varied from A, B, & C depending upon the participating teams.

At such circumstances, it can be well envisaged that the scatter, such as observed in Figs. 4.1 to 4.3, is not actually the real scatter of the bender element test. In order to show the actual waveform variation, the data from laboratories, which performed the experiments by using single pulse sine wave as an input and have submitted time history of both input and received waves, are extracted below for an illustration.

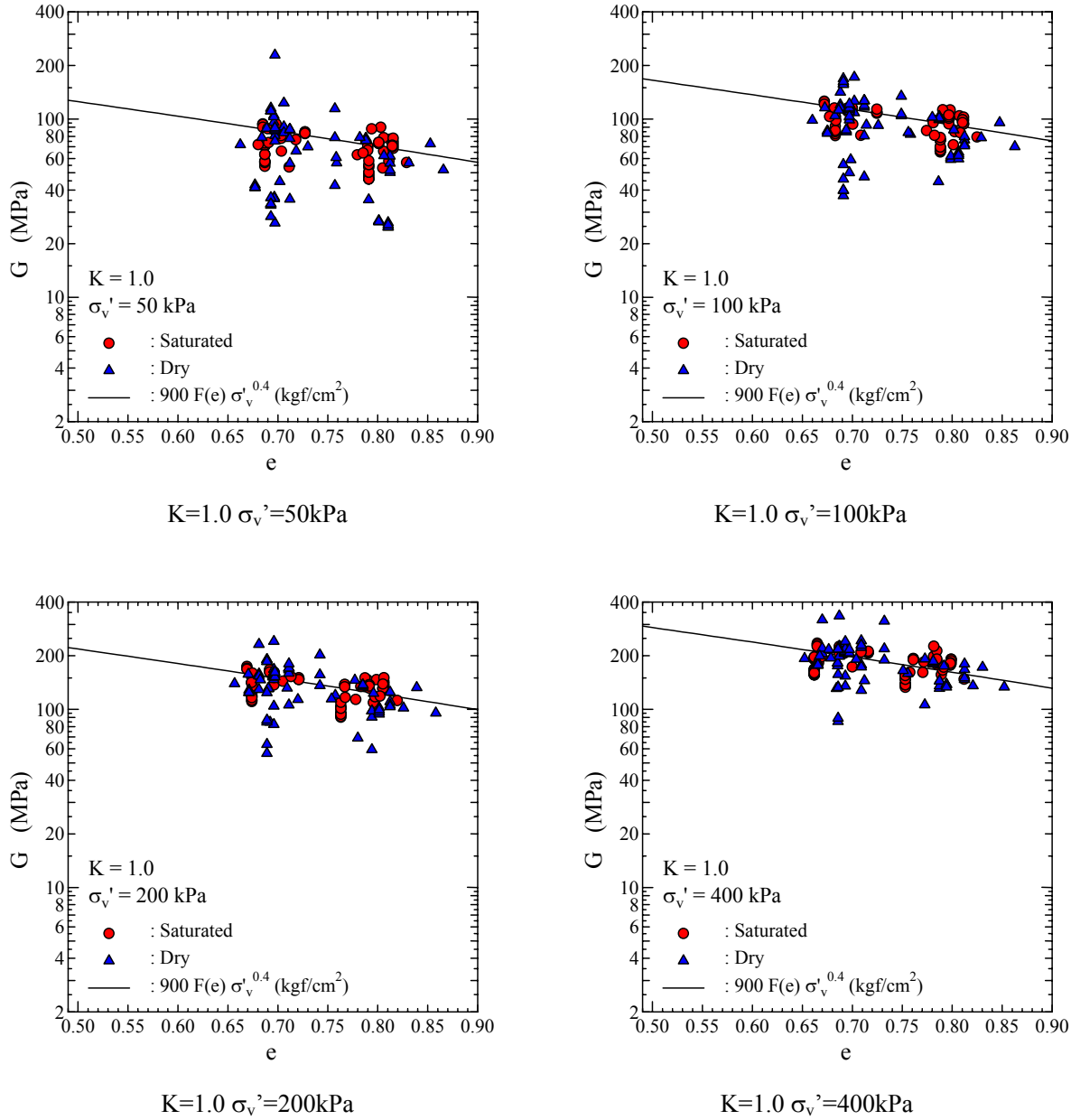

Fig. 4.1 Relations of G and e (isotropic consolidation)

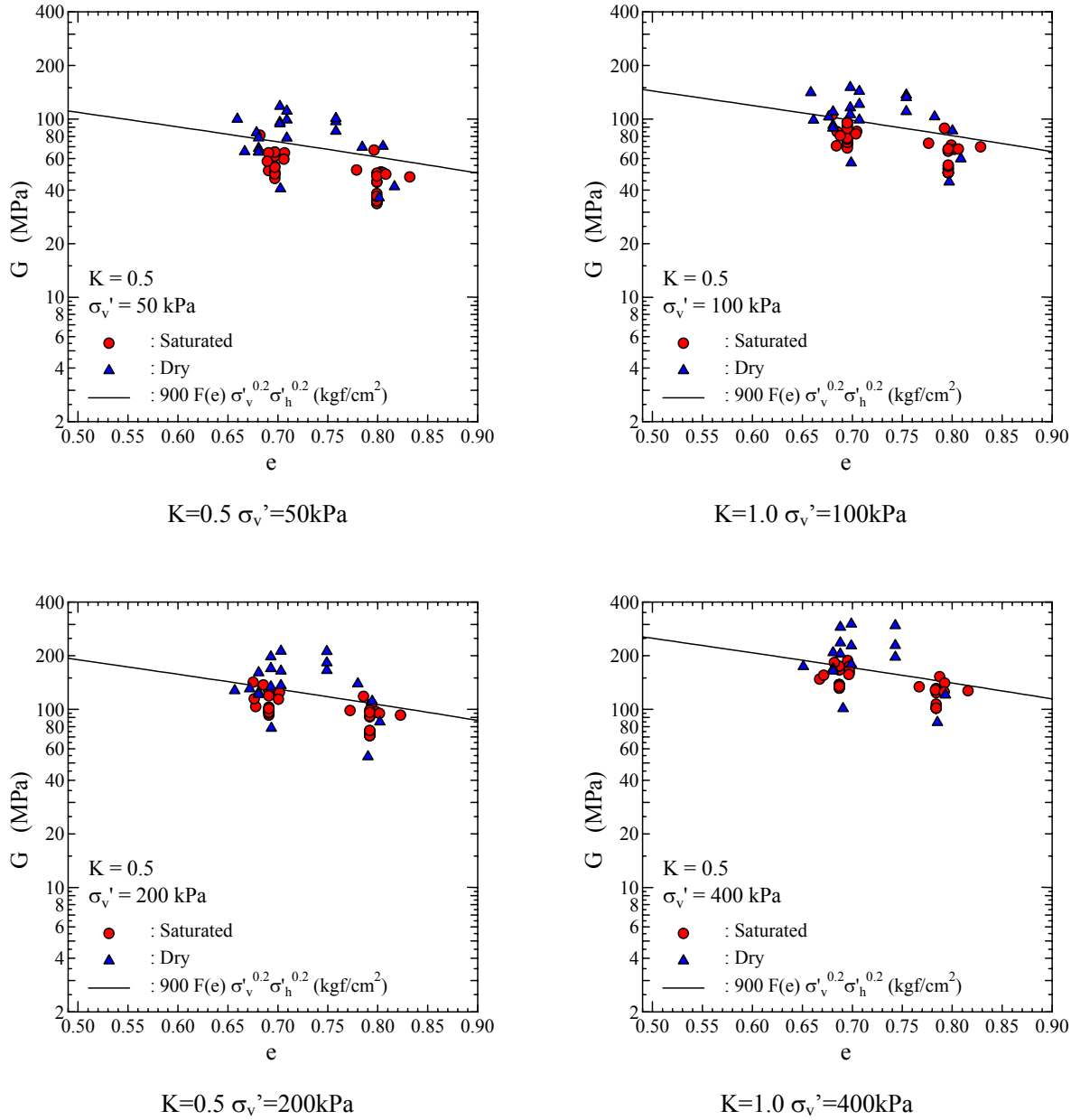

Fig. 4.2 Relations of G and e (K=0.5)

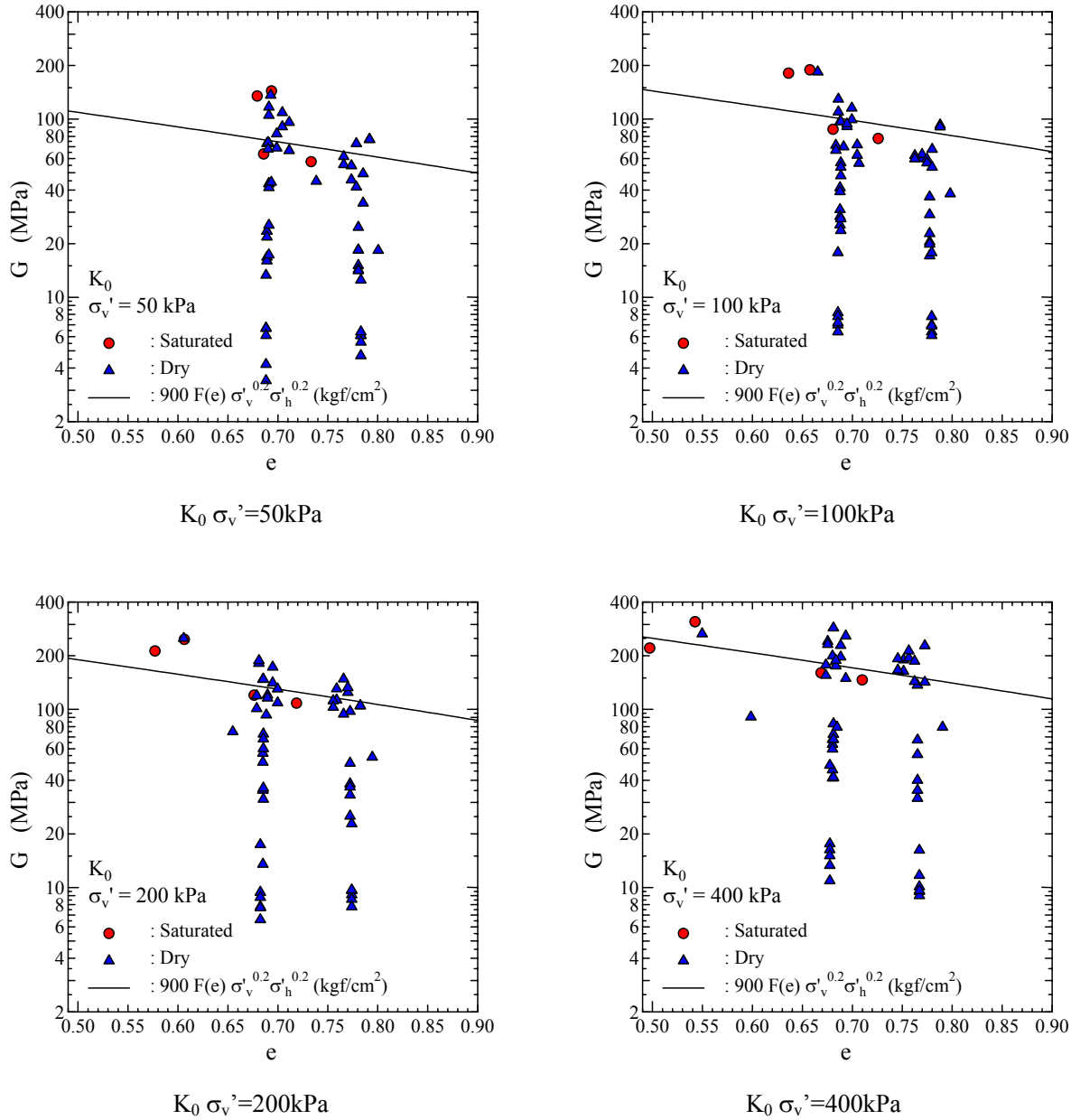

Fig. 4.3 Relations of G and e (one-dimensional K_0 consolidation)

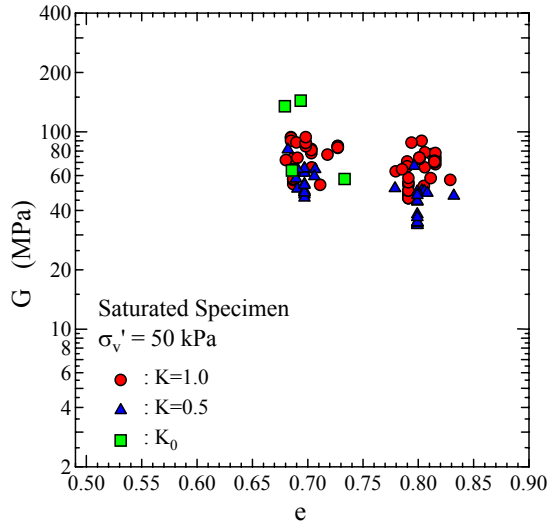

Saturated Specimen σ_v'=50kPa

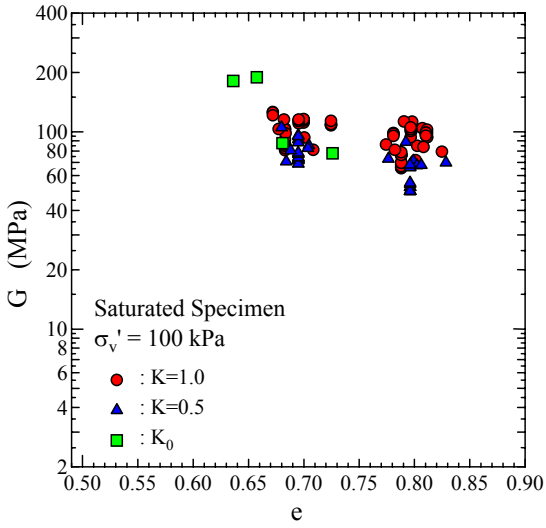

Saturated Specimen σ_v'=100kPa

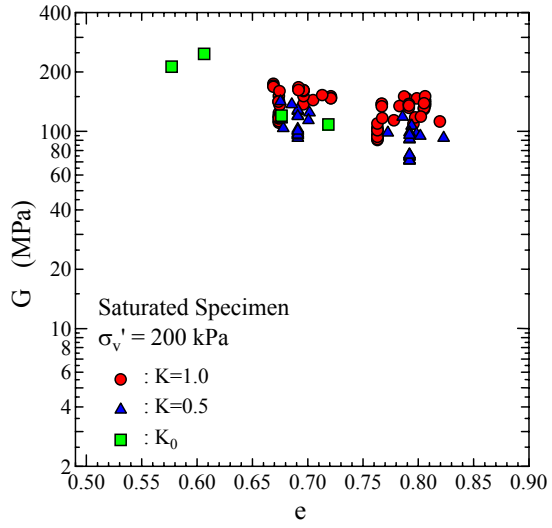

Saturated Specimen σ_v'=200kPa

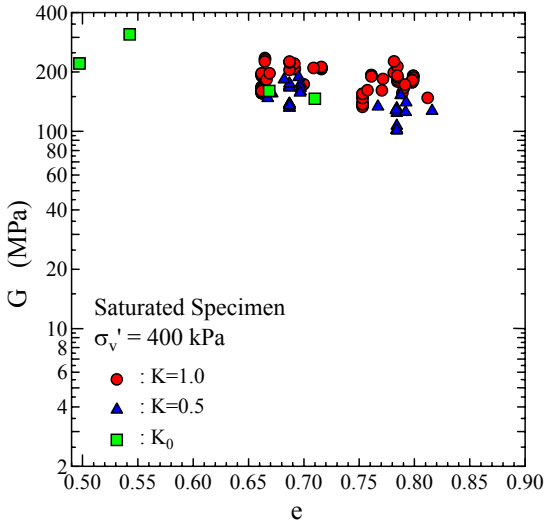

Saturated Specimen σ_v'=400kPa

Fig. 4.4 Relations of G and e (saturated specimens)

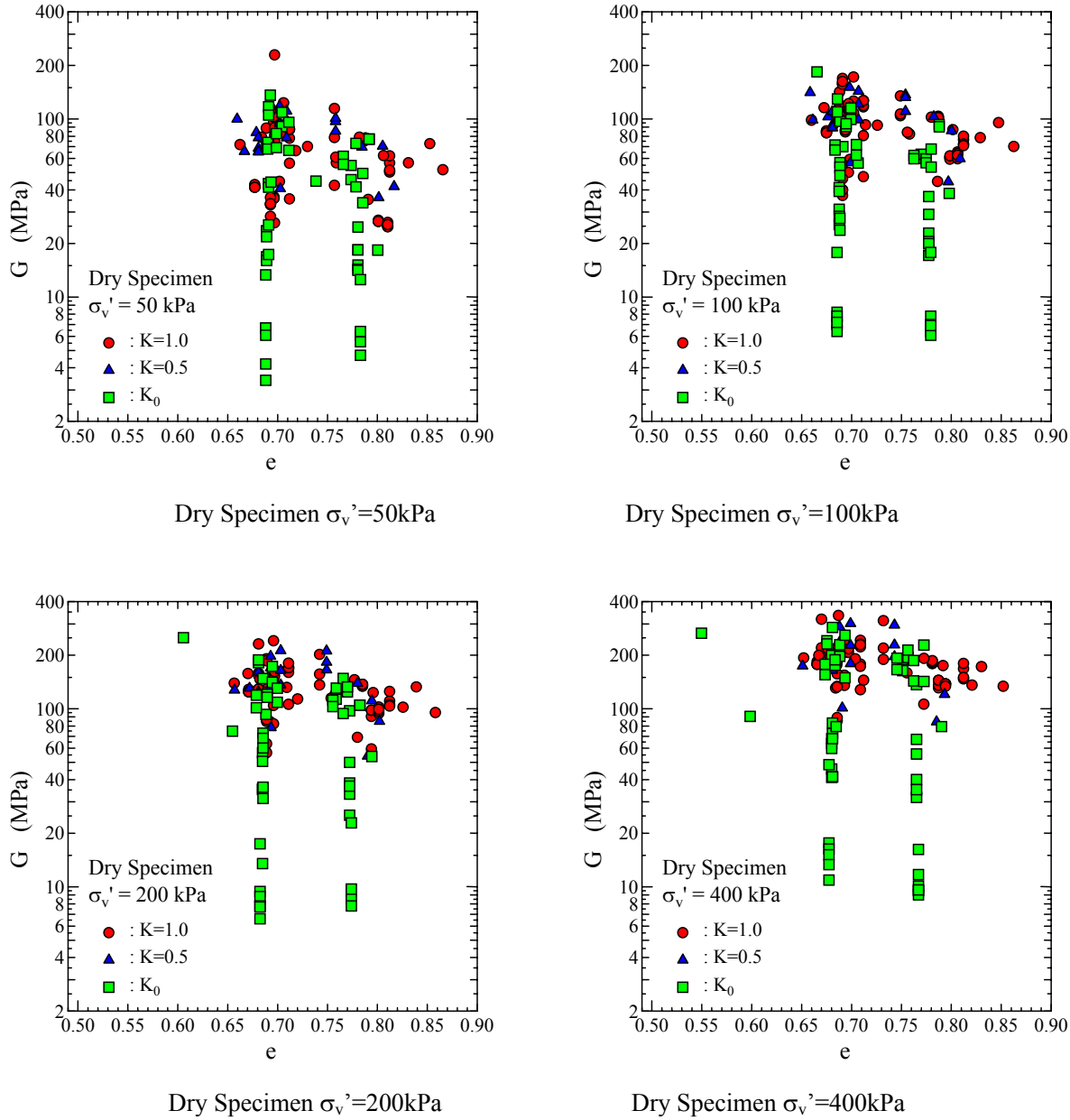

Fig. 4.5 Relations of G and e (dry specimens)

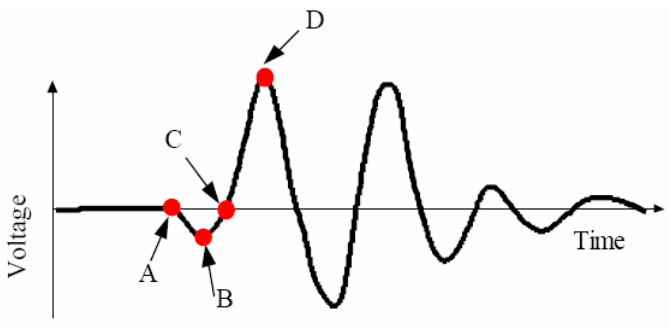

Fig. 4.6 An example of arrival point

4.2 Wave Data

Figure 4.7 to 4.14 show the received waveform obtained from the single cycle sine wave input for isotropically consolidated specimens at the confinement of 200 kPa. Figure 4.7 shows the data for saturated specimen at D_r=80%. In this figure, the time based lateral axis of the wave has been normalized with the respective tip-to-tip distance of benders for comparison. The horizontal axis thus becomes the inverse of shear wave velocity. The received waveforms are representative samples of different participating teams. The vertical arrow sign (↓) in the wave indicates the point which was considered as the shear wave arrival time by them. It can be noticed that the arrival point falls inside a relatively narrow band.

Figure 4.8 shows data for saturated specimen at D_r=80%. Normalization of horizontal axis and the width of the result band are quite similar to Figure 4.7. In both figures, the first peak in the wave from Laboratory No.09 is rather on the left as compared with others. In other words, G_{max} values for this case is comparatively larger than others. It is considered that such discrepancy comes from a smaller B value. On the other hand, the result of Laboratory No.02 lies on the right than others when square wave was used.

Figures 4.9 & 4.10 include the data for saturated specimens of relative densities, 80% & 50% as plotted in Figs. 4.7 & 4.8 respectively. In the plots, the horizontal axis in Figs. 4.7 & 4.8 are further normalized with a parameter, $(\rho_t/f(e))^{0.5}$, where, ρ_t =wet density, $f(e) = (2.17-e)^2/(1+e)$. In other words, the inverse of the square of the function plotted in horizontal axis takes the form of $G_{max}/f(e)$ (kPa). As shown in the figures, void ratio of the prepared samples differs among different laboratories. It is therefore, considered that introduction of void ratio function would eliminate the error introduced by the void ratio difference. Comparatively narrower scatter band width in Figs. 4.9 and 4.10 confirms this assumption. This means that if the wave reading is taken by following start-to-start method, the accuracy within the band width is ascertained. If converted into G_{max} value, the expected range is from 90 to 135 MPa.

Figure 4.11 & 4.12 show the result for dry specimen having respectively, 80% and 50% relative density. Very similar to Figures 4.7 and 4.8, the horizontal axis of the wave data has been normalized with the respective tip-to-tip distance of benders for comparison. The vertical arrow sign (↓) in the figures shows the reading considered by the respective laboratories. Excluding the result from Laboratory No. 16, the data lies in a narrow vertical band shown in the figure. The reason for such a large difference in the result of Laboratory 16 could be due to relatively smaller frequency of 1.5 kHz and low resolution of measuring equipment used in data reception. When compared with Figure 4.11, the result band in Figure 4.12 becomes a little wider but the reason may lie on the relatively larger scatter in void ratio values for samples at D_r=50%.

Figures 4.13 & 4.14, which include the data shown in Figs. 4.11 & 4.12, are redrawn with the axes similar to Figs. 4.9 & 4.10 discussed earlier. As the function $f(e)$ balances the effect of difference in void ratio in the tested specimens, the band width showing the range of the received wave arrival points becomes narrower as compared to Figs. 4.11 and 4.12. When compared between Figs. 4.13 and 4.14, one can easily notice that a band showing the scatter in result is larger with D_r=50% samples. The $G_{max}/f(e)$ values for Figs. 4.13 and 4.14 fall in the range of 93.6 to 126.0 MPa and 87.3 to 135.5 MPa, respectively. In both plots, it is understood that result from Laboratory No. 16 is substantially out of the range.

In summing up above discussions, if start-to-start method is considered for arrival time definition, the accuracy in getting G_{max} by using bender element test falls in a narrow range, indifferent of whether the tests are performed in dry or saturated condition.

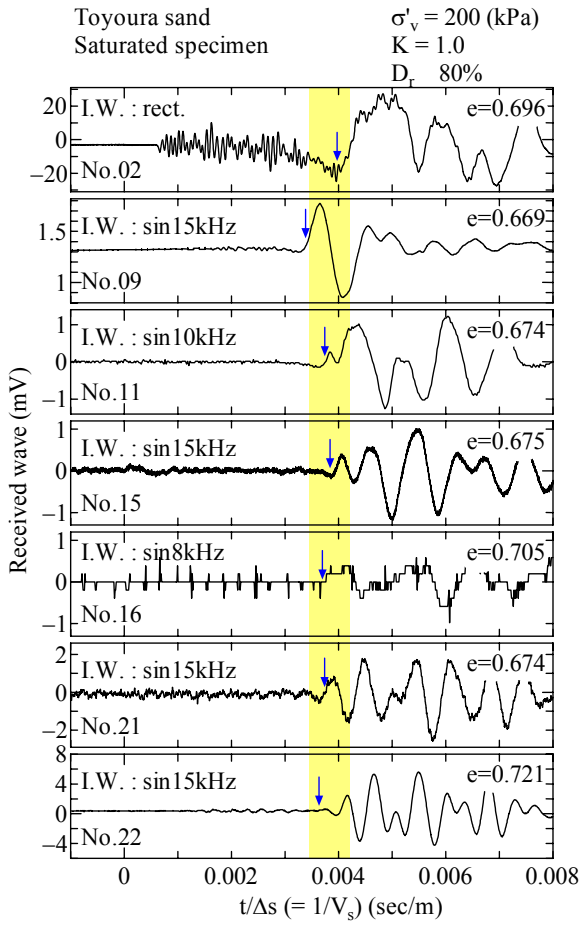

Fig. 4.7 Examples of wave data
(Saturated specimens, K=1.0, Dr=80%)

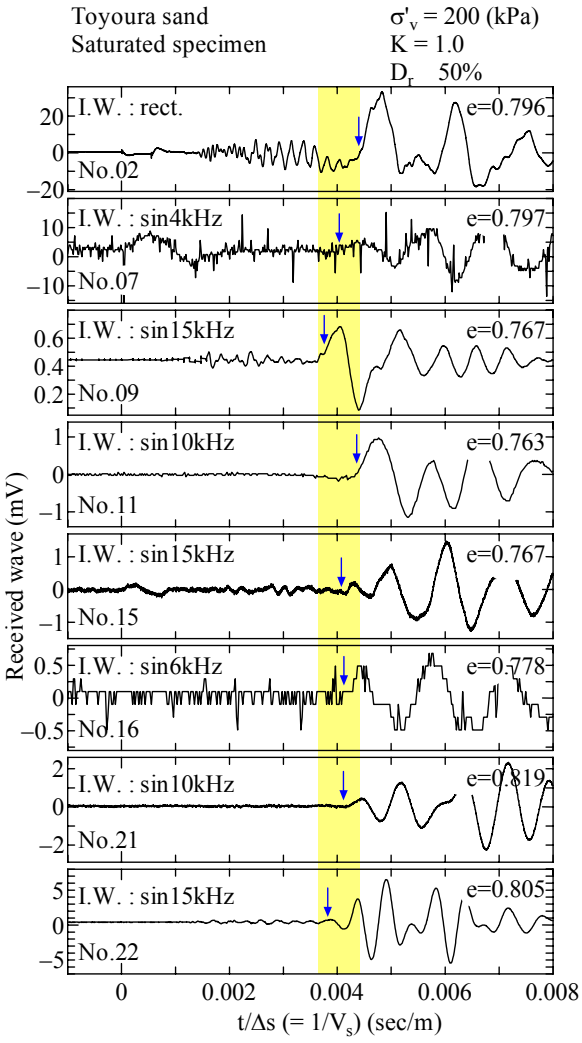

Fig. 4.8 Examples of wave data
(Saturated specimens, K=1.0, Dr=50%)

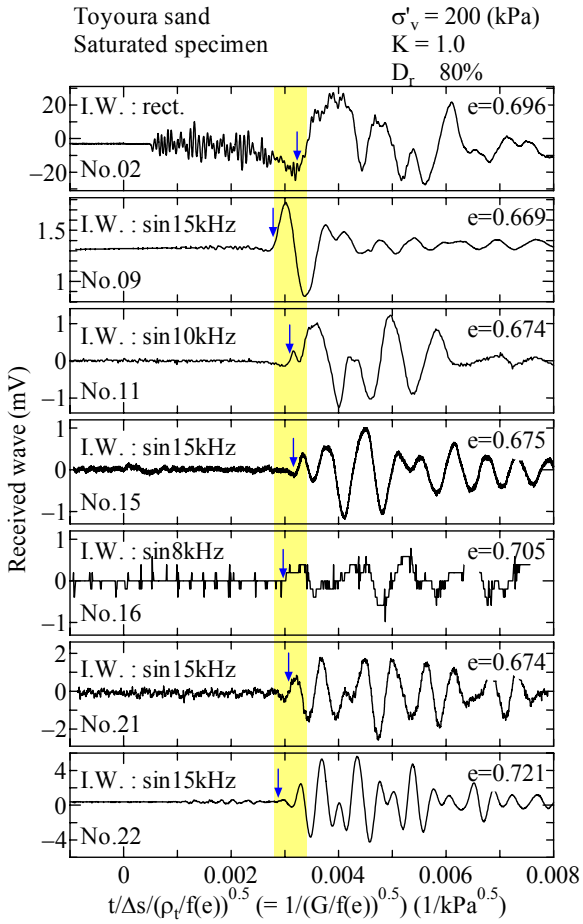

Fig. 4.9 Examples of wave data
(Saturated specimens, K=1.0, Dr=80%)

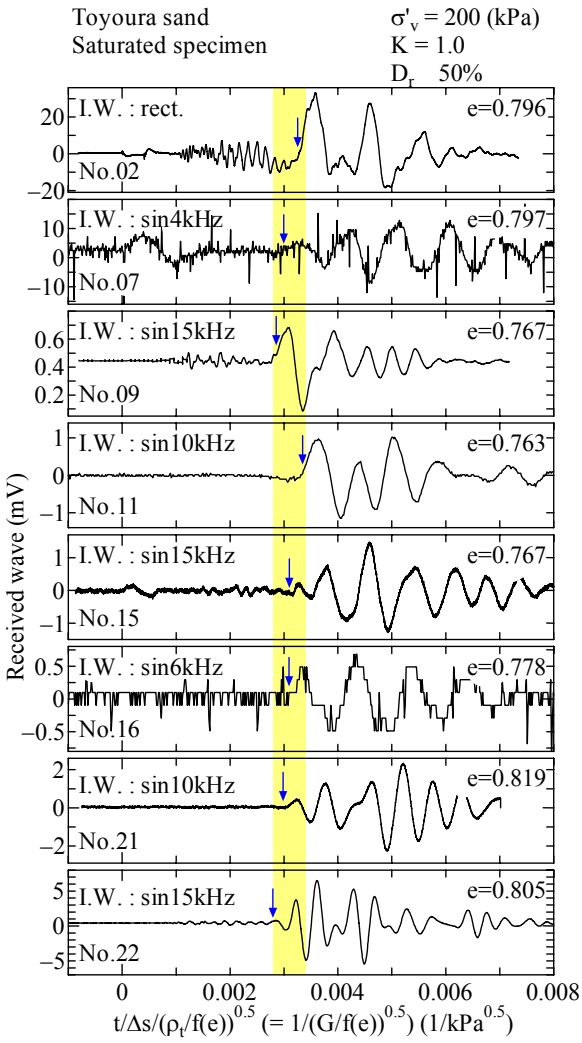

Fig. 4.10 Examples of wave data
(Saturated specimens, K=1.0, Dr=50%)

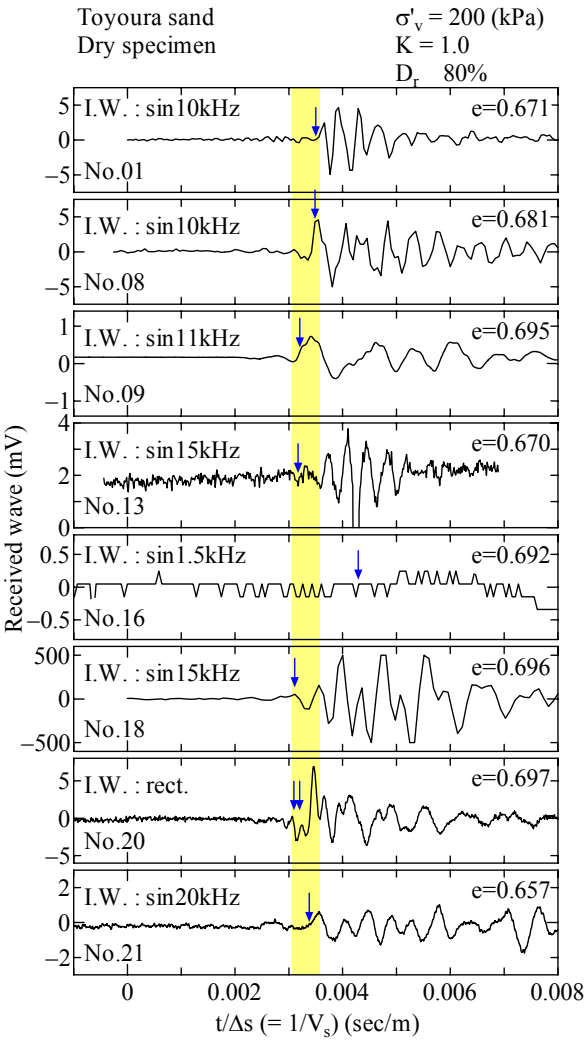

Fig. 4.11 Examples of wave data
(Dry specimens, K=1.0, Dr=80%)

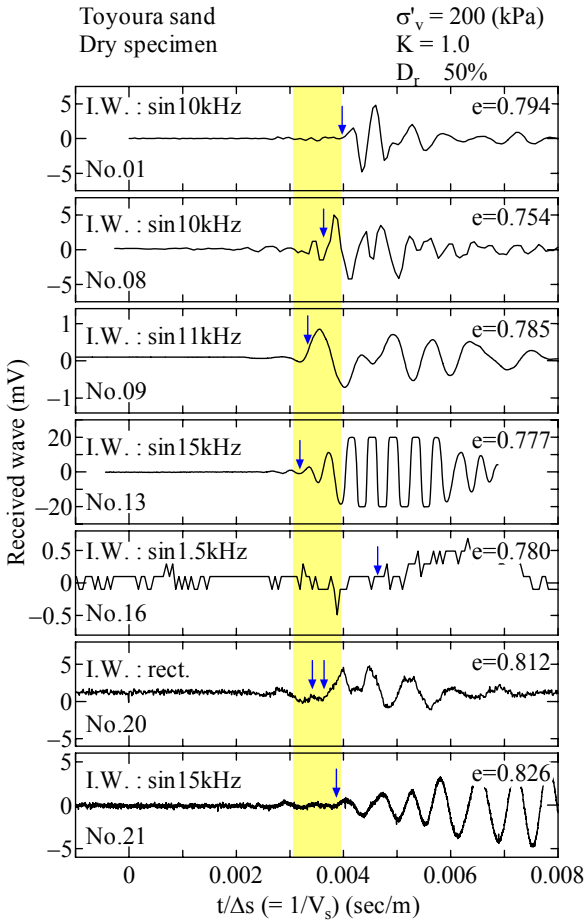

Fig. 4.12 Examples of wave data
(Dry specimens, K=1.0, Dr=50%)

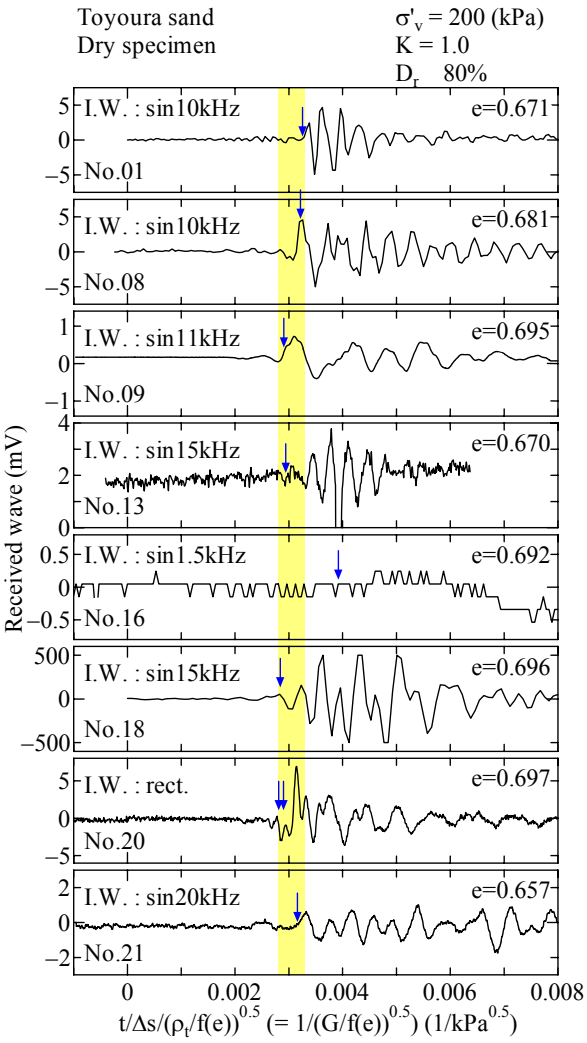

Fig. 4.13 Examples of wave data
(Dry specimens, K=1.0, Dr=80%)

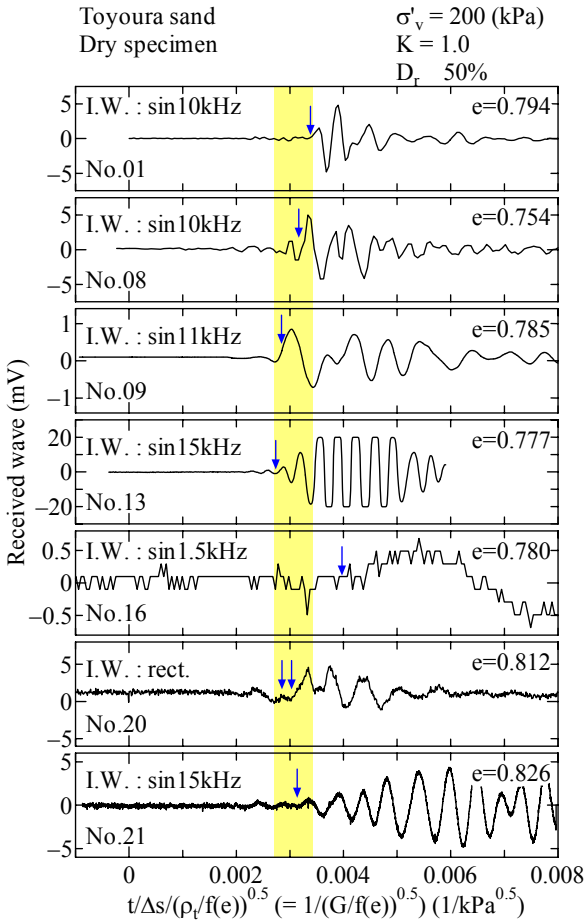

Fig. 4.14 Examples of wave data
(Dry specimens, K=1.0, Dr=50%)

4.3 Effect of Some Factors on Test Result

4.3.1 Effect of arrival time identification method

If the data reported from all laboratories were plotted, a large variation in G_{max} value, such as discussed in Section 4.1 was noticed. The following reasons are believed to be the main factors for such variations:

i) Method of arrival time identification differed with each laboratory.
ii) Even for the same identification method, reading points differed with laboratory.
iii) Some laboratories even considered multiple points in the received wave as arrival time and calculated multiple values of G_{max}.

On the other hand, when actual received wave was compared as discussed in Section 4.2, large variation did not exist. Therefore, comparison of the test results was done as hereunder, based on the difference in arrival time identification method.

Figure 4.15 plots the relationship of G_{max} vs. e at 200 kPa for isotropically consolidated (IC) specimens by using the data submitted from testing laboratories. The data points, which used the start-to-start identification method, were picked up and plotted in Figure 4.16. The solid line in the figure shows the relationship of G_{max} =900 f(e)σ_v'$^{0.4}$ (kg/cm^2) (γ=10^{-5}) and the dashed line, G_{max} =850 f(e)σ_v'$^{0.44}$ (kg/cm^2) (at γ=10^{-6}) (Iwasaki and Tatsuoka, 1977). The following points are noted from these figures:

1) Start-to-start method of identification results in a relatively smaller variation as compared with other methods. The data points also match well with the relations obtained independently in the past researches.
2) Peak-to-peak and Cross-correlation methods yield slightly smaller values of G_{max} as compared with start-to-start method.
3) It seems that G_{max} values are not affected by the saturation condition but larger scatter were found in the results for dry specimens.

Figure 4.17 plots the G_{max} vs. e relationship reported from different laboratories for anisotropically consolidated samples at K=0.5 and K_0-consolidated samples performed in a stiff metal containers when vertical stress was 200 kPa. Figure 4.18 is prepared by excluding K_0-consolidated test data from Fig. 4.17. Tests for K=0.5 and K_0-consolidated tests for which start-to-start has been taken as the definition of arrival time are plotted in Figure 4.19. Other data remaining the same, Figure 4.20 was redrawn from Figure 4.19 by removing the data from Laboratory No. 5. The following trends of behavior are observed from these figures:

1) G_{max} values obtained from K_0-tests, where specimens were put inside a stiff metal container, are relatively smaller and have large scatter than other results.
2) Results from anisotropically consolidated tests (K=0.5 & K_0) are relatively largely scattered as compared with isotropically consolidated tests.
3) Very similar to the isotropic specimens, G_{max} values from anisotropic tests calculated by defining arrival time with start-to-start method has comparatively smaller scatter. Besides, the data points are very close to the solid lines shown in the figure.

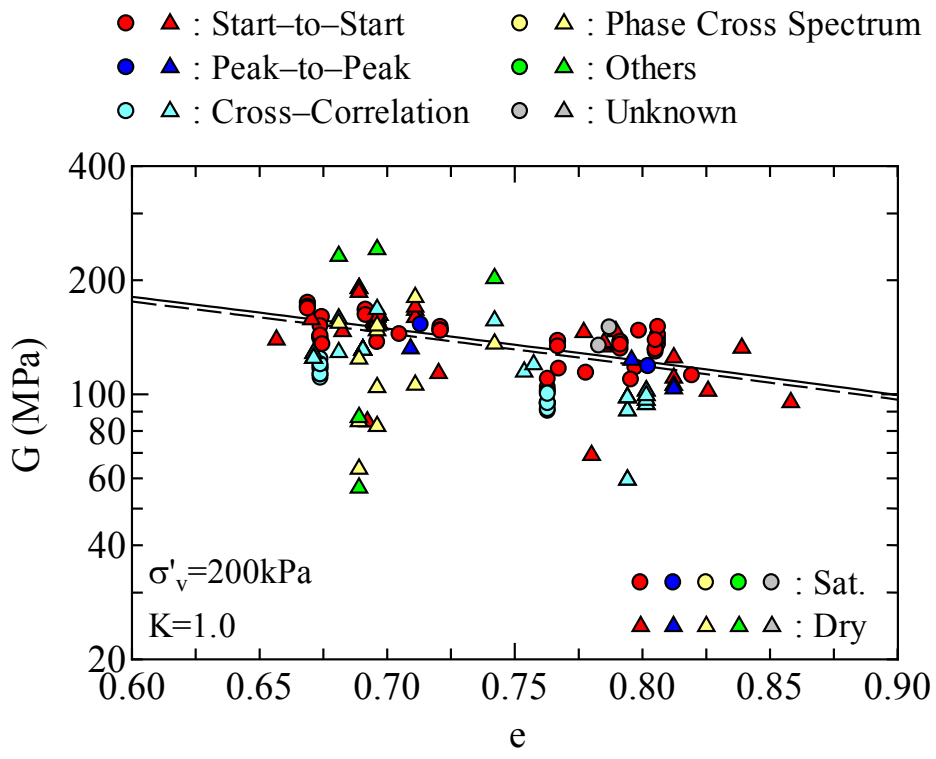

Fig. 4.15 Effect of identification method of travel time (isotropic consolidation)

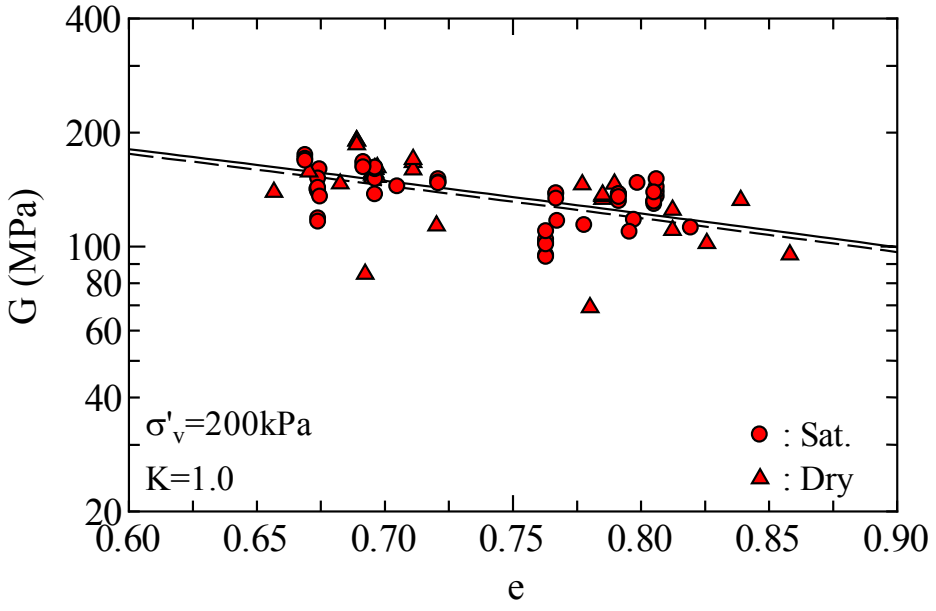

Fig. 4.16 Effect of identification method of travel time (isotropic consolidation, start-to start)

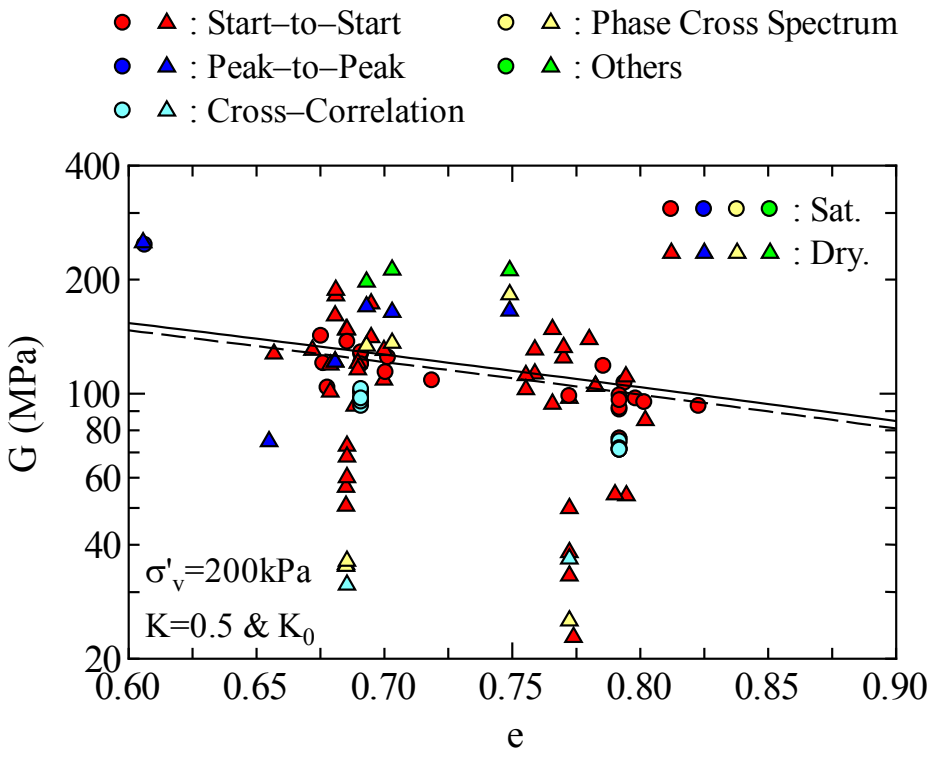

Fig. 4.17 Effect of identification method of travel time (K=0.5, K_0 consolidation)

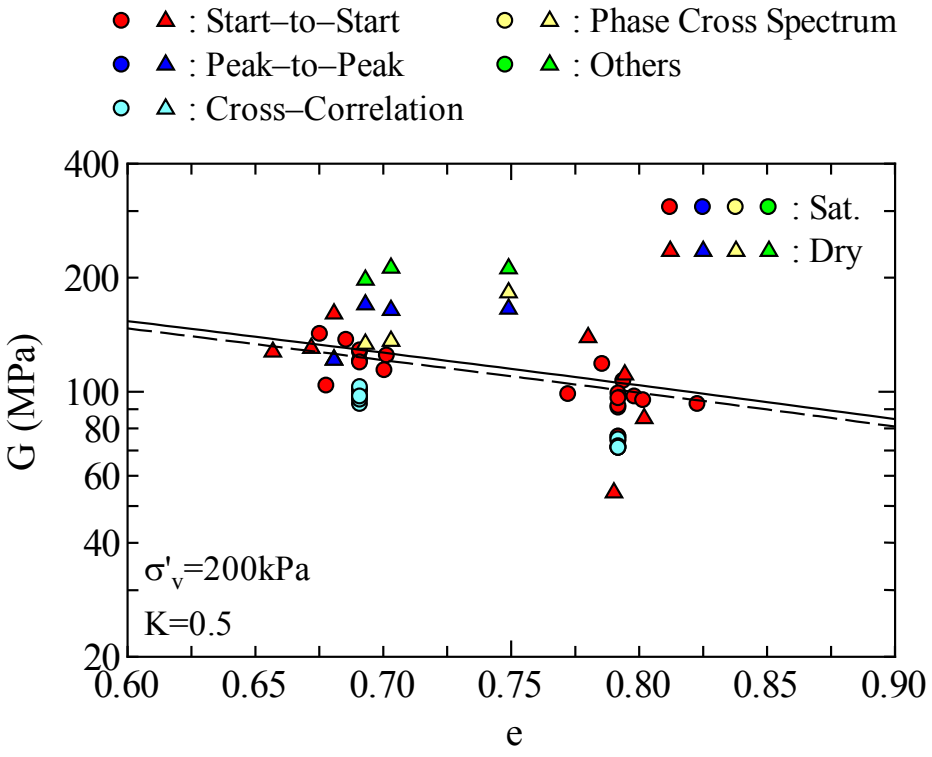

Fig. 4.18 Effect of identification method of travel time (K=0.5)

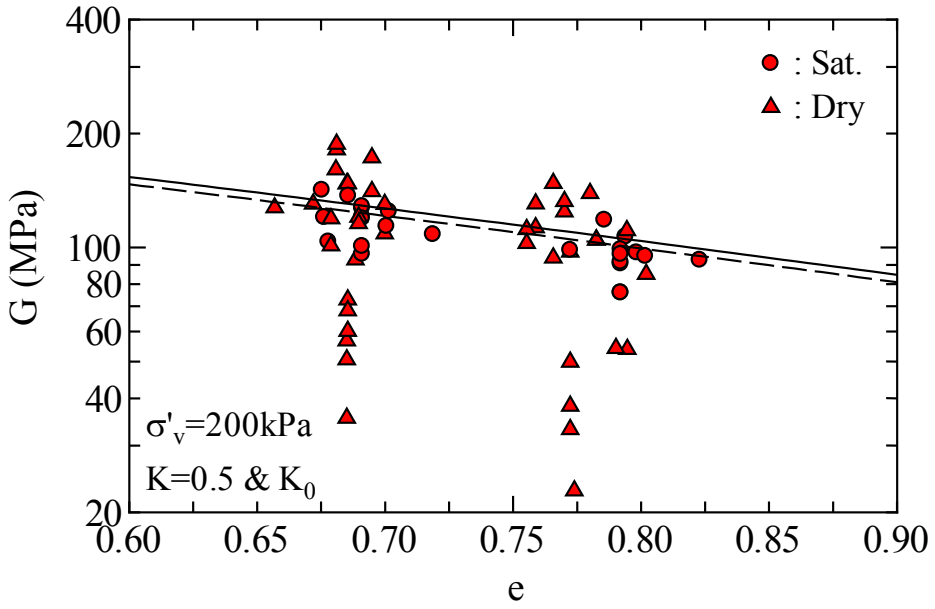

Fig. 4.19 Effect of identification method of travel time (K=0.5 and K_0, start-to start)

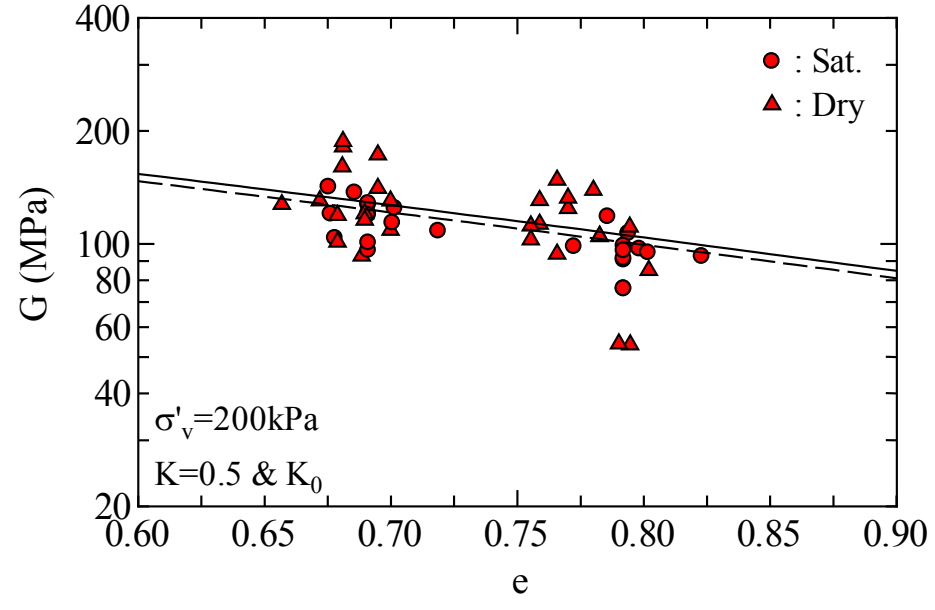

Fig. 4.20 Effect of identification method of travel time (K=0.5 and K_0, start-to start; remove Lab. No.5)

4.3.2 Cantilever length of BE

Figure 4.21 shows a scenario of percentage of BE insertion used by the different laboratories. Here, the % penetration means the ratio of cantilever length of a bender element that penetrates inside the specimen to the total sample length, expressed in %age. In general, larger the penetration, the voltage signal is clearer but at the same time, it creates larger disturbance to the sample. On the other hand, smaller penetration is better in the sense that they do not cause much disturbance but generated energy may not be sufficient to propagate to the other end of sample or for receiving.

As shown in Table 3.4, cantilever length of BE used in the tests by participated laboratories lies in the range of 2.4-27.85 mm. When specimen length is taken into account, BE penetration ratio comes out to be 1.6-58%. Among these, approximately half of the total laboratories use 7-20% BE penetration. Moreover, almost one-third of total use 7-10%.

Figure 4.22 shows an effect of the cantilever length of BE on G_{max} vs. e relationship for isotropically consolidated specimens at 200 kPa based on the data from different laboratories. Figure 4.23, on the other hand, plots the results for anisotropically consolidated specimens at K=0.5 and K_0-consolidated specimens at vertical stress of 200 kPa. The variation as shown in Figure 4.22 does not provide clear trend on the effect of cantilever length of BE for isotropically consolidated specimens. In Figure 4.23, larger scatter associated with increased cantilever length is well understood. For anisotropic tests with relatively smaller specimen lengths and having large scatter in original data, it is not possible to pinpoint that such scatter are the effect of cantilever length of BE. It is however, no doubt that increased cantilever length, which reduces the travel length of shear wave signal inside the specimen, is likely to introduce larger error in G_{max} values.

Therefore, as beneficial point of increasing the cantilever length is not recognized, we can say that there is no need to excessively increase the cantilever length of BE if arrival position of received wave is easily readable. The following three points about increased cantilever length need to pay the attention:

i. It results into reduced travel path between benders causing the possibility of inducing larger error in calculating G_{max} values.
ii. The degree of disturbance increases.
iii. It is most likely that noise due to reflections from the boundaries magnify.

With this background, it can be easily said that increasing the bender cantilever length recklessly cause no more than increasing a possibility of magnifying the error.

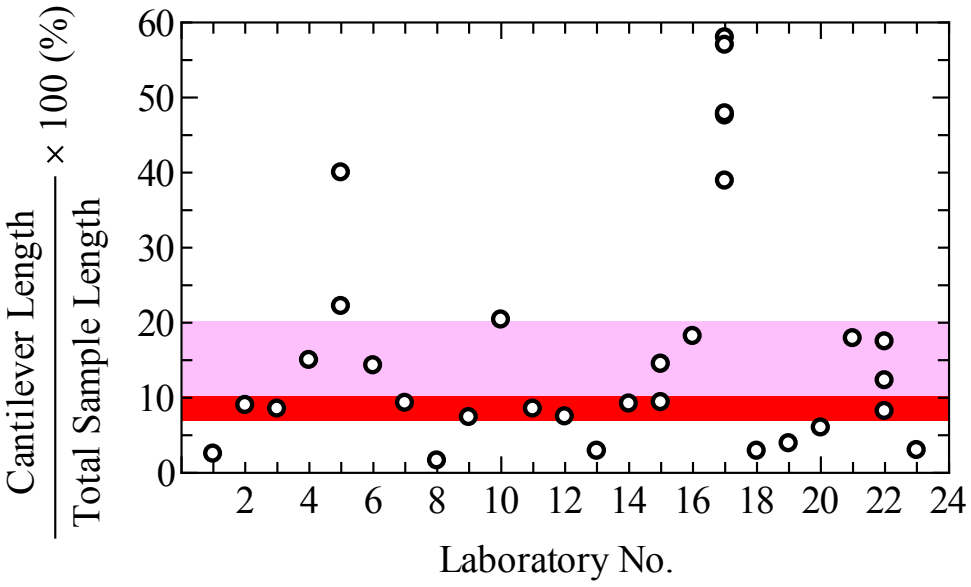

Fig. 4.21 Cantilever length of BE

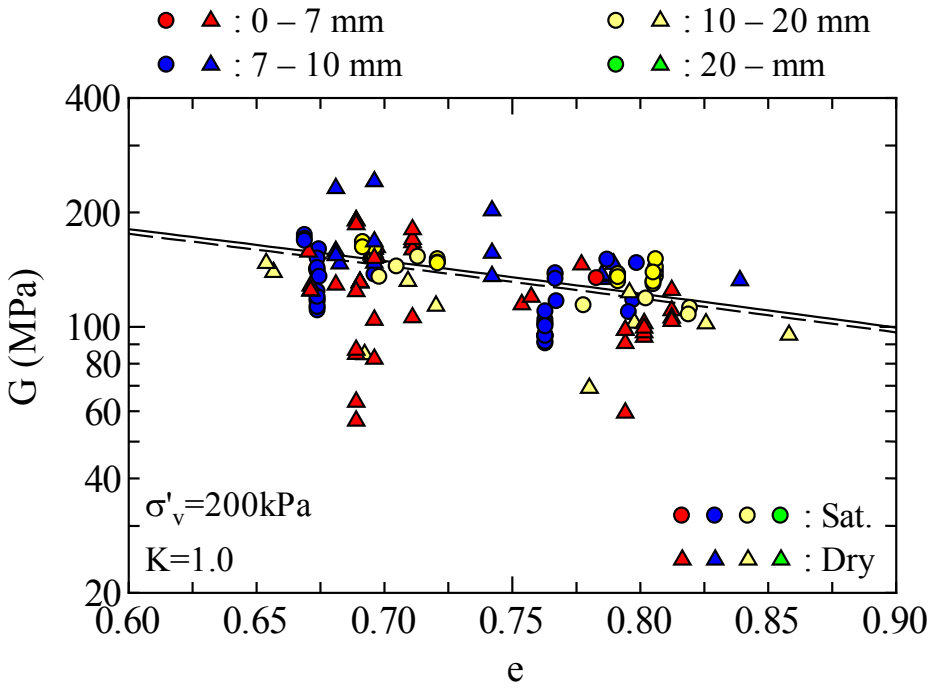

Fig. 4.22 Effects of cantilever length (isotropic consolidation)

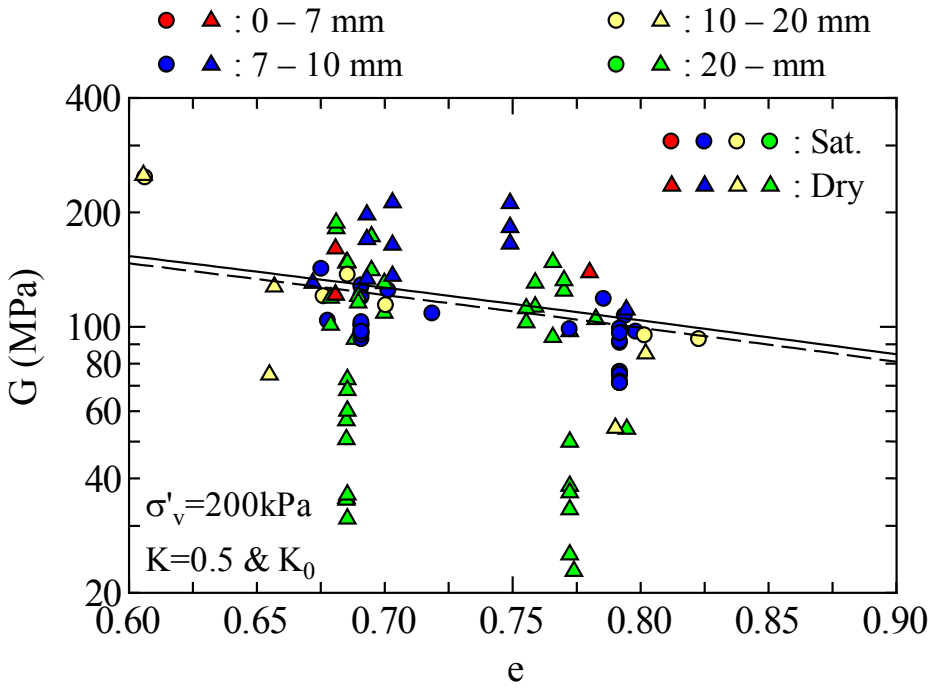

Fig. 4.23 Effects of cantilever length (K=0.5, K_0 consolidation)

4.4 Re-Evaluation of Test Data (rereading of travel time)

As expressed in the description above, scatter results due to the difference in identification method and also because the actual reading point differs according to the personal judgment when T.D. method is applied. Therefore, it is neither convincing nor appropriate to evaluate the bender element test method from only the reported test data. At this point, the whole wave data was reread by applying the single identification method from the digital records of the waveforms provided by testing laboratories.

4.4.1 Used Identification Methods

1) Start-to-Start Method

From among the digital waveform data received, laboratories which used single pulse of sine or square wave as an input were reread by using start-to-start method of arrival time definition. The near-field-effect (NFE) and direction of the initial motion of BE against the applied voltage was considered while deciding arrival point in the received signal.

There were very few laboratories which provided the information of initial movement of benders on applying electric voltage. In this regard, it was presumed that initial motion of BE for both transmitting and receiving side fell on the same side if such information was not supplied.

To consider NFE, receiving signals, obtained by exciting the transmitter bender with sinusoidal waves of different frequencies, needs to be compared and evaluated (if available). When first amplitude in reception time history matches the direction of initial motion, the point where the receiving signal takes-off from the zero line (a horizontal line of voltage output when there is no signal) is the time of shear wave arrival. In case if the first amplitude in reception time history does not match the direction of initial motion, the point on the wave when it first traverses to the direction of initial motion and intersects the no-signal line is the arrival time of shear waves (e.g. Kawaguchi et al. 2001).

2) Peak-to-Peak Method

Similar to the start-to-start method above, the data from laboratories that used single pulse of sine wave input were reread by using peak-to-peak method, i.e., the time lag in between the peak position of an input wave to the first peak of the received wave, as the definition for arrival time. At the time of identification, direction of the initial motion of BE was considered similarly as that for start-to-start method described earlier.

3) Cross Correlation Method

The shear wave arrival time was also reevaluated from cross correlation technique by using Equation 4.1 after selecting only those data from the whole pool which used single sine wave pulse as an input. If the first received signal has the biggest amplitude, the arrival time was defined at the position where the highest peak of correlation was located. However, when the first peak at reception was not the highest one, the first peak in the time history of cross correlation, rather than at highest amplitude, was taken as the required arrival time. Besides, direction of the initial motion of BE was considered similarly as described earlier.

$$CC_{xy}(\tau) = \lim_{T=\infty} \frac{1}{T} \int_{T} X(t).Y(t+\tau)d\tau \qquad \text{(Equation 4.1)}$$

Here, $CC_{xy}(\tau)$:cross correlation function, T: recording period, X(t): time history of input wave, Y(t): time history of received wave, τ:delay.

4) Phase Cross Spectrum Method

The cross spectrum and its associated phase angle is obtained by performing Fourier transformation of cross-correlation function. The average inclination of absolute phase angle at the cross spectrum, if evaluated at the prevalent frequency of match between input and received waves, phase velocity of shear wave propagation time can be obtained. For the details on this method, please refer Viggiani and Atkinson (1995). If this inclination is designated as α, shear wave propagation time, Δt is given by the following formula.

$$\Delta t = \alpha/360 \qquad \text{(Equation 4.2)}$$

4.4.2 Reevaluation by Start-to-Start Method

In Figures 4.24 to 4.29, the horizontal time axis of the reported wave data has been normalized with the distance between tip-to-tip of bender pairs and further normalized with the square root of the ratio of the wet density and a void ratio function f(*e*). The zero in the figure denotes the start of input wave and the ordinate is simply the amplitude of received voltage. In total, 12 plots are prepared based on saturation condition, specimen density and testing methods. The number at the bottom left of the figure is the Laboratory number and the vertical line corresponds to the defined arrival point. While plotting the figure, if only one signal record was found, the same was plotted irrespective of the input wave frequency. However, if there was data of more than single frequency, wave data in the range of 10-15 kHz was selected for plotting.

Figure 4.30 to 4.33, respectively representing IC, K_0 & K=0.5, K=0.5 and K_0 tests, compare the G_{max} values that were evaluated by a standard technique of the start-to-start method. Although a little variation in the G_{max} value still remained, the scatter remarkably narrowed down if compared with the original submissions from the laboratories. Encircled data points in Figs. 4.30 and 4.32, which are located away from other data, are from the Laboratory No.16. It is considered that such scatter is not only due to the relatively long sampling interval of received wave, but also because of a very low frequency of the input sine wave (1.5 kHz). For example, in Figure 4.27 for a saturated specimen, the result submitted from the same laboratory but at higher frequency of 6 kHz resulted in the G_{max} values in par with other laboratories. Therefore, when receiving voltage is small and the resolution is rough, it is difficult to pinpoint the arrival point accurately. For clear reception, it is either necessary to increase the data resolution or to enlarge the received signal by increasing transmission voltage or input wave frequency.

Excluding the data from Laboratories No.4 and No.16, the scatter of G_{max} values in Figs. 4.30 to 4.33 are from consolidation tests and dry specimens. It is unclear, why the result of dry specimens has more scatter but it was found that there were many tests on dry specimens performed in a consolidation container probably due to the difficulty of saturation. For these tests performed in consolidation apparatus, shear wave travel length is relatively small and identification of arrival point becomes difficult due to NFE and reflections of waves at specimen boundaries. Thus, the errors associated with K_0-tests may have some link with dry specimens as well.

If wave arrival point is properly reread, even the data from Laboratory No. 5, which locates quite away from the other data points in Fig. 4.19, comes closer as shown in Fig. 4.31. An example of the time history of receiving wave from the Laboratory No.5 is shown in Fig. 4.26. The wave record is not much different from other submissions. The scatter probably appeared due to the judgment of person in charge of interpretation. It is most likely that the initial shear wave signals which are quite weak are considered as a noise while judging the arrival point. The larger value of travel period considered at the highest amplitude points might have resulted into extremely low G_{max} values. In this way, although some experience is necessary, sufficiently reasonable values of G_{max} can be obtained, if the start-to-start method of wave arrival technique is applied and NFE is properly considered by paying attention in the direction of initial motion of BE, and wave patterns at different frequencies.

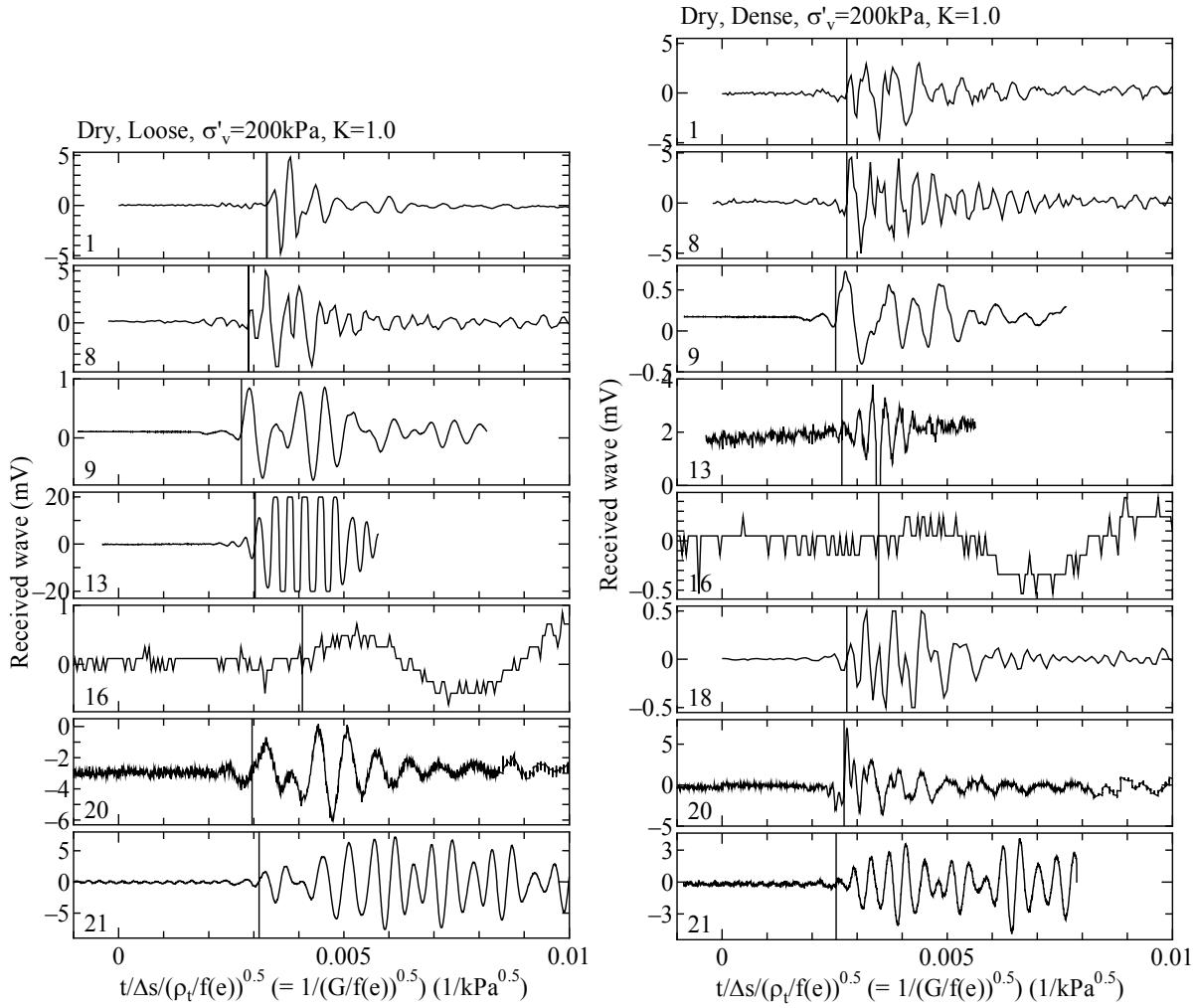

Fig. 4.24 Dry specimen (IC), 200kPa, start-to-start; (a) Dr=50%, (b) Dr=80%

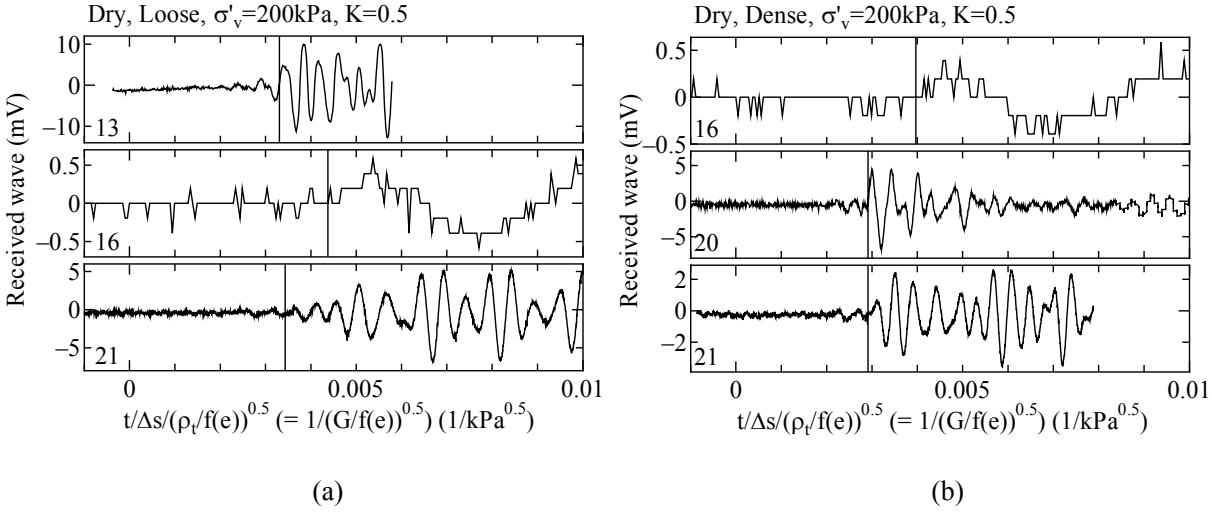

Fig. 4.25 Dry specimen (K=0.5), 200kPa, start-to-start; (a) Dr=50%, (b) Dr=80%

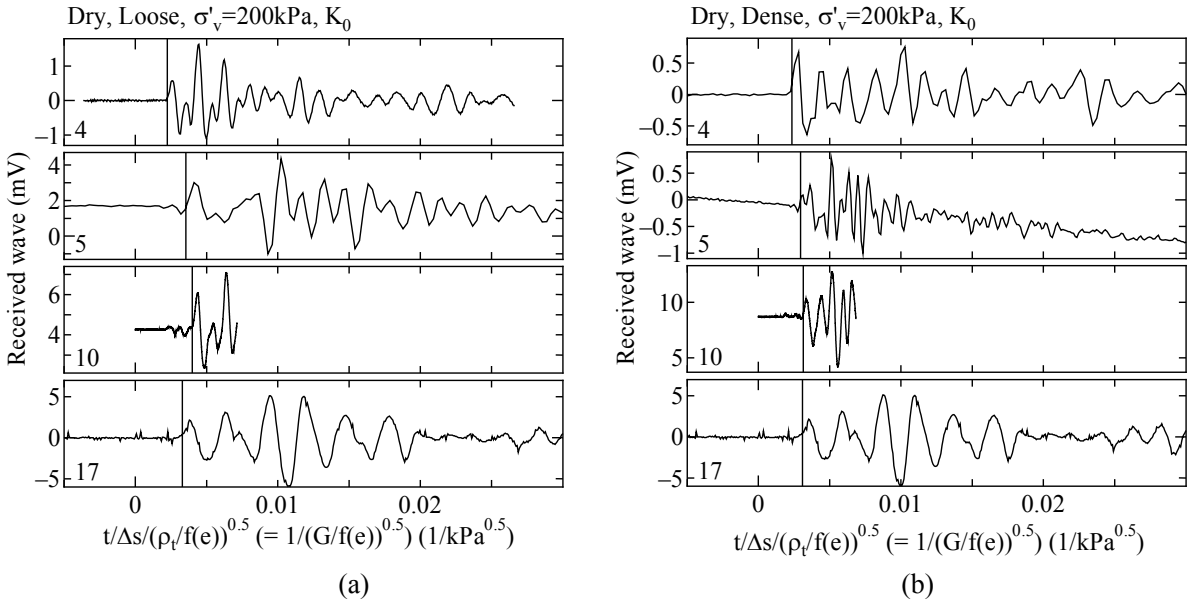

Fig. 4.26 Dry specimen (K_0), 200kPa, start-to-start; (a) Dr=50%, (b) Dr=80%

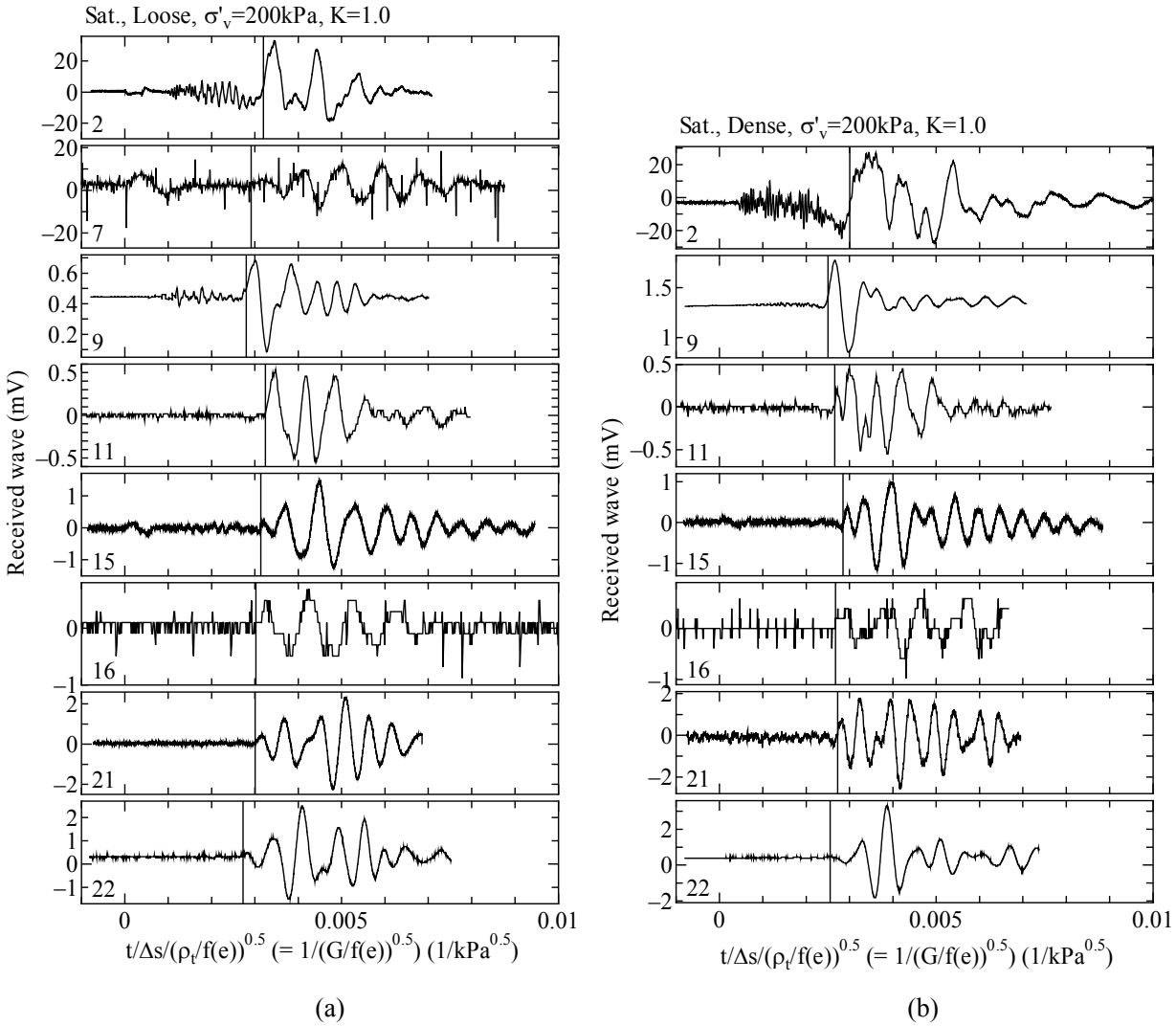

Fig. 4.27 Saturated specimen (IC), 200kPa, start-to-start; (a) Dr=50%, (b) Dr=80%

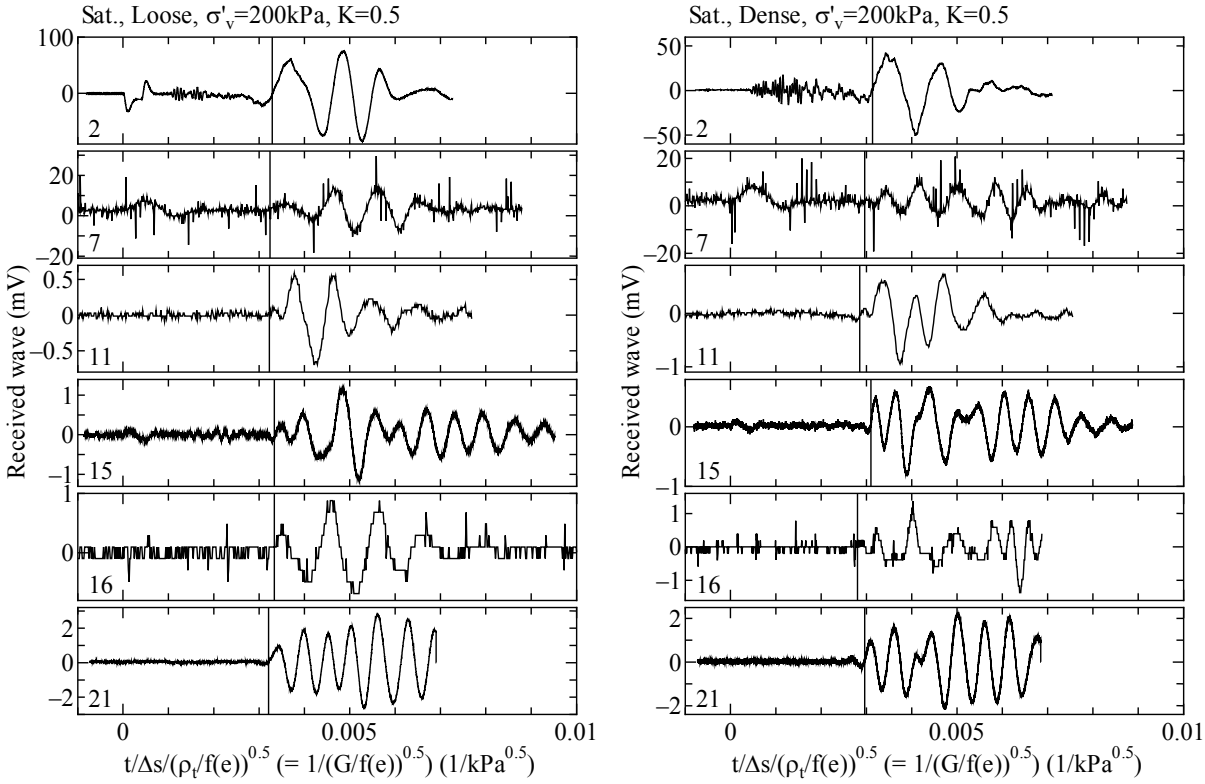

Fig. 4.28 Saturated specimen (K=0.5), 200kPa, start-to-start; (a) Dr=50%, (b) Dr=80%

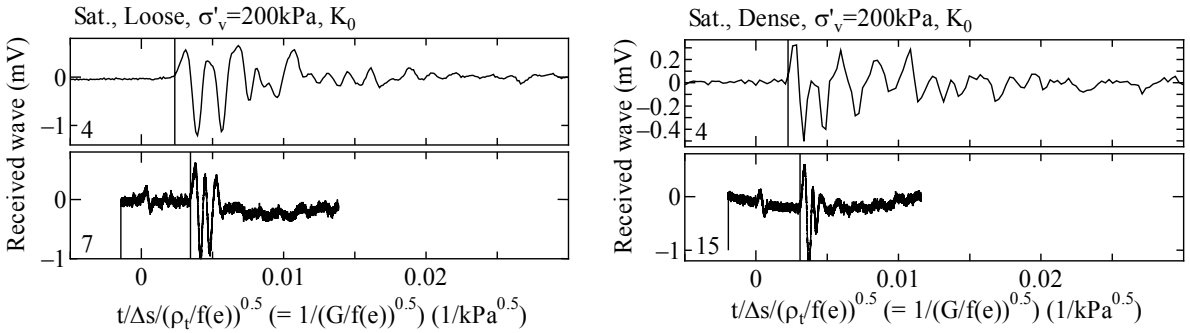

Fig. 4.29 Saturated specimen (K_0), 200kPa, start-to-start; (a) Dr=50%, (b) Dr=80%

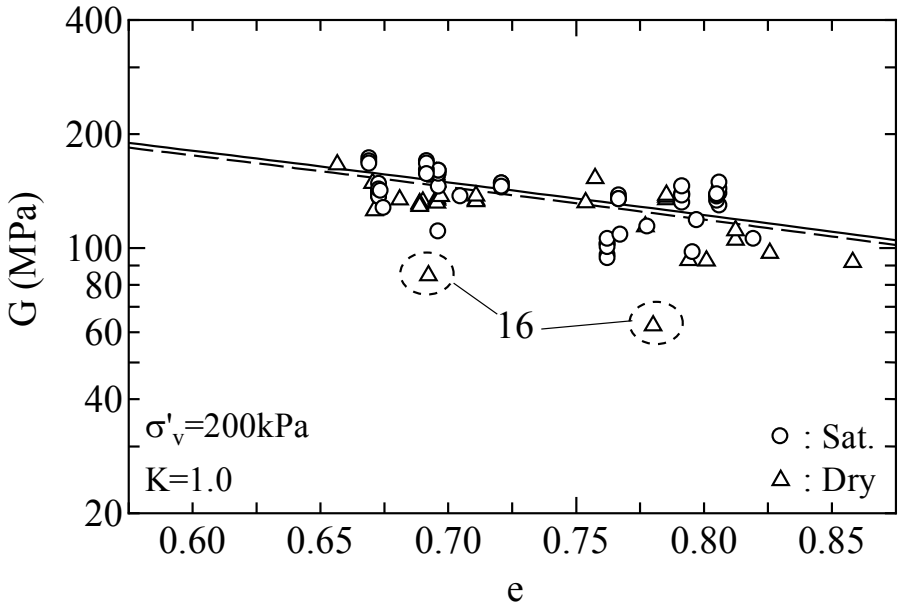

Fig. 4.30 Relation of G and e (re-evaluation results; 200kPa, IC, start to start)

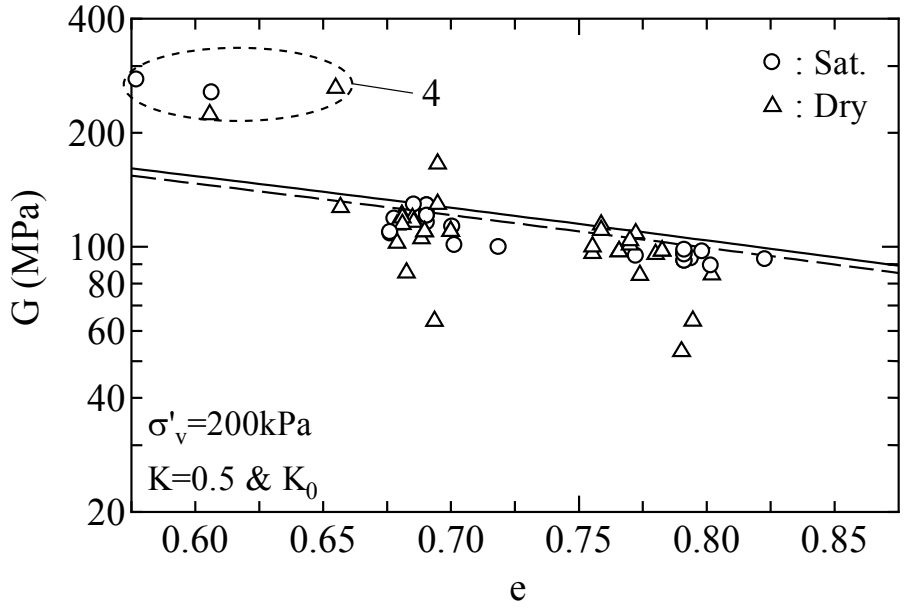

Fig. 4.31 Relation of G and e (re-evaluation results; 200kPa, K=0.5 and K_0, start to start)

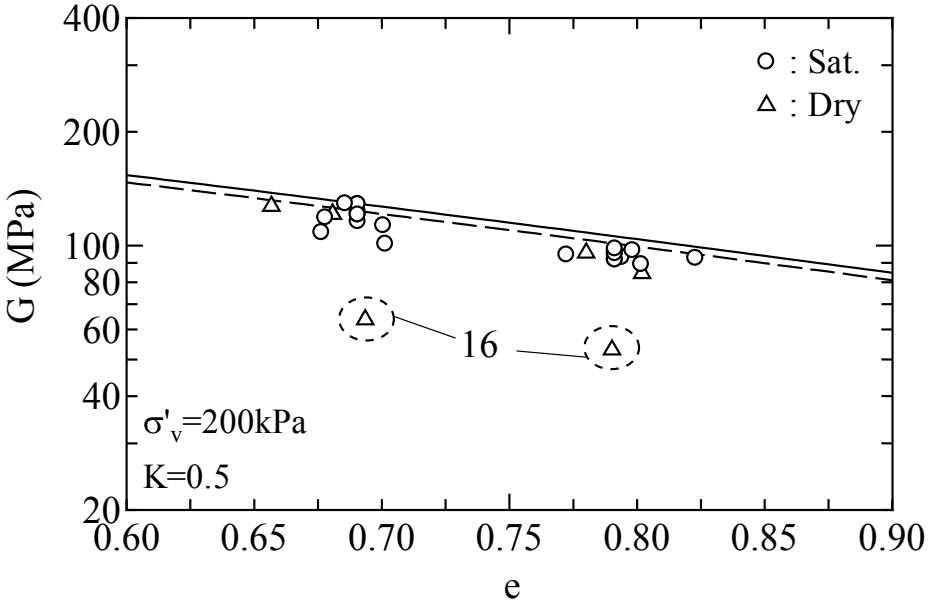

Fig. 4.32 Relation of G and e (re-evaluation results; 200kPa, K=0.5, start to start)

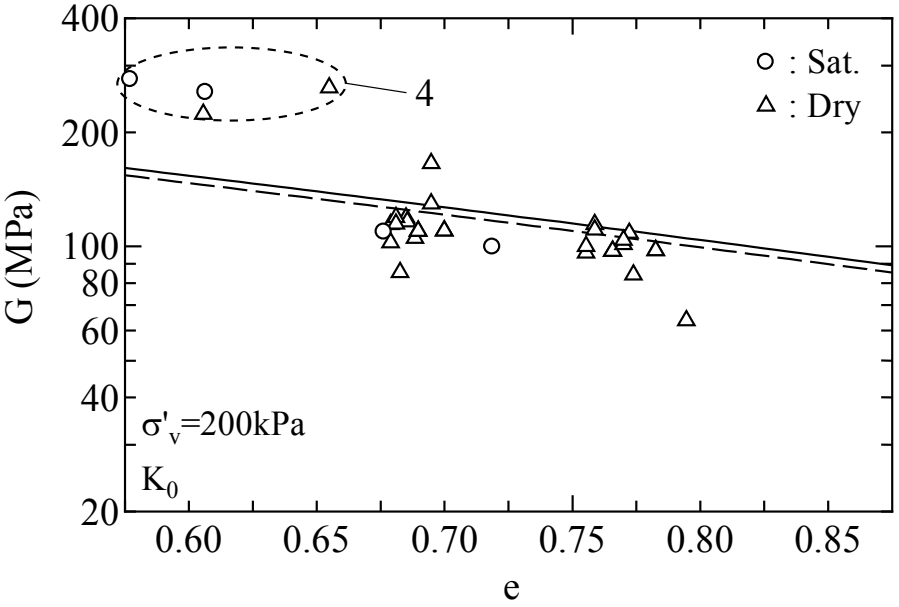

Fig. 4.33 Relation of G and e (re-evaluation results; 200kPa, K_0, start to start)

1) Effect of input wave frequency

Figures 4.34 to 4.37 compare the waveform data received from the same laboratory when the input frequency was altered. The vertical line in each figure shows the arrival time identified by the start-to-start technique. The following conclusions may be drawn from these figures:

i) In case of dry samples, where frequencies of transmitted wave and receiving wave differ remarkably, the peak-to-peak identification method is quite difficult.
ii) Changing the input frequency does not alter the frequency of the received wave appreciably (rather, the receiving wave is thought to be dictated by test equipment system).
iii) Reception voltage becomes small when frequency is high.
iv) At higher frequencies, such as with D_r=80%, amplitude of received voltage before the initial motion of benders becomes large.

Figure 4.38 shows the relationship between transmission frequency and shear modulus, G_{max}. Here, G_{max} in vertical axis is corrected for void ratio difference, i.e., current void ratio of the specimen and void ratio corresponding to D_r=50 or 80%, by using void ratio function f(e) There is no clear effect of input frequency in case of the saturated samples but for dry specimens it seems that scatter is slightly on the higher side at lower frequencies.

Figure 4.39 is plotted very similarly to that of Figure 4.38 and includes the wave data from the same laboratory performed with multiple input frequencies. In this way, it seems that the value of G_{max} increases upon the increase of frequency but the influence is comparatively smaller than other factors.

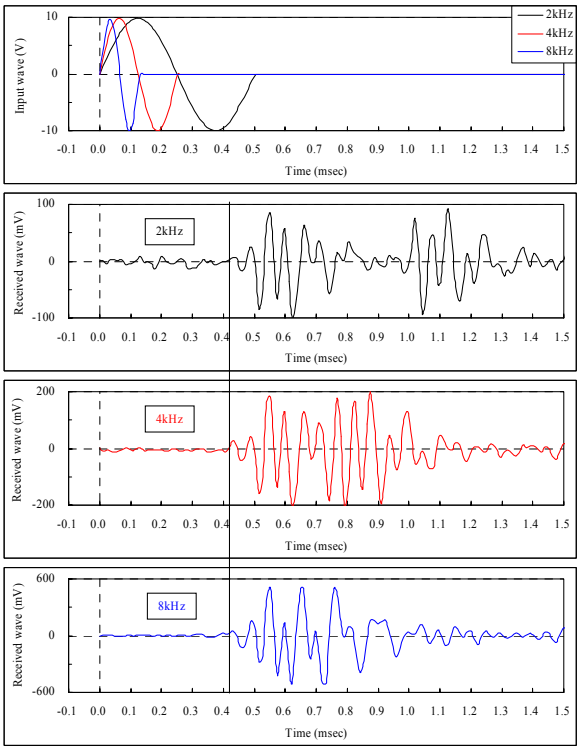

Fig. 4.34 Effect of frequency (200kPa, IC, Dr=80%, Dry, Lab.18)

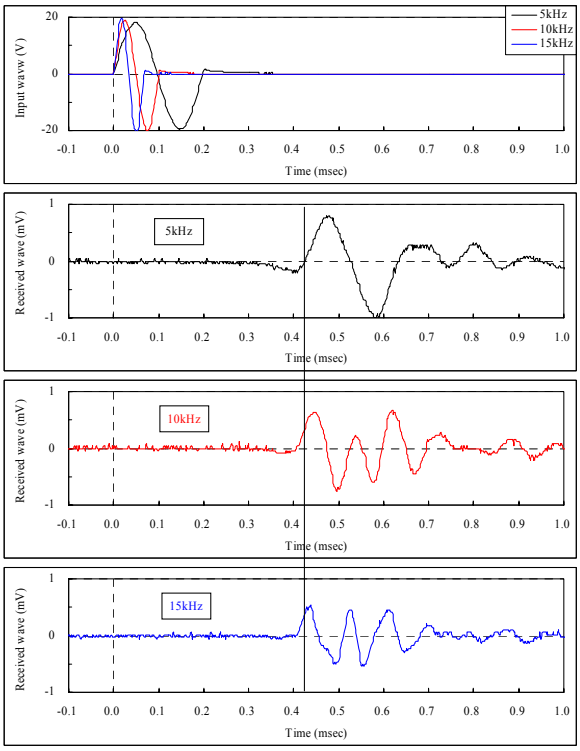

Fig. 4.35 Effect of frequency (200kPa, IC, Dr=50%, Saturated, Lab.11)

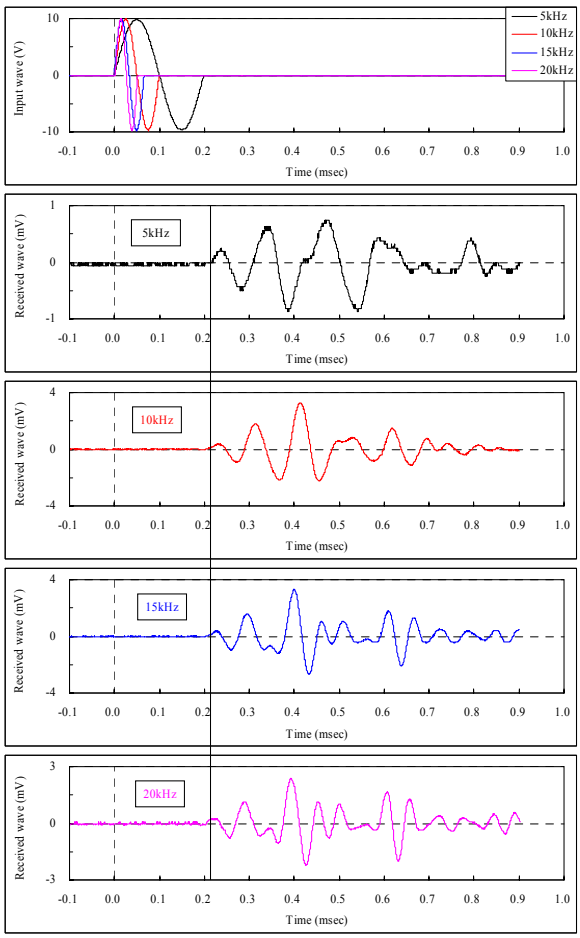

Fig. 4.36 Effect of frequency (200kPa, IC, Dr=50%, Saturated, Lab.22)

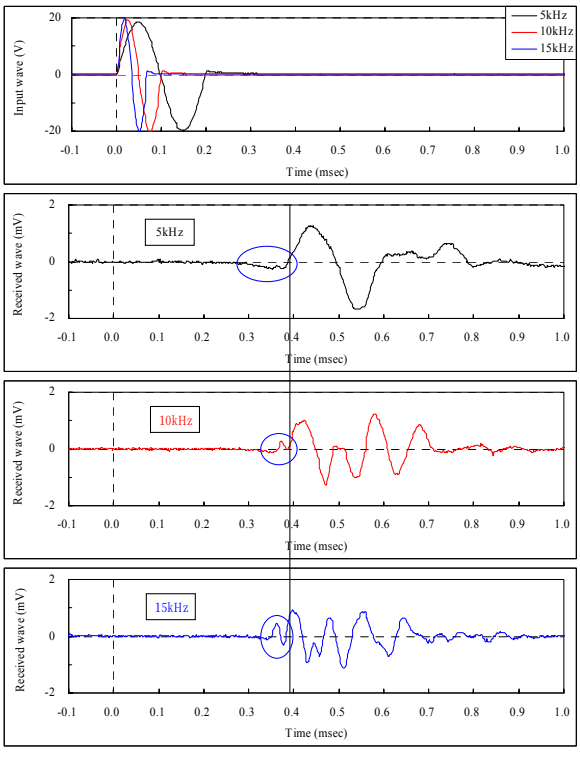

Fig. 4.37 Effect of frequency (200kPa, IC, Dr=80%, Saturated, Lab.11)

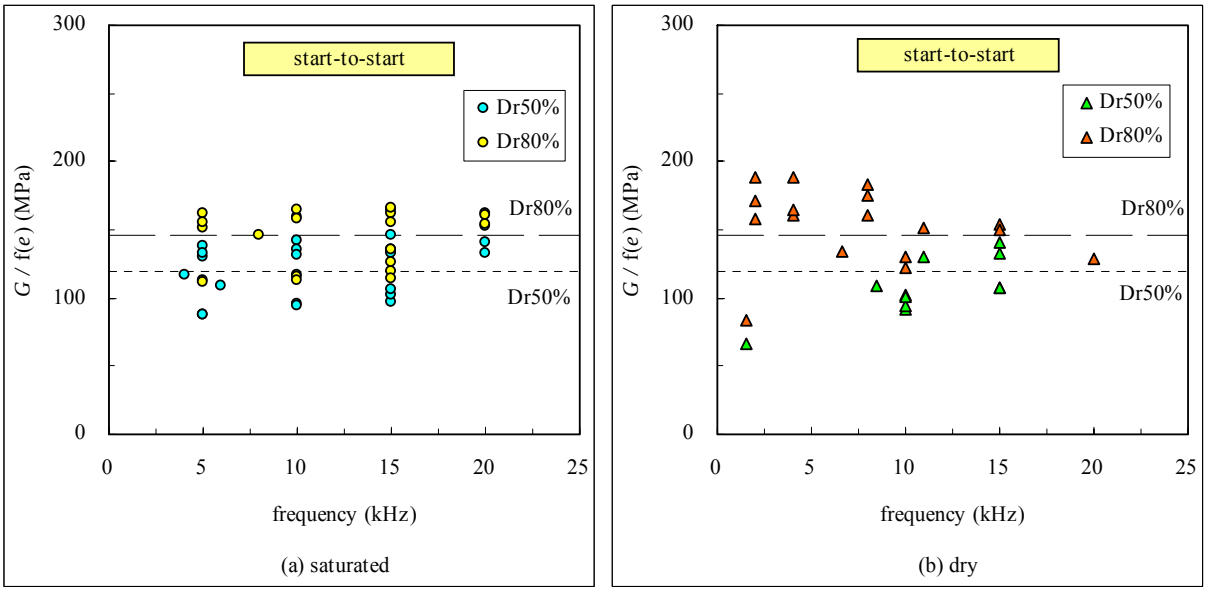

Fig. 4.38 Effect of frequency (IC, 200kPa); (a) saturated, (b) dry

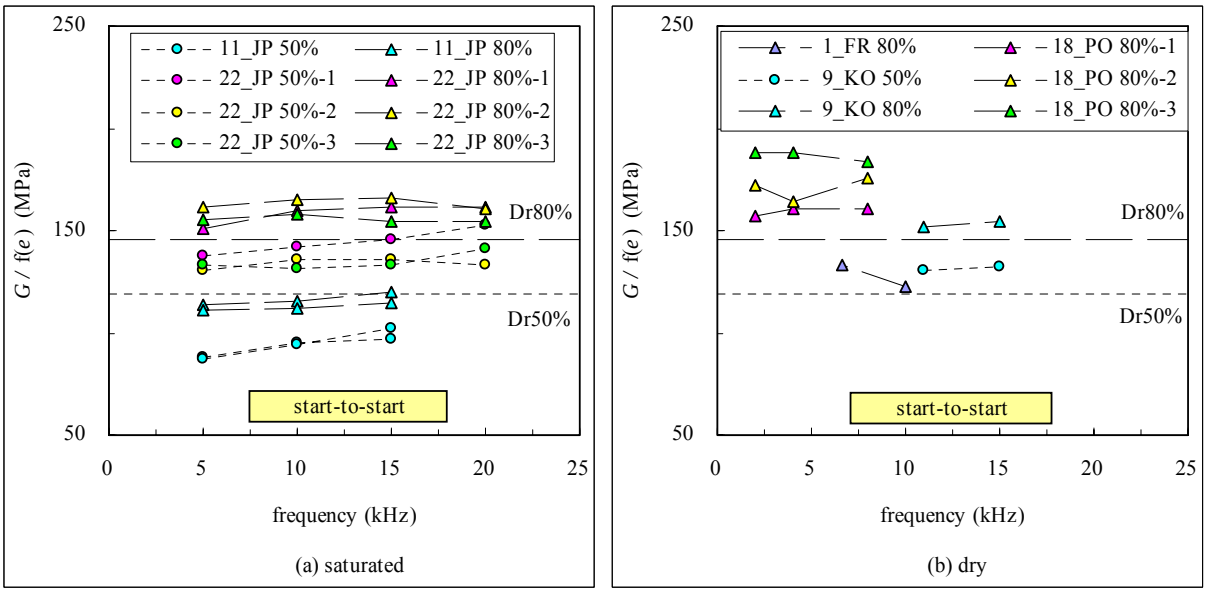

Fig. 4.39 Effect of frequency (IC, 200kPa); (a) saturated, (b) dry

2) Effect of penetration ratio of BE

Figure 4.40 shows the influence of penetration ratio of bender element to the shear modulus, G_{max}. In case of saturated specimens, no clear difference was found but the variation increased when penetration ratio was either small or large for dry specimens. However, looking on the responsible factors discussed so far and also considering the opposite trend observed for D_r = 50% and 80%, there is no tendency governed by the variation in cantilever length of BE.

Effect of penetration ratio is more clearly observed in Figure 4.41**,** which compares the waveform data from the same laboratory. The horizontal axis represents the distance between BE pairs normalized with the time. In the figure, a vertical line joining all plots indicates the shear wave arrival time identified with start-to-start technique. This figure also does not show any clear tendency of the influence of penetration ratio in BE test.

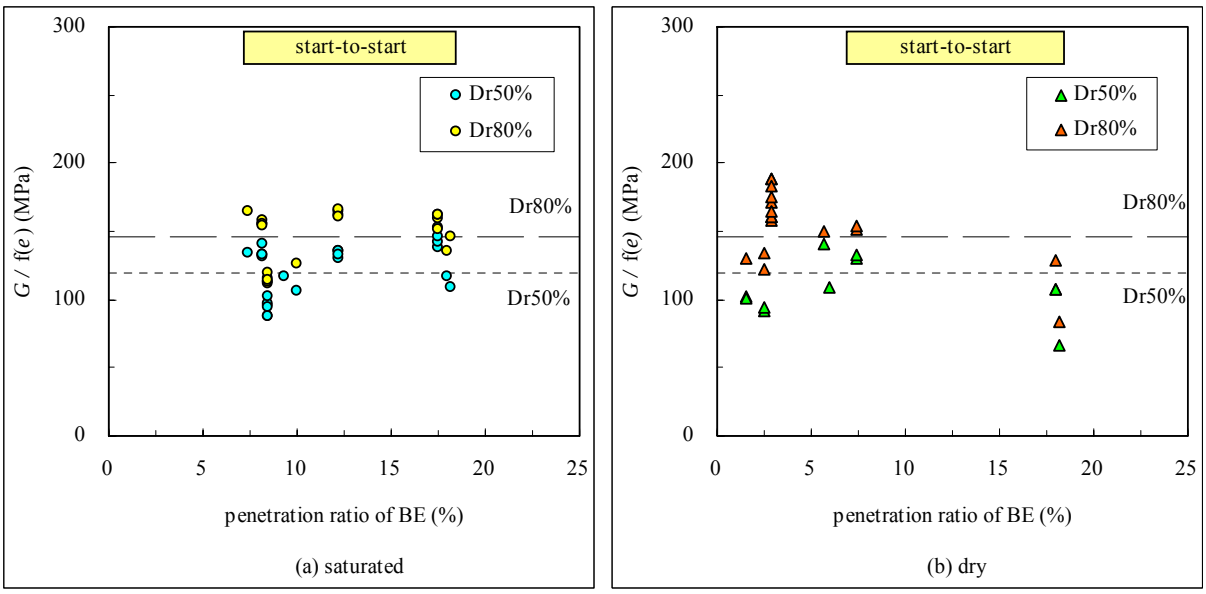

Fig. 4.40 Effect of penetration ratio of BE ; (a)saturated, (b)dry

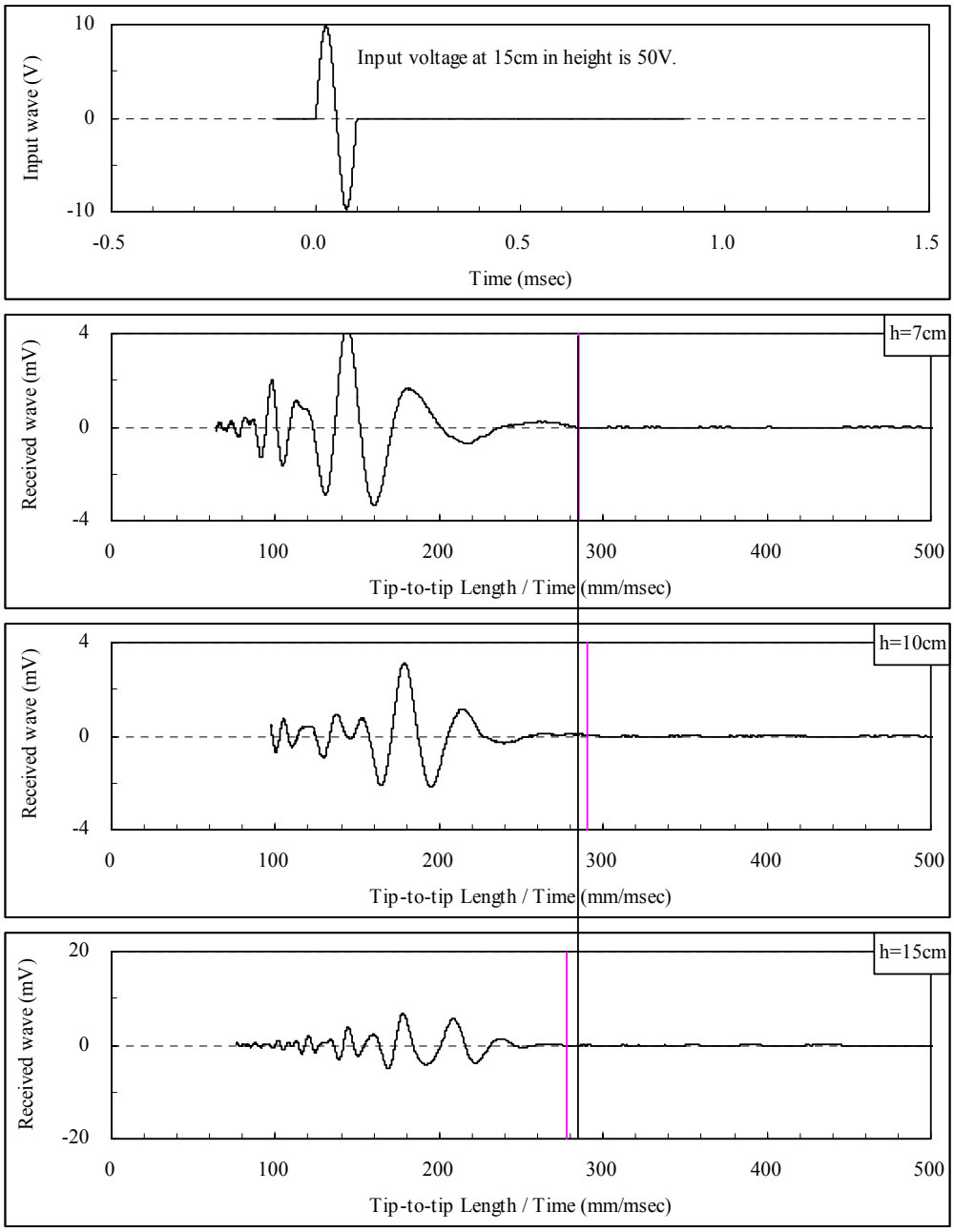

Fig. 4.41 Effect of penetration ratio of BE on received wave

4.4.3 Reevaluation by Peak-to-Peak Method

Figure 4.42, plots the reevaluated G_{max} values vs. void ratio, e when single sine wave pulse was used as input and arrival time was identified by the peak-to-peak method, i.e., the time lag between the peak points of transmitting and receiving waves. Although some scatter in data for dry specimen remained, the reevaluated results had far smaller scatter than the original data supplied by laboratories. An encircled data point in the figure, which lies away from other points, was obtained by an input of very small frequency of 2 kHz as compared with the input frequency used by other laboratories. As shown with examples in Figs. 4.34 to 4.37, the frequency of receiving wave does not change in the same proportion with input frequency. It is due to this reason that the chances of error in arrival time reading go up when the frequency difference between the input and receiving wave goes on increasing.

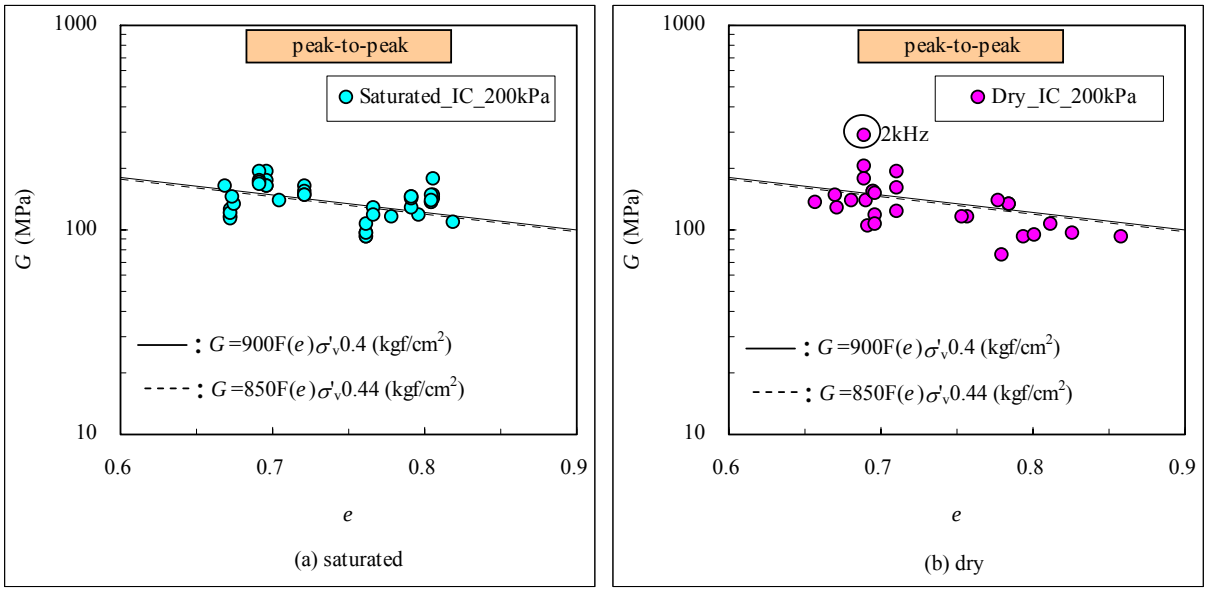

Fig. 4.42 Relation of G and e (re-evaluation results; 200kPa, IC, peak to peak)

4.4.4 Reevaluation by Cross-correlation Method

Figure 4.43 shows G_{max} vs. e plot for IC specimens at 200 kPa, by identifying the shear wave arrival time with the cross-correlation method. The data was however, limited to the cases where single pulse sine wave transmissions were adopted. As written in 4.4.1(3), if the first received signal had the biggest amplitude, the arrival time was defined at the position where highest peak of correlation was obtained. However, when the first peak at reception was not the highest one, the first ever peak in the time history of cross correlation (CC), rather than at highest amplitude (CC_{max}), was taken as the required arrival time.

As shown in the figure, the time corresponding to the cross-correlated CC data also has smaller scatter as observed in reread figures explained earlier. On the other hand, the encircled data in the figure representing dry specimens differ quite a lot. It is to be noted that the input frequency for these cases were quite low. As expressed earlier in the peak-to-peak method, the frequency of receiving wave does not always increase proportionately according to an input frequency. The error magnitude for cross-correlation method, which assumes the frequency similarity of input and received waves, is likely to increase when the frequency difference between them goes up, very similar to the peak-to-peak method.

Observing as a whole, the scatter in the dry specimen are higher than saturated ones in the same way as has occurred in previous cases. Figures 4.44 and 4.45 provide a comparative view of the waveform in saturated and dry sample that were submitted from the same laboratory. From this figure, it is well noted that the amplitude of the received wave for dry specimens is larger, it has longer reverberation time (after effect continues for long period), and there is bigger noise before the real shear wave signal than saturated cases. It is thought that the aforementioned effects associated with dry specimens, which create more disturbances in the wave shape, might be the reason behind the larger scatter in dry specimens. Furthermore, the arrival time evaluated by cross-correlation method is almost identical to that identified by other methods shown in the same figure. In the figure, a little rightward shift in the peak-to-peak identification method is not the real difference but because the zero point in the figure is the starting point of input wave, rather than the peak position needed for this method. In addition, CC_{max} that locates the maximum amplitude point in cross-correlation function, differs more largely than the other result. This clearly tells that when largest amplitude of the receiving wave is not the first wave, there is high chance of having big error by adopting CC_{max} method of definition.

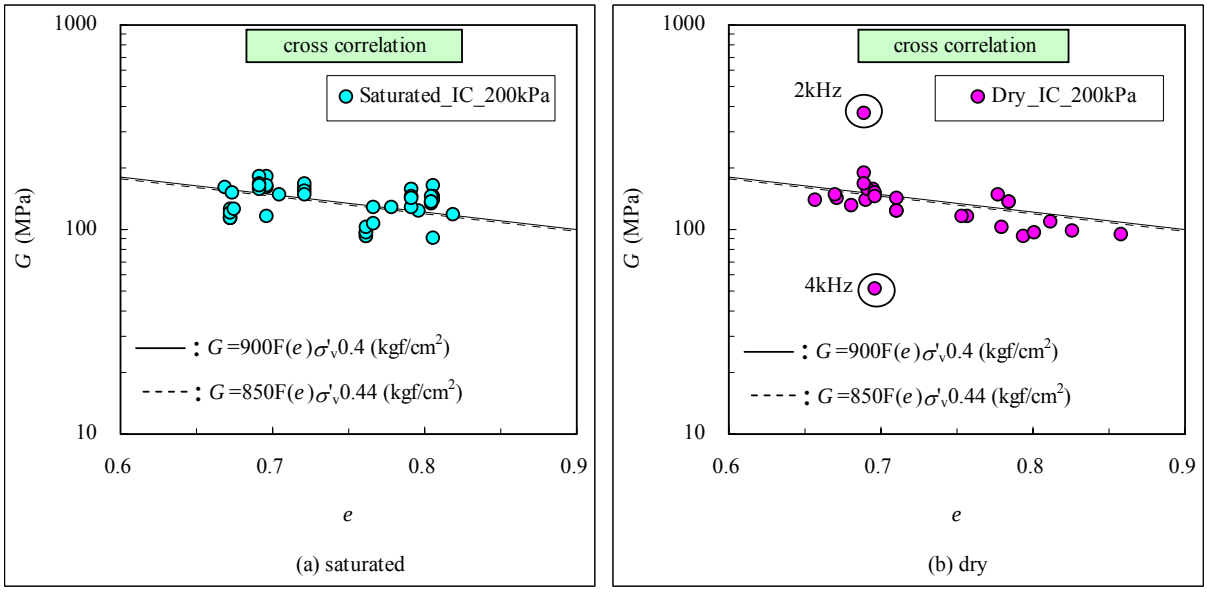

Fig. 4.43 Relation of G and e (re-evaluation results; 200kPa, IC, Cross correlation); (a)saturated, (b)dry

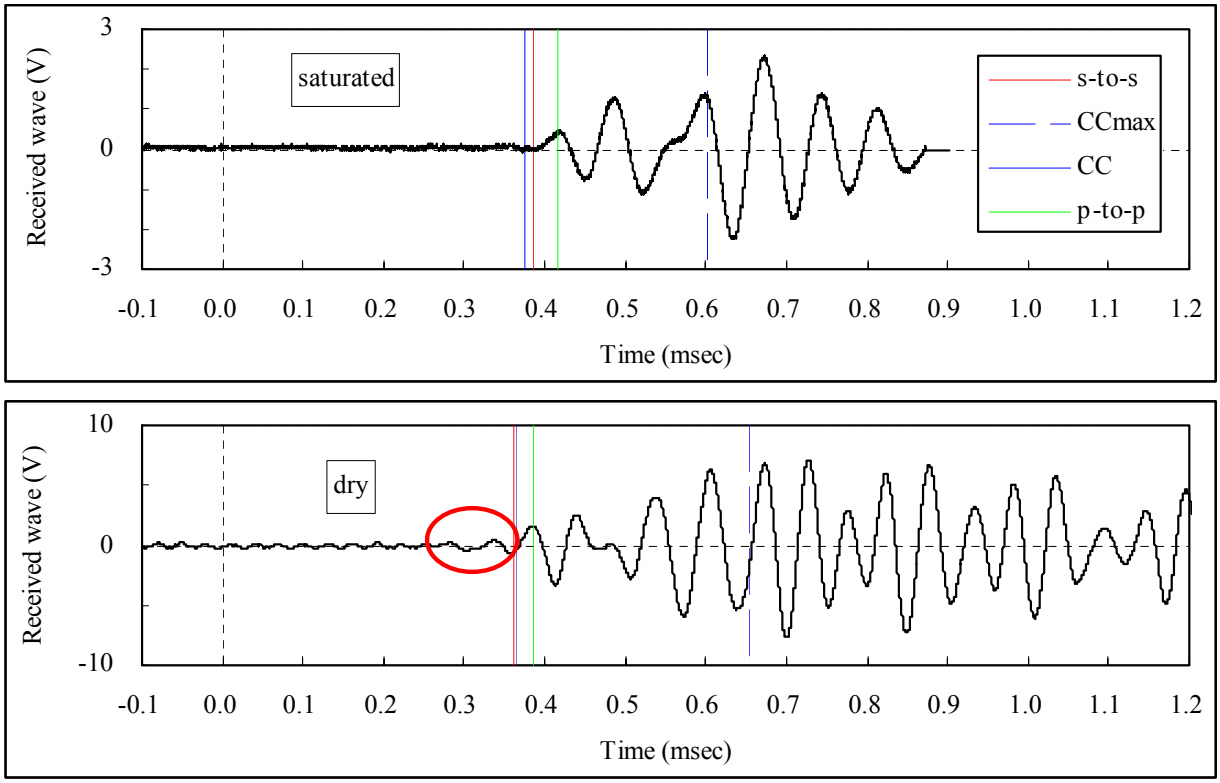

Fig. 4.44 Comparison of saturated and dry specimens (200kPa, IC, Lab.21)

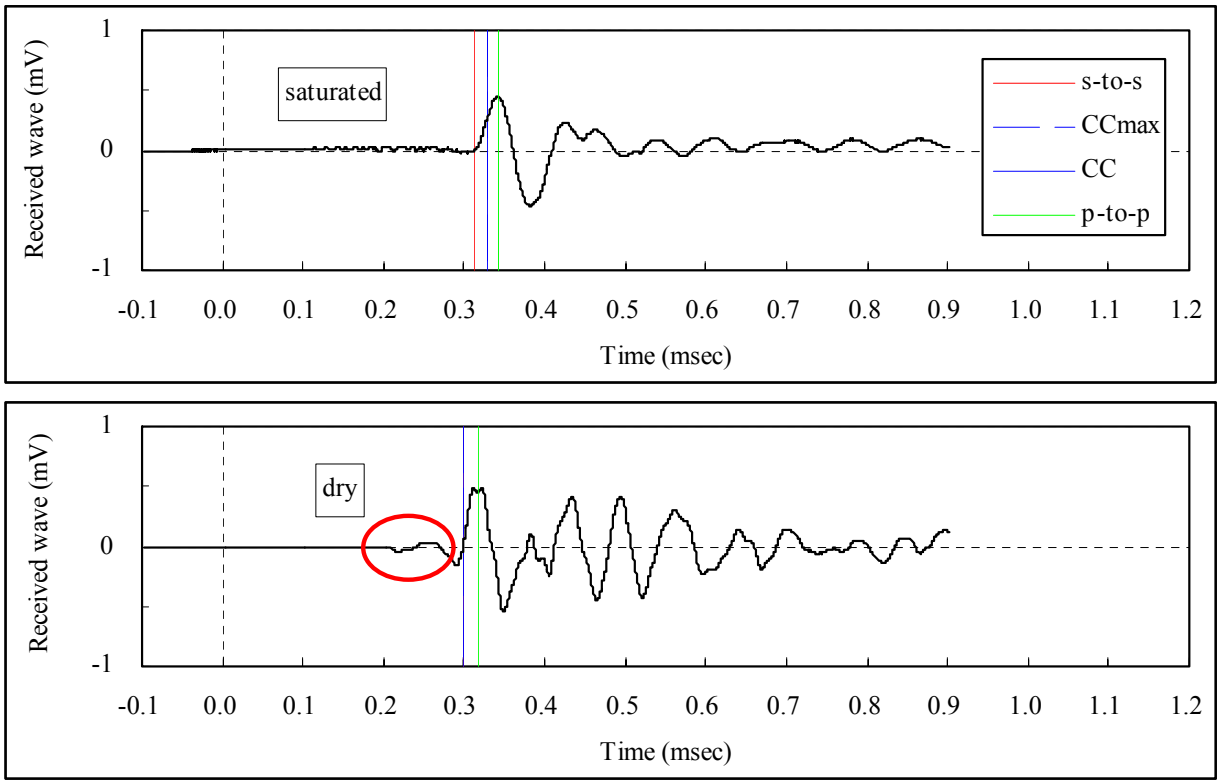

Fig. 4.45 Comparison of saturated and dry specimens (200kPa, IC, Lab.9)

4.4.5 Reevaluation by Phase Cross Spectrum Method

Figure 4.46, has been prepared for shear modulus, G_{max} by applying the arrival time identification method of the phase cross spectrum (yellow color) for IC saturated specimens at confinement of 200kPa. Similar to the peak-to-peak and cross correlation method, the wave data that used sine wave input was selected from among the whole list of submitted data.

In the figure, the values of G_{max} submitted by the laboratories are represented by circular symbol (red color). Coincidentally, all of the laboratories selected here used the start-to-start method of identification. Plotted in the same figure are the G_{max} values corresponding to the time defined by CC_{max} (green color) and two general relations obtained for the similar material in the past (solid and broken lines).

The results from some laboratories are almost identical irrespective to the evaluation method (blue circle on the left). But almost the G_{max} values obtained from the phase cross spectrum are considerably smaller than those evaluated by the start-to-start method and are quite scattered (see a typical example, the blue circle in the right). On the one hand, G_{max} values which is obtained from the phase cross spectrum are almost identical to the G_{max} values obtained from the maximum of cross-correlation function, CC_{max}.

Figure 4.47 is very similarly prepared to Figure 4.46 but for dry specimens. Similar to the saturated specimens, G_{max} values for dry specimens are remarkably smaller than those evaluated by start-to-start method and are quite scattered. Here, the G_{max} values obtained from the phase cross spectrum also differ from the G_{max} values obtained from CC_{max} method.

Figures 4.48 and 4.49 show the waveform data where the same G_{max} value was obtained by any method. If receiving wave is examined (the second tier, blue), the amplitude of the first signal is the largest. It is expected that this peak point in the receiving wave is considered while calculating the cross-correlation function at the maximum amplitude (CC_{max}). As a result, the arrival time calculated from the inclination of phase spectrum in the frequency range where amplitude of the cross spectrum is large (5-20 kHz), is almost equal to the arrival time defined by start-to-start method.

Figures 4.50 and 4.51 compares the arrival time defined by start-to-start method and by the phase cross spectrum. Unlike in Figs. 4.48 and 4.49, the results obtained from different methods differ largely. Looking on the receiving wave (the second tier, blue), the amplitude of the first peak of shear wave is not the largest. The maximum of cross-correlation function shown in the same figure (the third tier, green) clearly shows that CC_{max} does not correspond to this first peak. As a result, although the arrival time obtained from the maximum of cross-correlation function and inclination of the phase cross spectrum (10 to 20 kHz) match fairly, these differ largely with the arrival time determined by start-to-start method.

Recollecting the above discussions, if the value which is obtained from start-to-start method or the relational expression of G_{max} is taken as the appropriate arrival time, the value of G_{max} obtained from the time corresponding to the inclination of the phase cross spectrum will be appropriate only when frequency of input wave is made equal to the frequency of the first wave appeared in receiving wave.

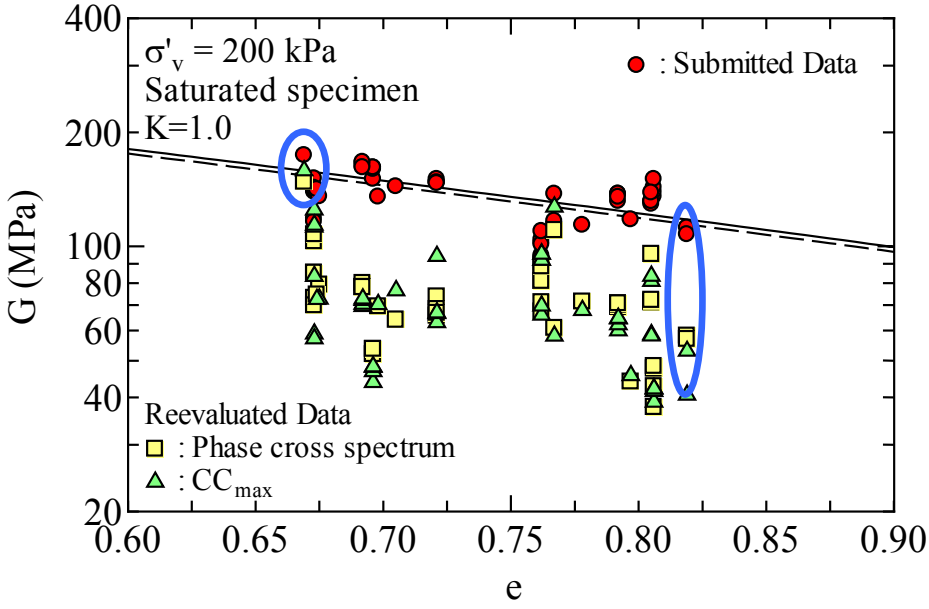

Fig. 4.46 Relation of G and e (200kPa, IC, Saturated)

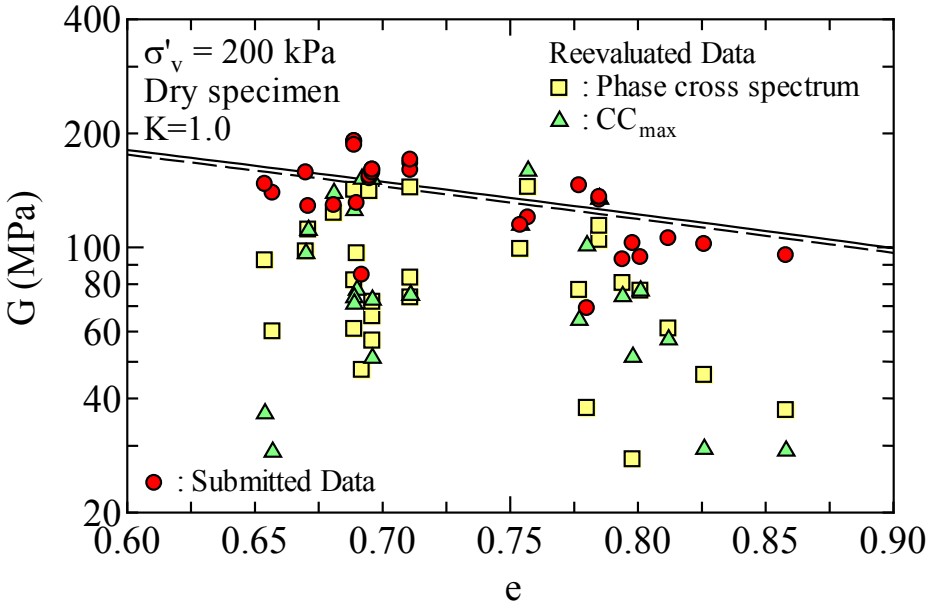

Fig. 4.47 Relation of G and e (200kPa, IC, dry)

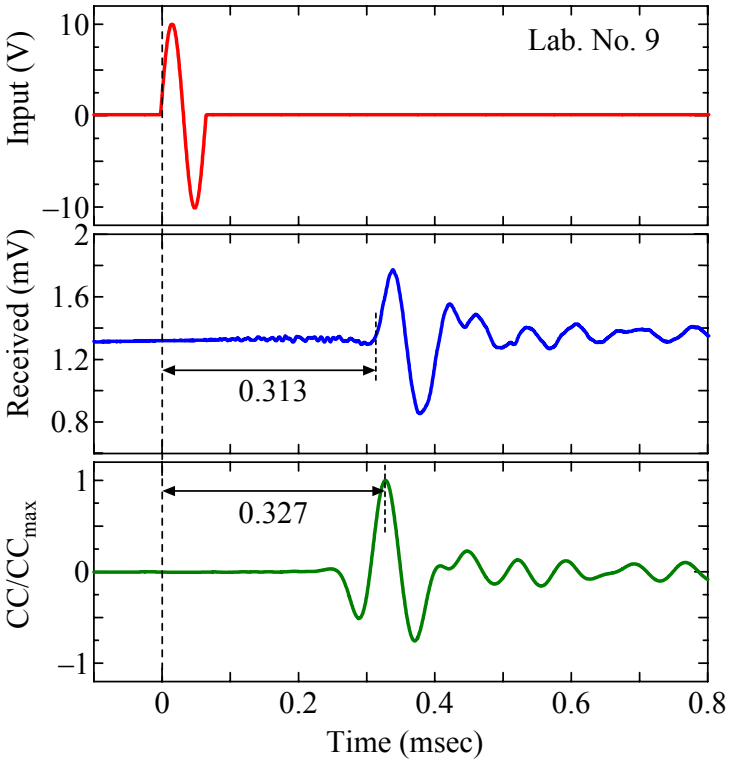

Fig. 4.48 An example of CC (Dry, 200kPa, IC)

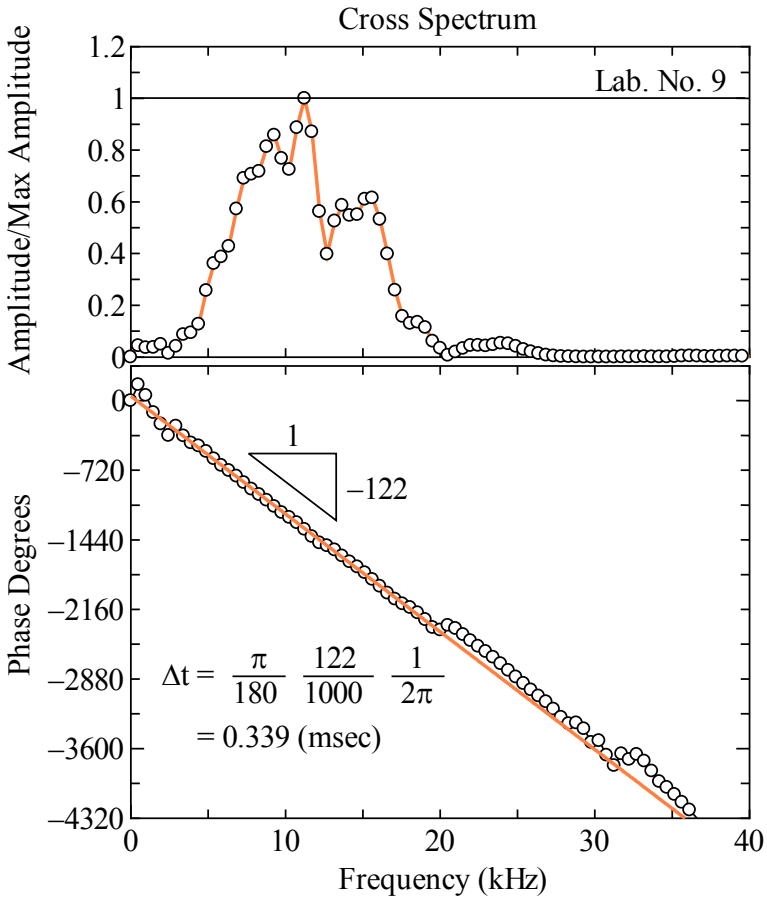

Fig. 4.49 An example of PCS (Dry, 200kPa, IC)

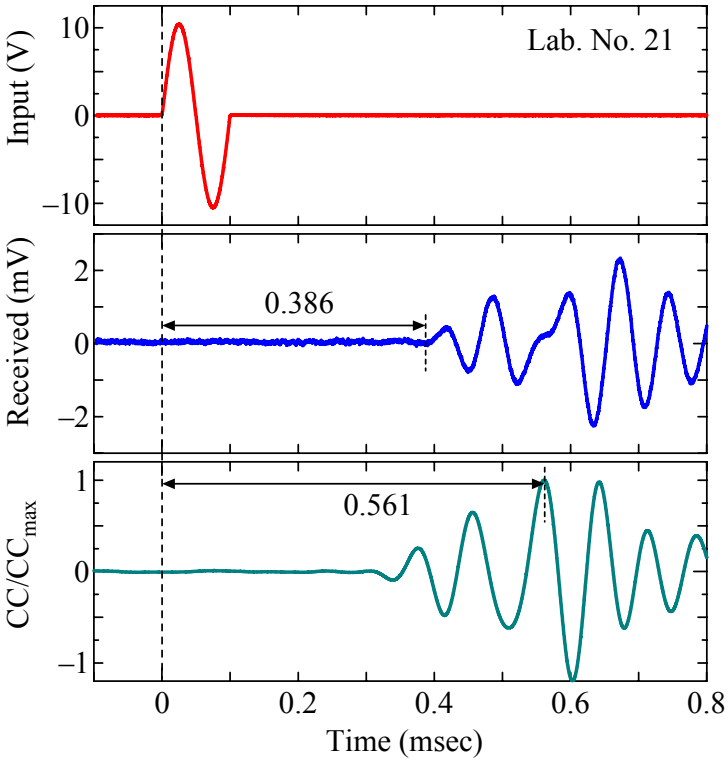

Fig. 4.50 An example of CC (Dry, 200kPa, IC)

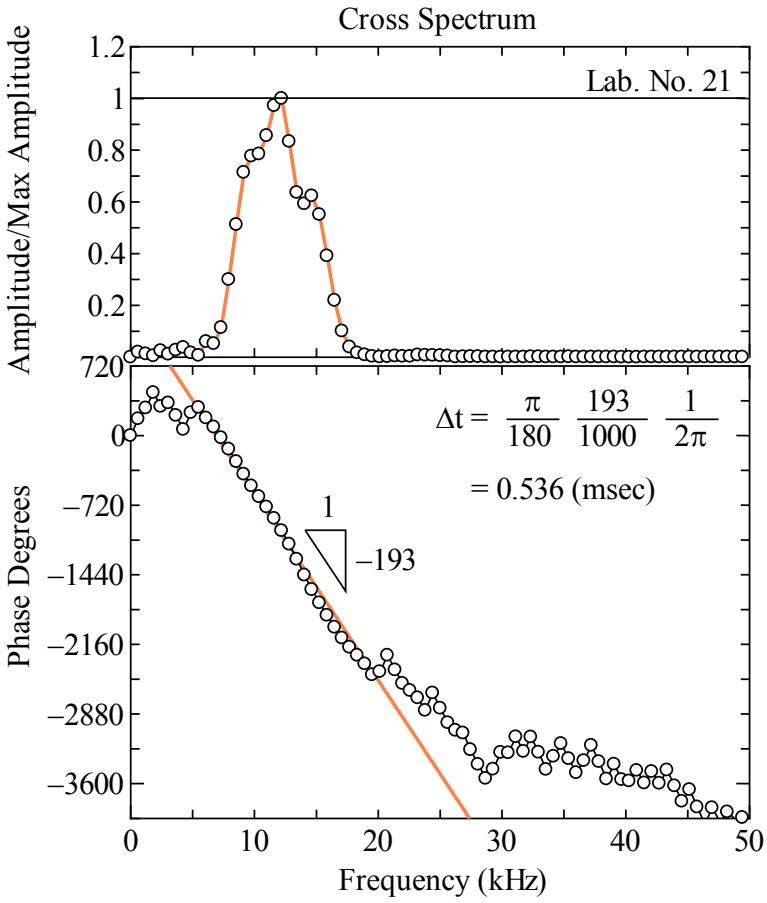

Fig. 4.51 An example of PCS (Dry, 200kPa, IC)

4.5 Effect of Difference of Identification Method

The following paragraph compares the result due to the difference in arrival time identification method. Figure 4.52 to 4.54 show the G_{max} values obtained by the travel time from the start-to-start, peak-to-peak and cross-correlation methods. In general, saturated specimens have smaller scatter than dry ones. In addition, the average relative relationships among different methods agree well irrespective of the identification method. Some scatter cases, such as for dry specimens, is due to lower transmission frequency and other reasons as already explained in previous paragraphs.

Figures 4.55 to 4.57 show the average relations of the shear modulus, G_{max} calculated with aforementioned three identification methods and the void ratio, e. Here, G_{max} values in vertical axis has been corrected to the required void ratio by using void ratio function, f(e) so that relative density, D_r reaches the required value of 50% or 80%. The figures show the mean value and the range of the maximum and minimum values for samples at D_r=50% and 80%.

Interestingly, it was found that although dry specimens had larger variation range than the saturated specimens, the mean value was almost identical irrespective to the identification method. In other words, factors affecting particular identification method may differ but the average calculated G_{max} values would not be much different.

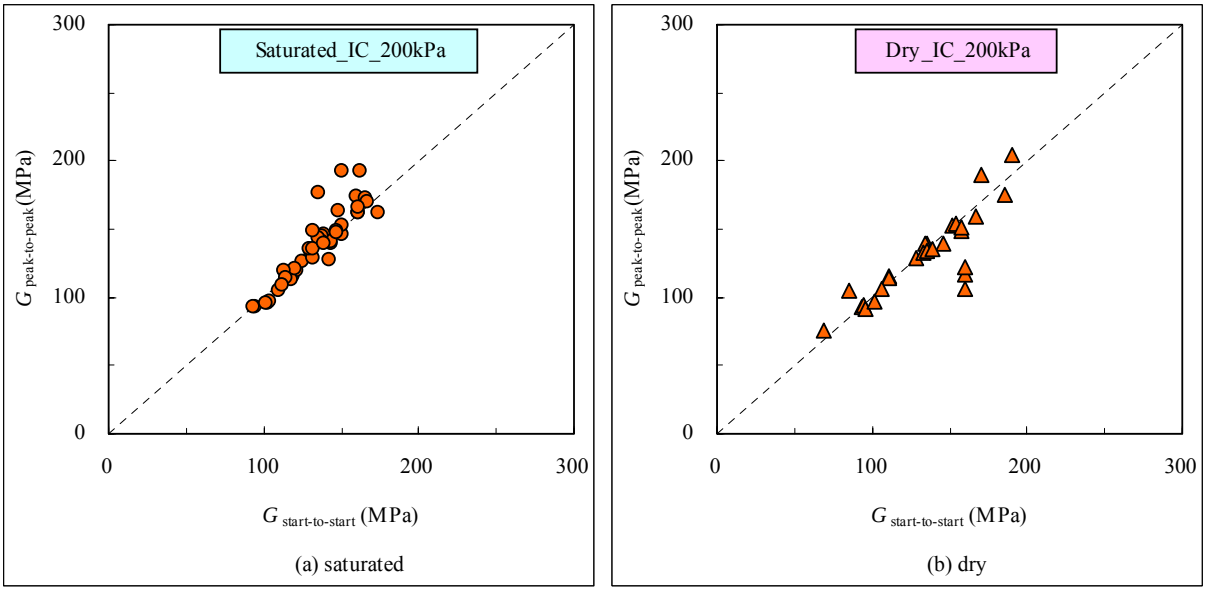

Fig. 4.52 Comparison of start-to-start and peak-to-peak; (a)saturated, (b)dry

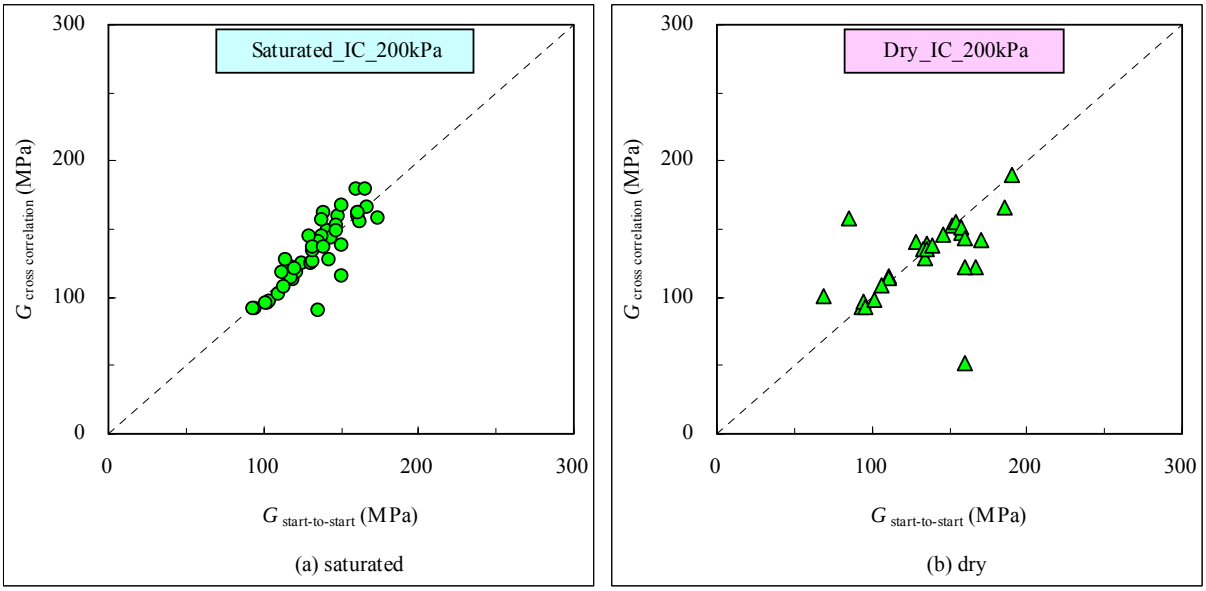

Fig. 4.53 Comparison of start-to-start and CC; (a)saturated, (b)dry

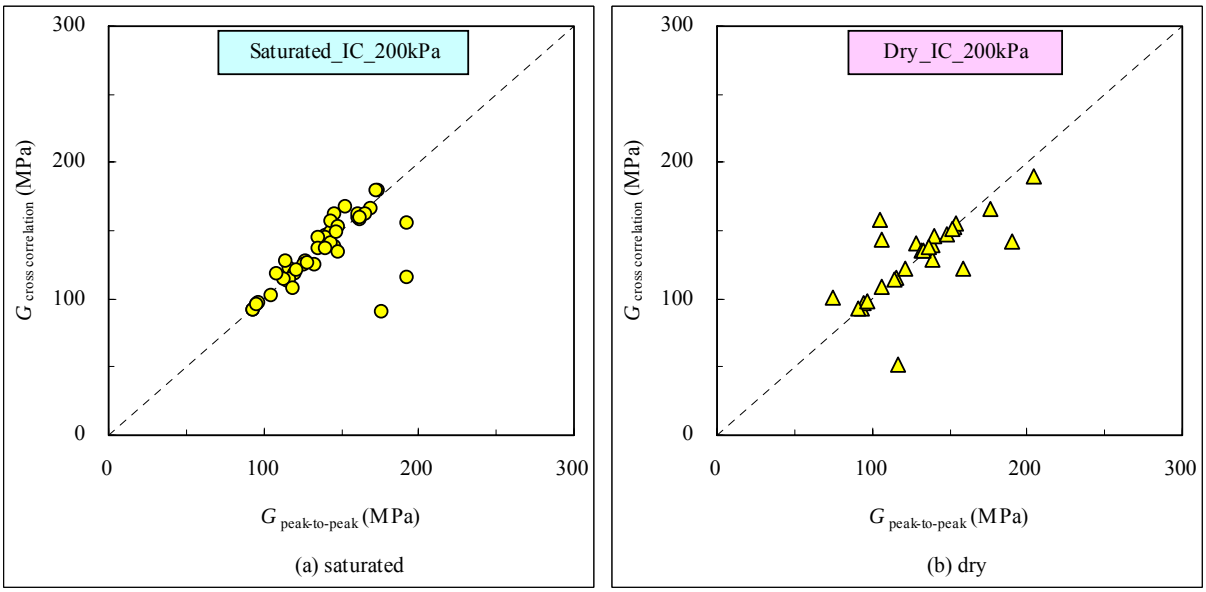

Fig. 4.54 Comparison of peak-to-peak and CC; (a)saturated, (b)dry

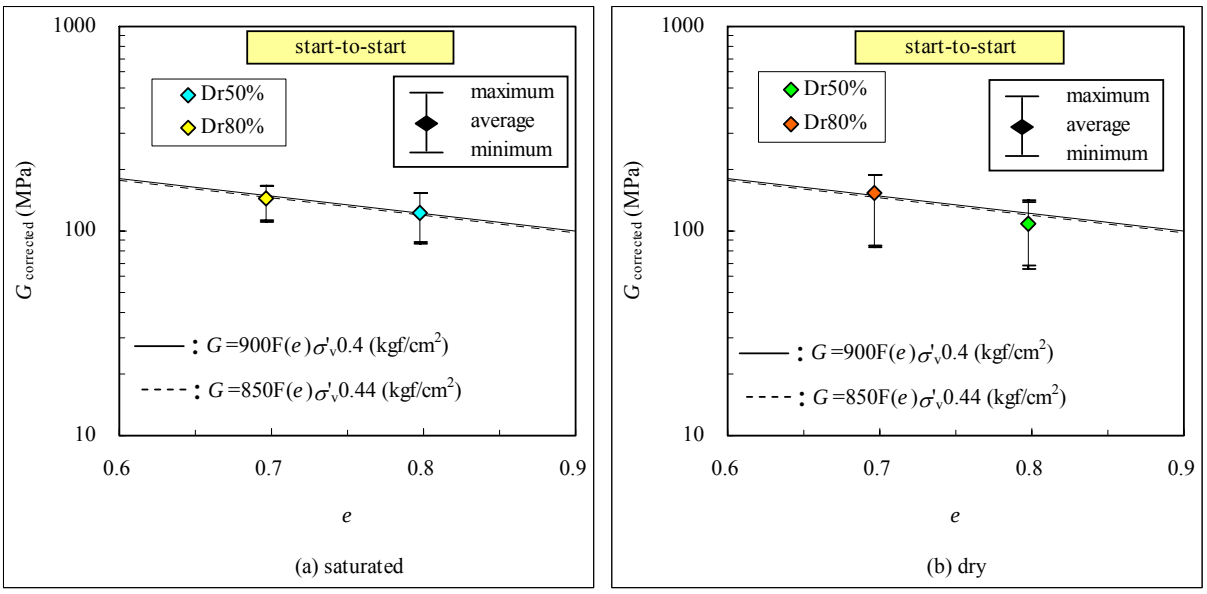

Fig. 4.55 Deviation of G (start-to-start); (a)saturated, (b)dry

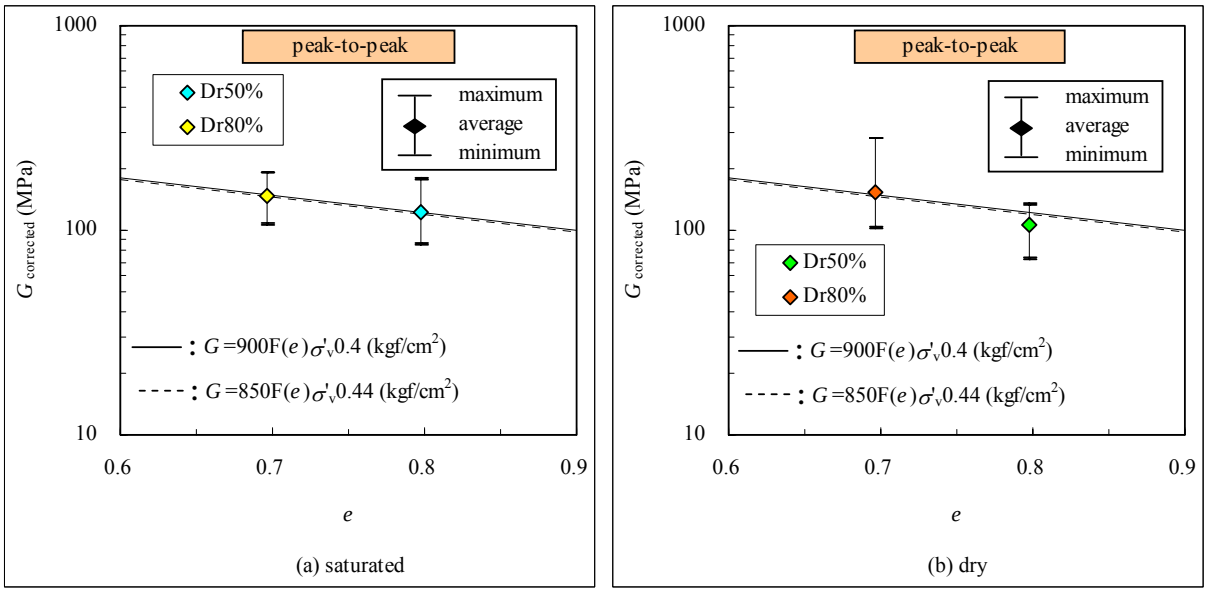

Fig. 4.56 Deviation of G (peak-to-peak); (a)saturated, (b)dry

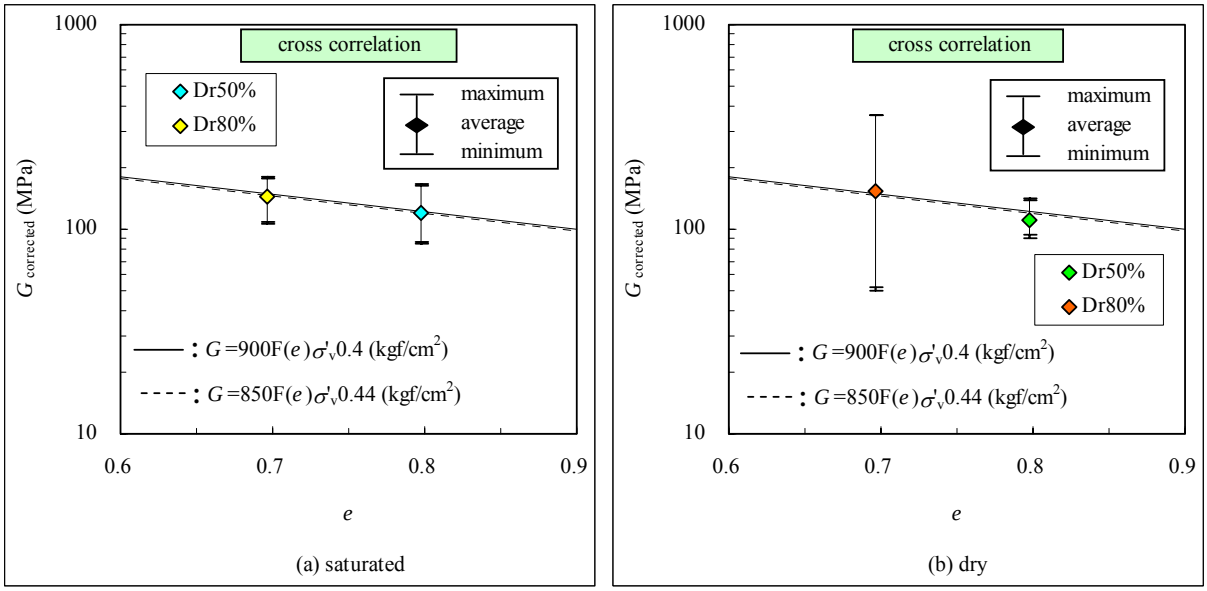

Fig. 4.57 Deviation of G (CC); (a)saturated, (b)dry

4.6 Comparison with Other Tests Results

In the current series of parallel test, besides finding shear wave velocity using the BE, it was also requested to find elastic moduli from the stress-strain curve by applying either monotonic or cyclic loads with strains 0.001% or less. Table 4.1 shows test condition and testing methods other than BE testing applied to determine the Young's modulus, E and shear modulus, G_{max}.

Among the laboratories which submitted reports, 12 out of 23 provided results obtained from other than BE method. Within those 12, nine of them obtained E values by using cyclic loads at very small strains (CTX). Besides this, Laboratory No. 1 obtained E values by measuring P- and S-wave velocities. Laboratory No. 9 & 10 obtained G_{max} values from resonant column (RC) or cyclic torsional test (CTS). Laboratory No. 20 fitted the piezoelectric actuator in the top cap, applied P- and S-wave signals, measured the acceleration with accelerometers fitted at the two ends of specimen along the side and obtained G_{max} values (Acc) from shear wave velocity and E values from P-wave velocity. G_{max} values were then calculated by assuming Poisson's ratio, ν. Furthermore, although Laboratory No. 23 evaluated the E values from cyclic loadings in the triaxial tests but as the strain level involved was quite large, it was not included in comparison below.

Figures 4.58 to 4.60 compare G_{max} values from BE test (G_{bender}) against those obtained from other type of tests (G_{other}) based upon different states of the sample (dry or saturated) and different consolidation conditions (isotropic or anisotropic). As G_{max} values from BE test submitted by different laboratories differed in input frequency as well as the identification method, the following guideline was adopted to obtain single G_{max} value:

i. If results from multiple methods (T.D., C.C. and F.D.) were submitted, the value from T.D. method was selected. If T.D. data was not available, the sequence of selection was in the order of C.C. and F.D.
ii. If the reports were available for square or sine input waves, sine wave was selected.
iii. If data at different frequencies were available within sine wave, the result obtained by input frequency closest to 10 kHz was selected.
iv. If multiple receiving points were considered for interpretation, the value calculated using start-to-start method was selected.

Regarding an isotropic stress state shown in Figs. 4.58(a) to 4.60(a), G_{max} obtained from resonant column test (□symbols) and torsional shear test (♦symbols) almost agree with the G_{max} values obtained from BE test. On the other hand, G_{max} values from triaxial test (●symbols) fall slightly below that of BE tests. In addition, G_{max} values obtained from shear wave velocity measured by accelerometer (○symbols) and P-waves (□symbols) locates a slightly on higher side. The measurement of shear wave arrival point with an accelerometer involves the decision about reading positions, similar to the BE methods described earlier. In the tests, the measurement was taken by considering multiple points, such as initial startup or the peak point. The calculated G_{max} values obviously differed with the reading positions and some of them are identical to the BE results. In addition, regarding the results for specimens at an anisotropic stress state (in plots (b) in these figures), resonant column test yields identical G_{max} value as the BE test, similar to the specimens at isotropic stress state. However, G_{max} values from triaxial tests are smaller than BE tests as for IC specimens.

Figures 4.61 and 4.62 show the relationship between G_{max} and void ratio, e with the tests other than BE. The values of G_{max} obtained from triaxial test also fall on lower side than other tests as discussed in the previous paragraph. The tendency of getting smaller G_{max} values from the triaxial test, for which G_{max} is calculated from Young's modulus, E and Poisson's ratio, ν has been recognized from the past parallel tests done so far. The difference existed in both drained triaxial tests, for which ν value calculated from the drained tests was used and also for undrained tests, for which ν value was simply taken as 0.5.

Figures 4.63 and 4.64 show the results of the past international parallel tests on the deformation behavior of geomaterials. The previous round robin test sponsored by TC29 (Yamashita et al. 2001) is shown in Figure 4.63. As compared with BE test, G_{max} values obtained from undrained triaxial test are slightly smaller. In addition, the other simultaneous test performed in Japan by using the triaxial test and torsional shear test device (Toki et al. 1995) also shows that (Figure 4.64) G_{max} values from the triaxial test are about 15% lower than torsional tests. Some of the factors for such lower values of G_{max} from triaxial test could be the effect of bedding error while measuring the axial displacement (Goto et al. 1991), lower B value and therefore smaller value of Poisson's ratio (ν<0.5) at undrained condition (Yamashita et al. 1996), influence of specimen anisotropy (Hoque & Tatsuoka 1998), the relation between the wave length of the shear wave and particle diameter (Tanaka et al 2000, Anhdan et al. 2002) and so on. G_{max} values, which were evaluated from the tests except BE in this parallel test, fell inside the scatter range indicated by past simultaneous tests and therefore, thought to be more reliable.

Figure 4.65 shows BE test data from the laboratories which evaluated moduli from other methods besides BE test. Although a little variation exists at lower confinements, the scatter is quite small as compared with Figure 4.1 that includes all of the data submitted from all laboratories. The reason for such uniformity lies on the fact that all of the laboratories use the same T.D. method for arrival time identification. In addition, they are expected to be more experienced on laboratory tests and have better quality. It is quite clear that G_{max} values obtained at anisotropic stress state (K=0.5) are smaller than those at isotropic stress state (K=1.0). The reason might be explained by the property of shear wave velocity that is governed by the stresses in propagation direction as well as in oscillating direction (Roesler 1979, Stokoe et al. 1995). Although vertical stress, which acts in the propagation direction, is identical in both isotropic and anisotropic tests, stress acting in lateral direction is smaller in the latter.

Lastly, Young's modulus evaluated with triaxial tests, for which the maximum number of reports was received, is shown in Figure 4.66. Variation is a little high in comparison with other tests. It is considered that factors affecting the test result, such as bedding error and others explained above, are more in triaxial test than other types.

Table 4.4 Test methods and test conditions

Lab. No.	Apparatus	Test method					Test condition				Remarks
		Acc.	P-wave	RC	CTS	CTX	Dry		Saturated		
							K=1	K=0.5	K=1	K=0.5	
1	TX		E				○				V_P by BE
2	TX					E, G			○	○	CTX(undrained), ν=0.5
7	TX					E, G			○	○	p' const CTX
8	TX					E	○				CTX(drained)
9	RC/TS			G	G		○		○		TS, RC
12	RC			G			○	○	○	○	RC
13	TX					E, G	○	○			CTX(drained)
14	TX					E, G			○		CTX(undrained), ν=0.5
20	TX	G	E, G			E, G	○	○			
21	TX					E, G	○	○	○	○	CTX(draine, undrained), ν=0.5
22	TX					E, G			○		CTX(undrained), ν=0.5
23	TX					E, G	○		○		CTX(drained), ν=0.25

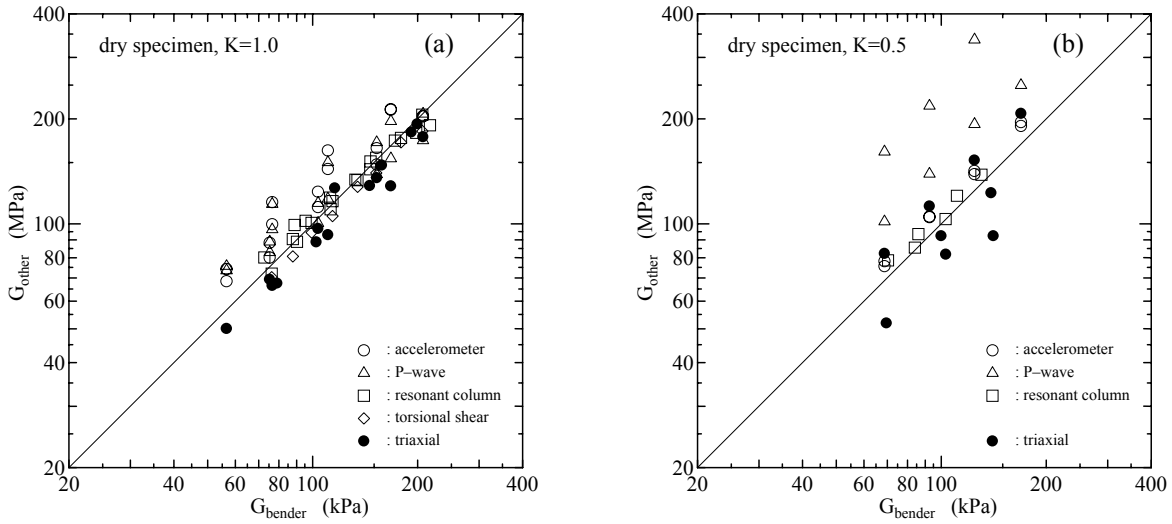

Fig. 4.58 Comparison of BE and others test results (dry); (a)IC, (b)K=0.5

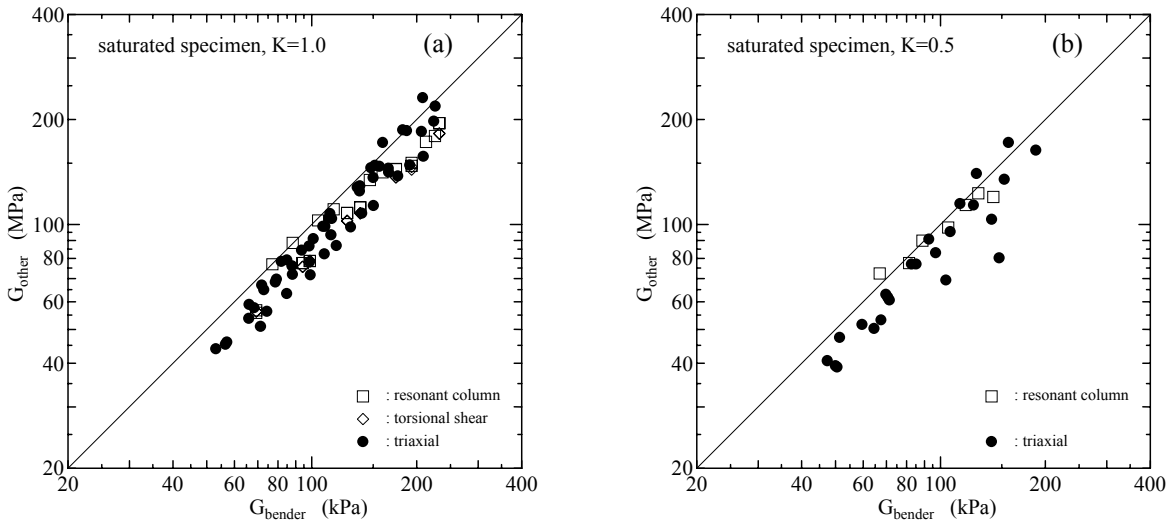

Fig. 4.59 Comparison of BE and others test results (saturated); (a)IC, (b)K=0.5

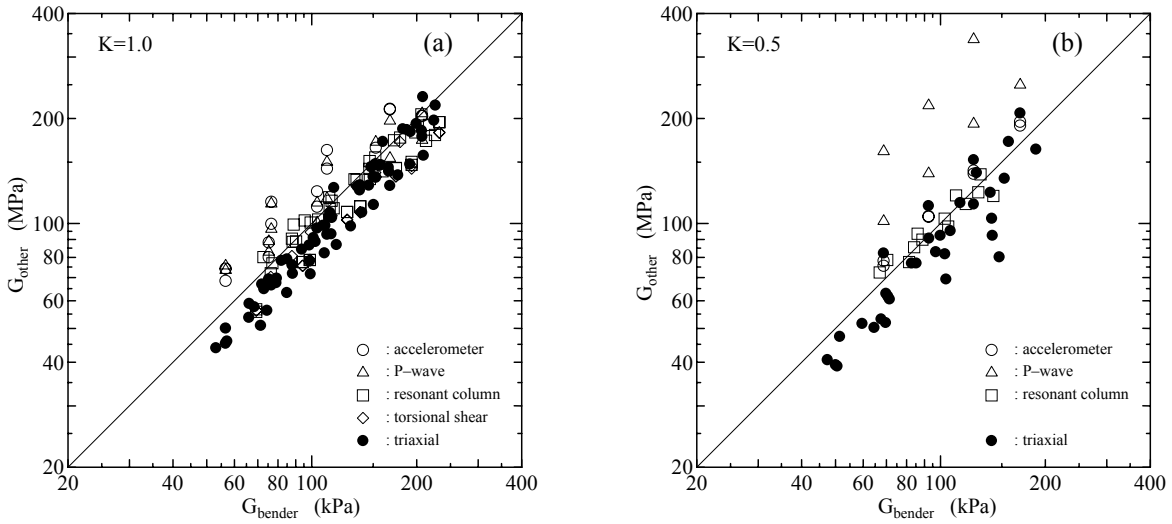

Fig. 4.60 Comparison of BE and others test results; (a)IC, (b)K=0.5

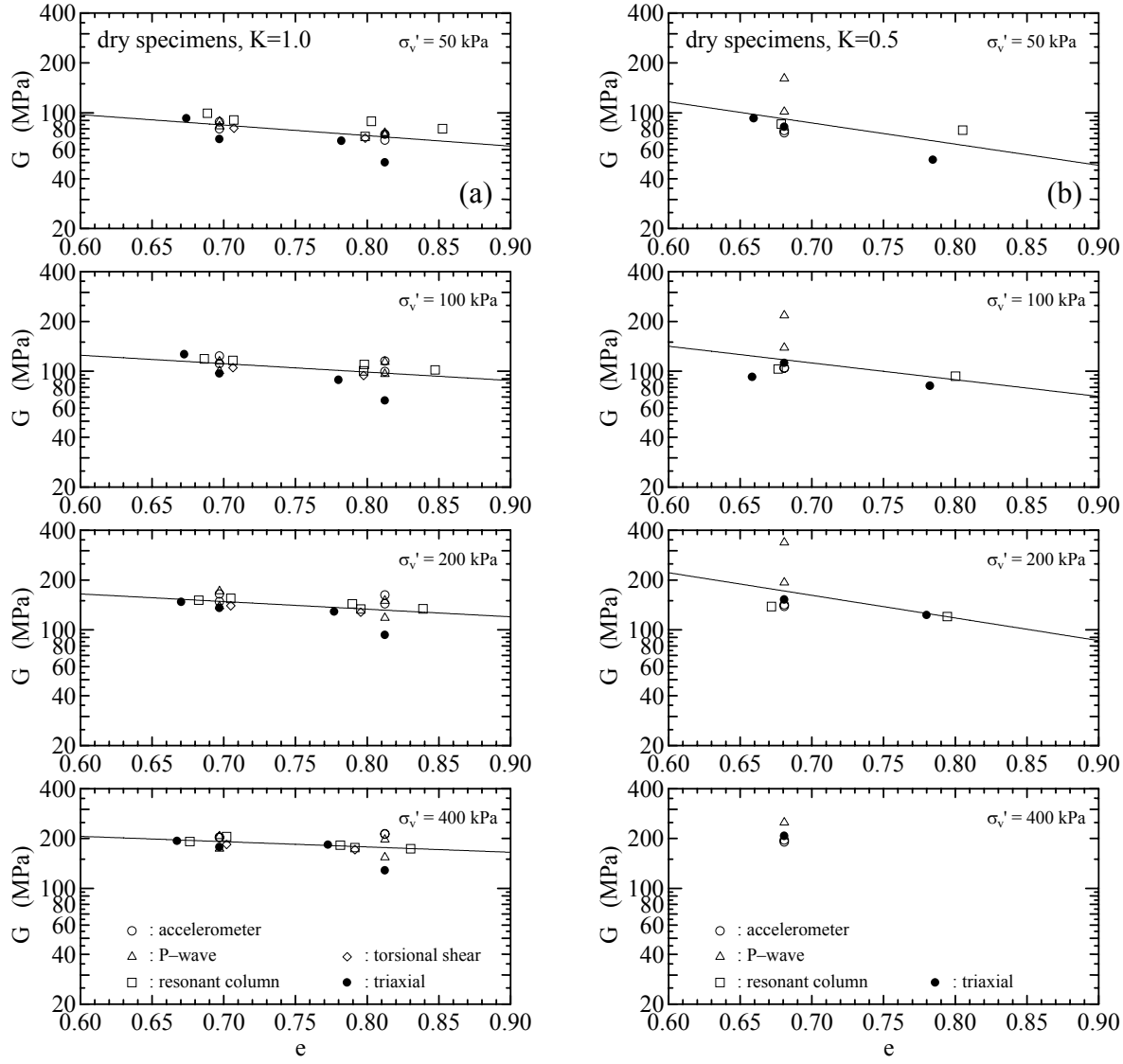

Fig. 4.61 Others test results (dry); (a)IC, (b)K=0.5

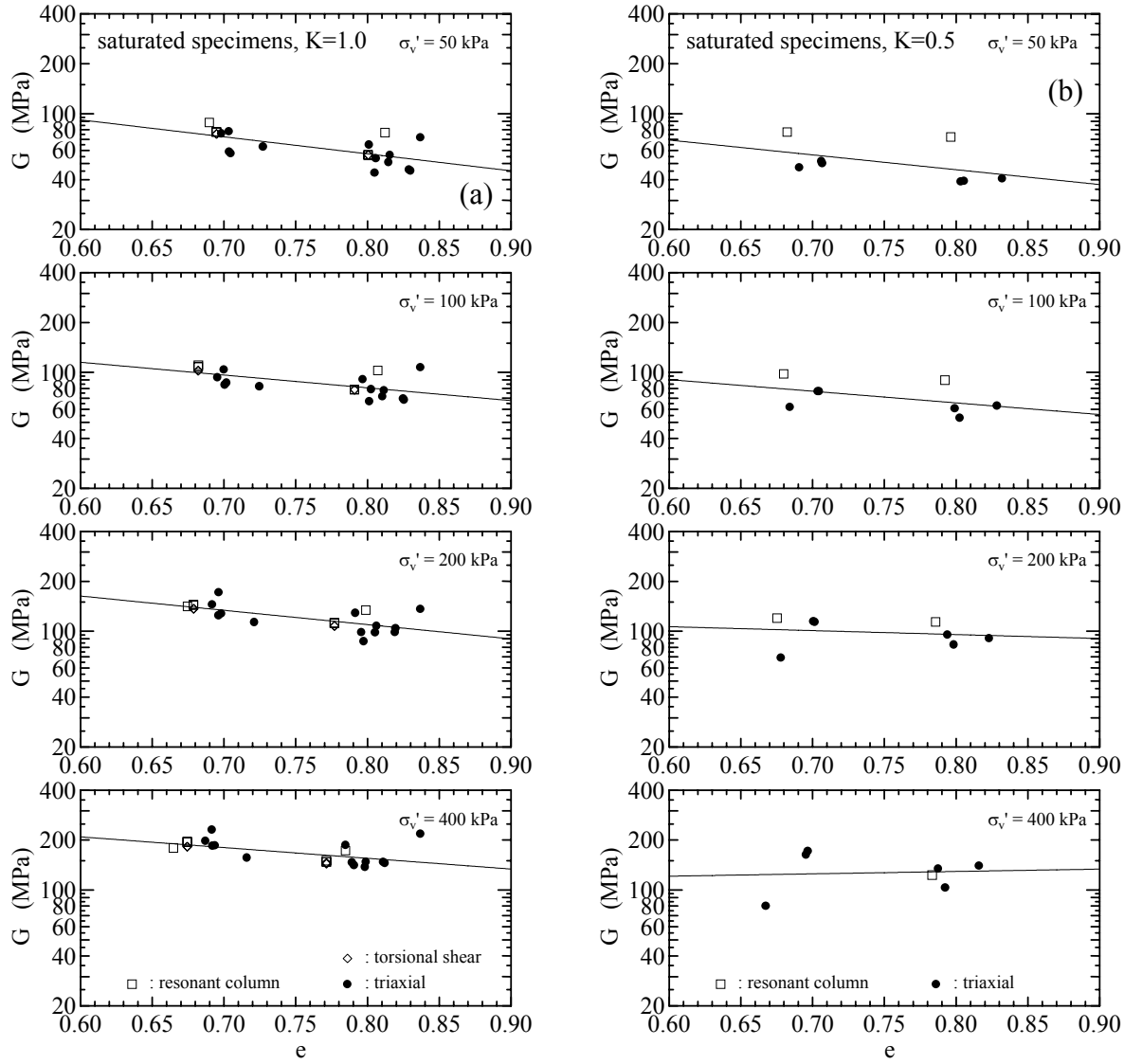

Fig. 4.62 Others test results (saturated); (a)IC, (b)K=0.5

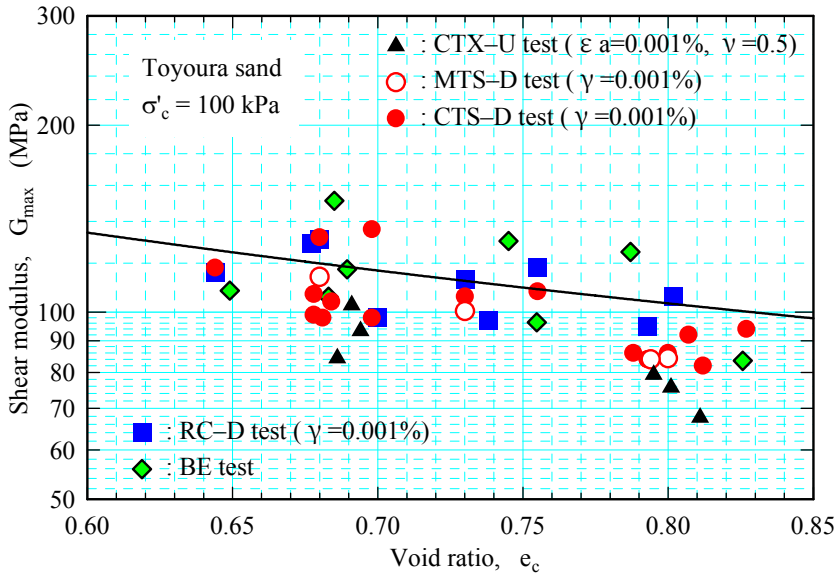

Fig. 4.63 Last RR test results (Yamashita et al 2001)

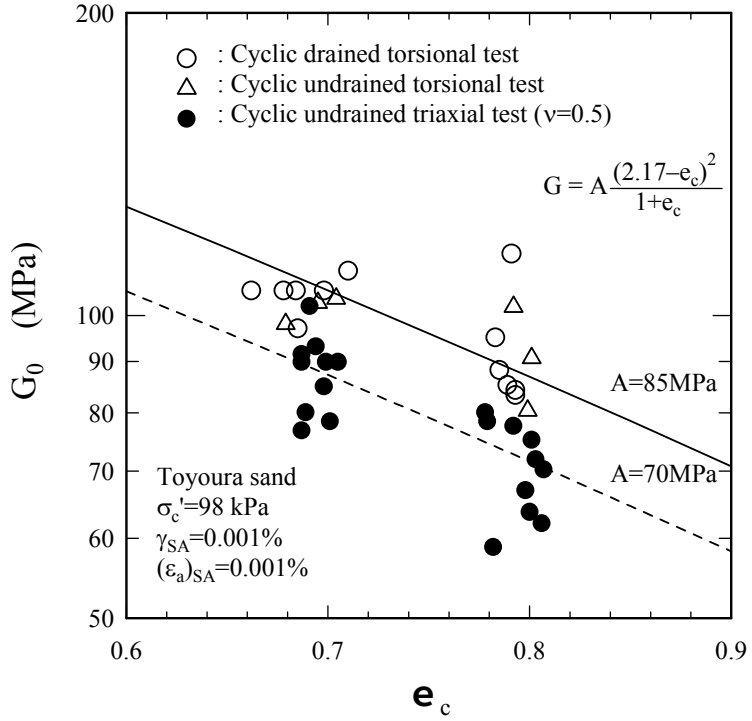

Fig. 4.64 Past RR test results (Toki et al 1995)

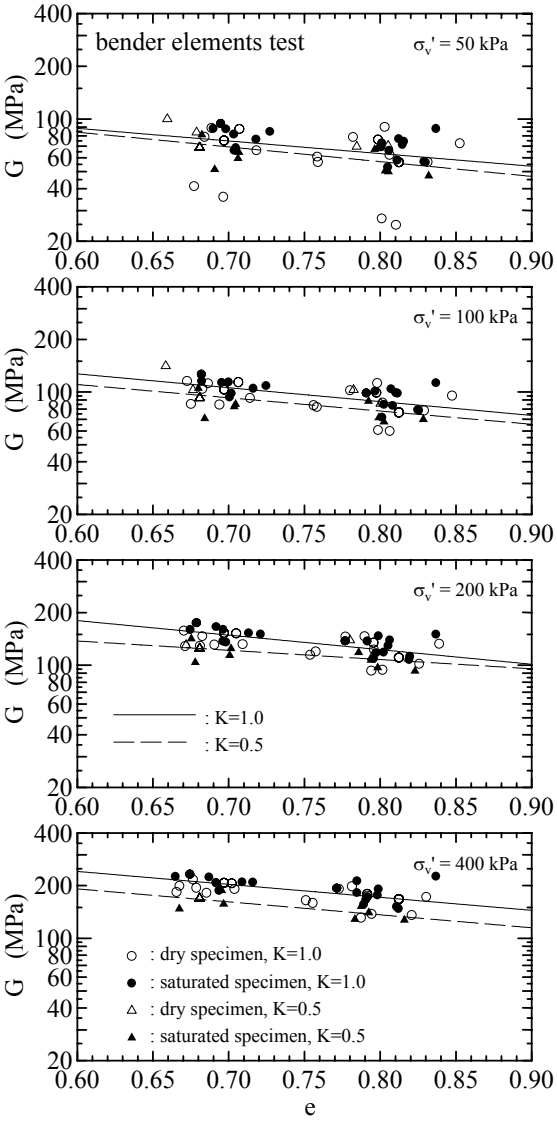

Fig. 4.65 BE test results

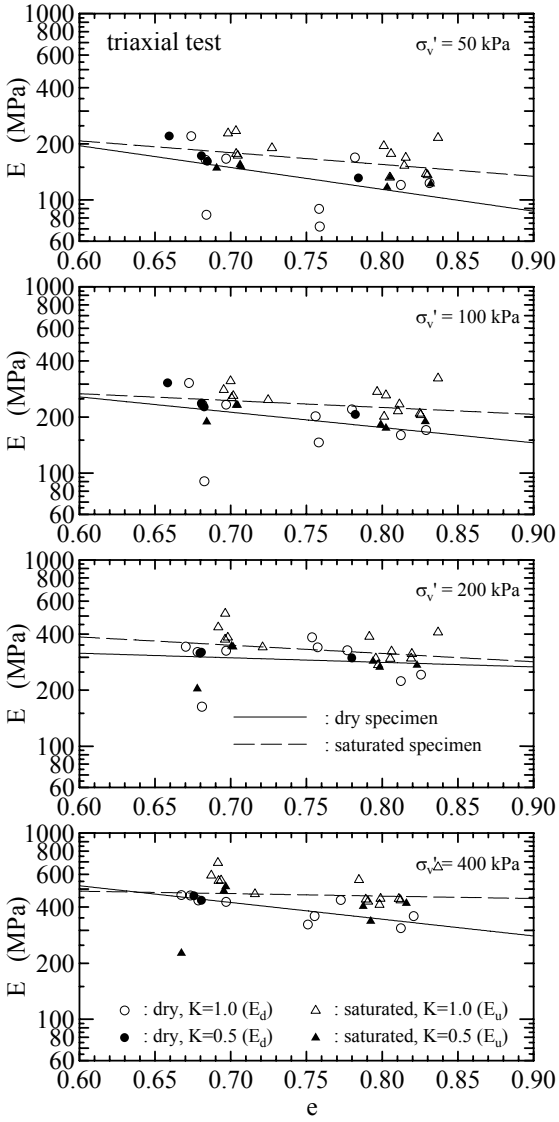

Fig. 4.66 CTX test results

5. STANDARD BE TEST METHOD (PROPOSE)

By evaluating the bender element (BE) test results from 23 institutions from 11 countries, the following standard test procedures for bender element testing has been proposed to obtain the most appropriate test result. The test process below is for a pulse of sine wave as input.

Among the result reported this time, the rectangular wave and continuous waves were also adopted other than single sine wave pulse. However, as the case records were only a few and it was not possible to judge their appropriateness, this report is relevant only with the single sinusoidal wave as an input.

- No clear influence of the difference in bender size, its structure, cantilever length and wiring method was recognized, but the average dimension used by the most laboratories was the width of 10 mm, thickness of 0.5 to 1.0 mm and cantilever length of 5 mm.
- Before starting the test, bender element pairs for transmission and reception are made to contact directly and delay time of the whole system as well as the polarity of initial motion need to be verified.
- Frequency of transmitting wave is adjusted so that it becomes equal to the frequency of the receiving wave. Otherwise, multiple input frequencies are used.
- Sampling interval shall be smaller than $1/100^{th}$ of expected arrival time. In case of very small distance between the benders and required resolution cannot be satisfied, the precision may be increased by using multiple frequencies.
- Voltage resolution shall be more that $1/100^{th}$ of the largest amplitude of the receiving wave. For example, when largest amplitude is 5 mV, the required resolution becomes 0.05 mV. This value is normally present in the digital oscilloscopes being used presently. When resolution cannot be satisfied, transmission voltage may be increased.
- The same value can be obtained by making use of either of the start-to-start or peak-to-peak or cross-correlation method of identification so, no specific method is recommended. However, when peak-to-peak method or cross-correlation method is used, frequency of input wave and the receiving wave shall be almost equal. In addition, when cross-correlation method is used and the 1^{st} wave in the receiving end does not have the largest amplitude, the attention shall be paid not to calculate the arrival time at the location of the maximum amplitude in cross-correlation function.
- When a test is conducted in a consolidation apparatus that use hard metal container or when the distance between the benders is short, the decision shall be taken relatively by using input waves of multiple frequencies and taking care of using wave length shorter than half the distance between benders.
- Regarding the F.D. method, reliable method for obtaining most appropriate data has not been concluded at present. From the fact that the scatter in F.D. method was quite large in the submitted data, it is quite dangerous to identify the arrival time with only this method.

6. CONCLUSIONS

The international parallel test for shear modulus evaluation was conducted from 2003 to 2005 by using bender elements and Toyoura sand as a sample. Altogether, the participation of 23 laboratories from 11 countries was confirmed. The purpose was to clarify the existing state of evaluation techniques for the bender element test and to recommend a standard test procedure for obtaining most appropriate test result by clarifying the influence of various factors. The following is what could be deduced from the submitted test results:

1) Report of the test result was submitted by 23 laboratories from 11 countries. The participated institutions were total of 15 from 3 countries in Asia, 9 from 7 countries in Europe and one from a country in North America. By comparing the participated international institutions in the previous parallel test organized by TC29 that was just 19, it is quite understandable that bender element test is spreading worldwide and being quite popular.
2) As for the test equipment, 17 laboratories used triaxial test, 5 laboratories used consolidation or direct shear test equipment that use hard metal containers and 2 laboratories used the resonant column test equipment. It is understandable that laboratories using the triaxial test device were the most. Besides, total of 105 tests, 60 on saturation specimen and 45 on saturation specimen, were conducted.
3) All of the BE used in the tests were of bimorph type and most of the laboratories used parallel type connection at transmitting end and series type at receiving end. Regarding the dimensions, 12 to 20 mm length, 10 to 12 mm width and 0.5 to 1.0 mm thickness was most common. In addition, penetration length inside the specimen was 5 mm in average.
4) Regarding the identification method of arrival time, the maximum number of laboratories (10) used T.D. method, 5 laboratories used C.C. method and 3 laboratories used F.D. method besides that some laboratories even investigated with multiple methods. On counting the teams using T.D. method, 13 laboratories used the start-to-start method, 2 used the peak-to-peak method and 3 laboratories used multiple methods.
5) On plotting the entire data reported from the laboratories, the scatter was quite large. In general, the scatter was large in dry specimens than the saturated specimens. Similarly, the results from K_0-tests performed in consolidation apparatus had larger scatter as compared to the isotropically consolidated specimens. The reasons for such scatter is not only the difference in identification method but also that some laboratories have evaluated the G_{max} value by assuming multiple arrival points in a received wave.
6) Concerning the difference in arrival time identification method, 1) the scatter in start-to-start method is small in comparison with other methods, 2) there is a tendency that peak-to-peak and the cross-correlation methods yield relatively small value of G_{max} than the start-to-start method, and 3) it is expected that there is no difference in G_{max} value due to saturation condition, i.e., dry or saturated, but larger scatters are associated with dry specimens.
7) When compared with the other test result, G_{max} obtained from resonant column and torsional shear tests almost agree with BE test. On the other hand, G_{max} values obtained from triaxial test are slightly smaller as compared to BE test. This tendency agreed with the similar parallel tests in the past.

The digital data submitted by laboratories was rearranged by using unified identification method. As a result, the following points were noted:

1) If arrival time is identified with start-to-start method, the scatter in the value of G_{max} reduced remarkably as compared with the originally submitted data from each laboratory. However, there still remain large scatter in the data for dry sample and K_0 consolidation sample as compared to the saturated samples and isotropically consolidated samples. A few of the data also deviated from the mean value.

   For most cases, reading an arrival point in the received wave was quite difficult due to a very low frequency of input wave and low resolution of sampling.
2) The data scatter decreases even if the peak-to-peak method is used for interpretation. Variation in wave scatter still remains for dry sample. In addition, in case of the peak-to-peak method, error is easy to occur when low frequency input wave is used.
3) With cross-correlation method, frequency of the input wave and the receiving wave is presumed to be equal so, the extent of error is likely to increase whenever the frequency of the input and the receiving wave differs, very similar to the peak-to-peak method. It is well noted that slight scatter is found for dry specimens than the saturated ones even with cross-correlation method.
4) The reason for larger variation in dry specimens is thought to lie on the relatively large noise before true shear wave signal and the longer reverberation time, among others.
5) As one of the methods of F.D. technique, phase cross spectrum was evaluated. In order to obtain appropriate value of G_{max} using this method, the two of the following conditions shall be fulfilled:

i. Amplitude of the first peak in the receiving wave showing the shear wave arrival shall be the maximum, and
ii. The frequency of input shear wave shall be almost equal to the frequency of the first wave at reception.

6) Irrespective of the applied identification methods, i.e., start-to-start, peak-to-peak or cross-correlation method, the measured mean value of arrival time remains almost the same. Therefore, provided that appropriate frequency of the input wave is used, the calculated shear modulus values do not depend on the identification method.

On the basis of the results as described above, standard procedure for bender element test has been proposed here to obtain the appropriate test result in the present condition.

REFERENCES

Anhdan, L., Koseki, J. and Sato, T.: Comparison of Young's moduli of dense sand and gravel measured by dynamic and static methods, *G*eotechnical Testing Journal, ASTM, Vol.25, No.4, pp.349-368, 2002.

Dyvik, R. and Madshus, C.: Laboratory measurement of G_{max} using bender elements, Advances in the Art of Testing Soils under Cyclic Conditions, ASCE, pp.186-196, 1985.

Goto, S., Tatsuoka, F., Shibuya, S., Kim, Y-S. and Sato, T.: A simple gauge for local small strain measurements in the laboratory, Soils and Foundations, JGS, Vol.31, No.1, pp.169-180, 1991.

Greenig, P.D. and Nash, A.F.T.: Frequency domain determination of G_0 using bender elements, Geotechnical Testing Journal, ASTM, Vo.27, No.3, pp.288-294, 2004.

Hoque, E. and Tatsuoka, F.: Anisotropy in elastic deformation of granular materials, Soils and Foundations, JGS, Vol.38, No.1, pp.163-179, 1998.

Iwasaki, T. and Tatsuoka, F.: Effect of grain size and grading on dynamic shear moduli of sands, Soils and Foundations, Vol.17, No.3, pp.19-35, 1977.

Kawaguchi, T., Mitachi, T. and Shibuya, S.: Evaluation of shear wave travel time in laboratory bender element test, Proc. of the 15th International Conference on Soil Mechanics and Geotechnical Engineering, Vol.1, pp.155-158, 2001.

Lings, M.L. and Greening, P.D.: A novel bender/extender element for soil testing, Gèotechnique, ICE, Vol.51, No.8, pp.713-717, 2001.

Miura, S., Toki, S. and Tatsuoka, F.: Cyclic undrained triaxial behavior of sand by a cooperative test program in Japan, Dynamic Geotechnical Testing, Vol.2, ASTM STP 1213, pp.246-260, 1994.

Roesler, S.K.: Anisotropic shear modulus due to stress anisotropy. Journal of Geotechnical Engineering, ASCE, Vol.105, No.7, pp.871-880, 1979.

Stokoe, K.H.II, Hwang, S.K., Lee, N.K.J. and Andrus, R.D.: Effect of various parameters on the stiffness and damping of soils at small to medium strains. Keynote lecture, Proceedings of the 1st International Conference on Pre-failure Deformation of Geomaterials, Sapporo, Balkema, pp.785-816, 1995.

Tanaka, Y., Kudo, K., Nishi, K., Okamoto, T., Kataoka, T. and Ueshima, T.: Small strain characteristics of soils in Hualian, Taiwan, Soils and Foundations, JGS, Vol.40, No.3, pp.111-125, 2000.

Tatsuoka, F., Shibuya, S. and Kuwano, E. (eds): Advanced Laboratory Stress-Strain Testing of Geomaterials, Balkema, 2001.

Tatsuoka, F., Toki, S., Miura, S., Kato, H., Okamoto, M., Yamada, S., Yasuda, S. and Tanizawa, F.: Some factors affecting cyclic undrained triaxial strength of sand, Soils and Foundations, JGS, Vol.26, No.3, pp.99-116, 1986.

Toki, S., Shibuya, S. and Yamashita, S.: Standardization of laboratory test methods to determine the cyclic deformation properties of geomaterials in Japan, Pre-failure Deformation of Geomaterials, Vol.2, Balkema, pp.741-789, 1995.

Toki, S., Tatsuoka, F., Miura, S., Yoshimi, Y., Yasuda, S. and Makihara, Y.: Cyclic undrained triaxial strength of sand by a cooperative test program, Soils and Foundations, JGS, Vol.26, No.3, pp.117-156, 1986.

Yamashita, S., Kohata, H., Kawaguchi, T. and Shibuya, S.: International round robin test organized by TC29, Advanced laboratory stress strain testing of geomaterials, Balkema, pp.65-110, 2001.

Yamashita, S., Toki, S. and Suzuki, S.: Effect of membrane penetration on modulus and Poisson's ratio for undrained cyclic triaxial conditions, Soils and Foundations, JGS, Vol.36, No.4, pp.127-133, 1996.

Viggiani, G. and Atkinson, J.H.: Interpretation of bender element test, Gèotechnique, ICE, Vol.45, No.1, pp.149-154, 1995.

APPENDIX 1

STANDARD TEST SPECIFICATION FOR INTERNATIONAL PARALLEL TEST ON THE MEASUREMENT OF Gmax USING BENDER ELEMRNTS BY TC-29

1 Test material and testing apparatus

- The test material is Toyoura sand. The results obtained from the international round-robin tests of monotonic and cyclic tests using triaxial, torsional shear and resonant column apparatuses on same sand are described in the paper "Ref.: Yamashita, S., Kohata, H., Kawaguchi, T. and Shibuya, S. (2001): International round robin test organized by TC29, Advanced laboratory stress strain testing of geomaterials, Balkema, pp.65-110."
- 5 kg of Toyoura sand will be distributed to each laboratory.
- Testing apparatus is triaxial, consolidometer, resonant column or etc. equipped with bender elements.

2 Sample preparation

- Specimens which will have D_r equal to 50 and 80 % (dry densities ρ_d equal to 1.465 and 1.553 g/cm^3) as determined at initial stress condition (σ_v'=25kPa) are prepared by the air-pluviation method; air-dried sand is poured from a copper nozzle with a rectangular inner cross-section of 1.5mm×15.0mm, while maintaining a constant drop-height throughout the preparation.
- The final top surface of specimen is made level and smooth by scraping with a thin plate having a straight edge.
- These nozzles will be produced by the Japanese domestic committee of TC-29, and will be distributed to the members of TC-29.

3 Specimen set-up (except for consolidometer)

- Before the mold is disassembled, a partial vacuum of 10 kPa is applied to the specimen, while the loading piston is unclamped.
- Subsequently, the mold is dismantled, and then the vacuum is raised to 25 kPa while ensuring that the specimen can deform freely both in the axial and lateral directions.
- Then, initial specimen height and diameter are measured, and the results are reported.
- The partial vacuum is replaced with a cell pressure of 25 kPa while keeping the effective stress constant throughout the procedure.

4 Consolidation and Measurements of shear wave velocity

- Sample conditions in testing are dry or fully saturated.
- In the case of saturated specimen, the specimen is saturated using any of or a combination of appropriate saturation techniques. A back pressure of 100 kPa is applied.
- Consolidation condition is isotropic or anisotropic [K=0.5 or K_0 (consolidometer)], and the consolidation stresses are σ_v' = 50, 100, 200 and 400 kPa (see Fig.1). e.g.; in the case of K=0.5, σ_v'=50, 100, 200, 400 kPa (σ_h'=25, 50, 100, 200 kPa).

4.1 Isotropic consolidation

a) Keeping the isotropic stress state in the drained condition, increase the confining stress to the next isotropic stress state (σ_c' = 50, 100, 200 or 400 kPa) in one or two minutes as shown in Fig.1.
b) Consolidate 10 minutes on each stress state (open circle marks in Fig.1).
c) Measure the changes in the height and volume of the specimen.
d) Measure the shear wave velocities using the bender element.
e) Measure the secant stiffness from stress-strain curve at small strains (less than 0.001%) by applying monotonic or cyclic loading in the drained and/or undrained conditions when possible.
f) Measure the changes in the height and volume of the specimen after the measurement of Vs and/or stiffness.
g) Repeat the processes a) to f) until the final stress state (σ_c' = 400 kPa) is reached.

4.2 Anisotropic consolidation (K=0.5)

a) In the drained condition, apply the vertical stress up to 50 kPa (σ_h'=25 kPa and K=0.5).

b) Consolidate 10 minutes on K = 0.5 stress state (solid circle marks in Fig.1).
c) Measure the changes in the height and volume of the specimen.
d) Measure the shear wave velocities using the bender element.
e) Measure the secant stiffness from stress-strain curve at small strains (less than 0.001%) by applying monotonic or cyclic loading in the drained and/or undrained conditions when possible.
f) Measure the changes in the height and volume of the specimen after the measurement of Vs and/or stiffness.
g) Increase the horizontal and vertical stresses step by step until next anisotropic stress state (solid circle marks in Fig.1) in one or two minutes on each step. The increment of horizontal and vertical stresses, $\Delta\sigma_h$, $\Delta\sigma_v$ are 25 and 50 kPa, respectively.
h) Repeat the processes b) to g) until the final stress state (σ_v'= 400kPa and σ_h'= 200 kPa) is reached.

4.3 K_0 consolidation (consolidometer)
a) In the drained condition, increase the vertical stress to the next stress state (σ_v' = 50, 100, 200 or 400 kPa) in one or two minutes.
b) Consolidate 10 minutes on each stress state.
c) Measure the changes in the height of the specimen.
d) Measure the shear wave velocities using the bender element.
e) Measure the changes in the height of the specimen after the measurement of Vs.
f) Repeat the processes a) to e) until the final stress state (σ_v' = 400 kPa) is reached.

5 Report
1) Outline of the test apparatus used.
2) Details of benders employed (e.g., maker, shape, dimension, thickness and material of Piezoelectric Ceramics, mounting, the tip-to-tip distance, electrical connections(series or parallel), etc.). Schematic figure indicated dimension of cap and/or pedestal with bender elements.
3) Fill up the items listed in Form attached.
4) Input and received wave record in digital data or hardcopy of screen. Sampling frequency and whether filter used or not.
5) Determination of arrival time (Vs), special treatment (cross correlation, self monitoring, etc).
6) Strain rate of monotonic loading, and/or frequency and number of loading cycle of cyclic loading.
7) Stress and strain records on monotonic and/or cyclic loadings in digital data.
8) Any deviations from the procedure outlined in this specification.

6 Schedule:
Report of test results: end of June 2004
Contact : Dr. Satoshi Yamashita; yamast@mail.kitami-it.ac.jp

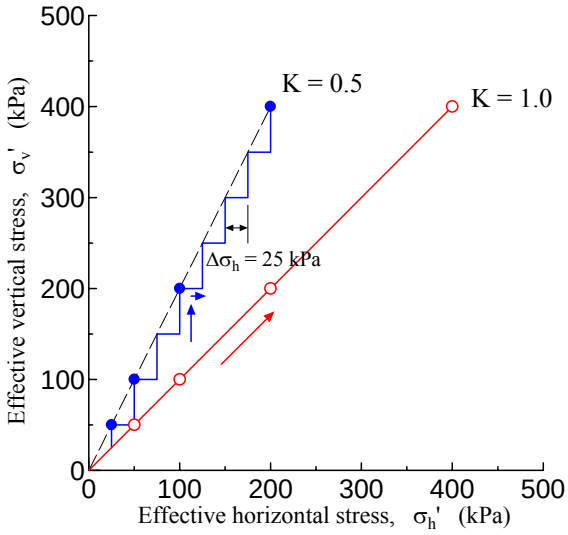

Figure 1.

APPENDIX 2

Round-Robin Test Form (Example)

Lab. Name	Kitami Institute of Technology
Test apparatus	Triaxial
Test No.	1

Sand name	Toyoura sand
Dry or Saturated specimen	saturated
density of soil particle, ρs (g/cm3)	2.635

	Initial				
Effective vertical stress, σv' (kPa)	25	50	100	200	400
Effective horizontal stress, σh' (kPa)	25	50	100	200	400
Back pressure, u (kPa)	0	100	100	100	100
Consolidation stress condition, K	1.0	1.0	1.0	1.0	1.0
Change of height during consolidation from initial state, ΔH	0	0.001	0.007	0.014	0.027
Volume change during consolidation from initial state, ΔV (	0	0.147	0.528	0.909	1.543
Outer diameter of specimen, Do (cm)	5.044	5.042	5.039	5.036	5.031
Inner diameter of specimen, Di (cm)	-	-	-	-	-
Hight of specimen, H (cm)	9.975	9.974	9.968	9.961	9.948
Volume of specimen, V (cm3)	199.321	199.174	198.793	198.412	197.778
Change of height after the measurement of Vs, ΔH (cm)		0.001	0.007	0.014	0.027
Volume change after the measurement of Vs, ΔV (cm3)		0.147	0.528	0.909	1.543
Dry mass, ms (g)	310.480	310.480	310.480	310.480	310.480
Mass of specimen, m (g)	391.972	391.825	391.444	391.063	390.429
Dry density, ρd=ms/V (g/cm3)	1.558	1.559	1.562	1.565	1.570
Total density, ρt=m/V (g/cm3)	1.967	1.967	1.969	1.971	1.974
Void ratio, e	0.692	0.690	0.687	0.684	0.679
Distance of BE, Δs (cm)	9.296	9.295	9.289	9.282	9.269

Bender Elements

Stage	σv' (kPa)	σh' (kPa)	Input wave (V)	Input wave f (Hz)	Input wave Shape	Δt (msec)	Δs (mm)	Vs (m/sec)	ρt (kg/m3)	G (MPa)
1	50	50	±10V	15kHz	sin	0.409	92.95	227.262	1971	101.80
2	100	100	±10V	15kHz	sin	0.342	92.89	271.608	1972	145.48
3	200	200	±10V	15kHz	sin	0.304	92.82	305.329	1974	184.03
4	400	400	±10V	15kHz	sin	0.281	92.69	329.858	1977	215.11

Monotonic or Cyclic test

Stage	σv' (kPa)	σh' (kPa)	E (MPa)	εa	ν	G (MPa)	γ
1	50	50					
2	100	100					
3	200	200					
4	400	400					

APPENDIX 3

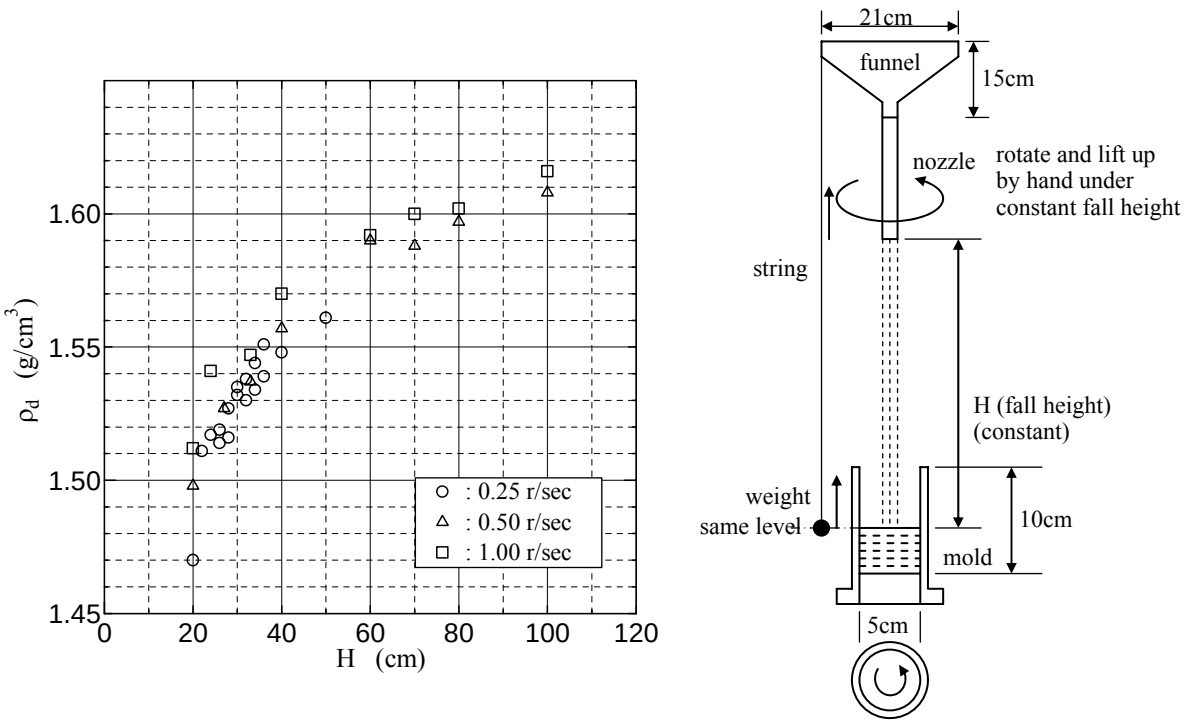

FIG. Relationship between dry density and fall height

Above figure shows an example of relation between the dry density and the fall height in Air-Pluviation method. However, this relation varies with the size of funnel, room humidity, rotation speed of nozzle, size of specimen, operator, etc.